Mathematical Models of Androgen Resistance in Prostate Cancer Patients under Intermittent Androgen Suppression Therapy

by

Javier Baez

A Dissertation Presented in Partial Fulfillment
of the Requirements for the Degree
Doctor of Philosophy

Approved November 2017 by the
Graduate Supervisory Committee:

Yang Kuang, Chair
Eric Kostelich
Sharon Crook
Carl Gardner
John Nagy

ARIZONA STATE UNIVERSITY

December 2017

ABSTRACT

Predicting resistant prostate cancer is critical for lowering medical costs and improving the quality of life of advanced prostate cancer patients. I formulate, compare, and analyze two mathematical models that aim to forecast future levels of prostate-specific antigen (PSA). I accomplish these tasks by employing clinical data of locally advanced prostate cancer patients undergoing androgen deprivation therapy (ADT). I demonstrate that the inverse problem of parameter estimation might be too complicated and simply relying on data fitting can give incorrect conclusions, since there is a large error in parameter values estimated and parameters might be unidentifiable. I provide confidence intervals to give estimate forecasts using data assimilation via an ensemble Kalman Filter. Using the ensemble Kalman Filter, I perform dual estimation of parameters and state variables to test the prediction accuracy of the models. Finally, I present a novel model with time delay and a delay-dependent parameter. I provide a geometric stability result to study the behavior of this model and show that the inclusion of time delay may improve the accuracy of predictions. Also, I demonstrate with clinical data that the inclusion of the delay-dependent parameter facilitates the identification and estimation of parameters.

To my wife, Rubi

ACKNOWLEDGMENTS

I want to sincerely thank my advisor, Dr. Yang Kuang, for his incredible support. Working with him has been extremely rewarding, enjoyable, and inspiring. I am deeply grateful for all his help and understanding. Also, I want to thank Dr. Eric Kostelich, for his guidance on a significant portion of this dissertation. Next, I want to thank my committee members Dr. John Nagy, Dr. Carl Gardner, and Dr. Sharon Crook, from whom I learned immensely through the courses I took from them. Also, I want to express my gratitude to my parents for their love and support and for inspiring me to do my best. I also want to thank the rest of my family and in-laws for their constant love and encouragement. Lastly, but certainly not least, I want to thank my wife, Rubi, for her unconditional love and for always believing in me and telling me to never give up.

TABLE OF CONTENTS

CHAPTER Page

CHAPTER Page

LIST OF TABLES

LIST OF FIGURES

Figure Page

Figure Page

Chapter 1

INTRODUCTION

1.1 Biological Background

Prostate cancer is the most common non-skin cancer among men (Bard *et al.* (2013)). A non-smoking man is more likely to develop prostate cancer than colon, bladder, melanoma, lymphoma, and kidney cancer combined (Bard *et al.* (2013); Heinlein and Chang (2004)). In most cases, the prostate tumor grows slowly, and takes years to become large enough to be diagnosed, and even longer to spread to other body locations (Folkman (1996)) However, a small percentage of men experience more rapidly growing and aggressive forms of prostate cancer (Feldman and Feldman (2001)). Hence, it is difficult to know for sure which prostate cancers will grow slowly and which will grow aggressively. The design of cancer chemotherapy is becoming increasingly sophisticated, however, the uncertainty of cancer growth can still complicate treatment strategies (Khayat and Hortobagyi (2013)). Currently, there is no cancer treatment that is 100% effective against metastatic cancer (Gottesman (2002)). Even though there are targeted treatments after chemotherapy has failed, treatment resistance that occurs as cancerous cells evolve is the main obstacle of targeted cancer treatments today (Holohan *et al.* (2013)).

1.2 Pathways to Androgen Resistant Prostate Cancer

There are five identified pathways for cancerous prostate cells to develop androgen resistance (Feldman and Feldman (2001)). The hypersensitive pathway happens when more androgen receptors are produced or the androgen receptors become more

sensitive to lower levels or androgen (Feldman and Feldman (2001)). In the promiscuous pathway, the androgen receptors are not only activated by androgen molecules but also other non-androgen molecules such as corticosteroids (Feldman and Feldman (2001)). In the outlaw pathway, receptor tyrosine kinases are activated, and the AR is activated by the protein kinase B (Feldman and Feldman (2001)). In the bypass pathway, parallel survival pathways, such as that involving the anti-apoptotic protein BCL2 (B-cell lymphoma 2), obviate the need for AR or its ligand. The first four pathways are due to mutations in castration sensitive prostate cells that make the cells resistant to lower levels of androgen. However, in the lurker cell pathway, androgen resistant cancer cells that are present all the time in the prostate. The resistant cells had been lurking as a sub-population of the tumor and androgen suppression therapy selected for the lurking cells until they take over the majority of the tumor and the patient no longer responds to ADT (Feldman and Feldman (2001)). The above mentioned pathways are described in great detail in a great paper review paper by Feldman and Feldman (2001). In order to asses a models ability to model androgen resistant prostate cancer, we need to check whether a model can incorporate as many of the possible pathways to resistance with the data that is available.

1.3 Androgen Suppression Therapy

Since the discovery of androgen dependency of prostate cells, androgen deprivation therapy (ADT) has been the main treatment of metastatic and locally advanced prostate cancer (Heinlein and Chang (2004); Shafi *et al.* (2013); Tsao *et al.* (2012)). In ADT, the goal is to reduce the levels of male hormones, androgens, or to prevent them from affecting prostate cells (Feldman and Feldman (2001)). The main androgens in the body are testosterone and dihydrotestosterone (DHT) (Feldman and Feldman (2001)). Most of the androgens are made by the testicles, but the adrenal glands produce

about 5% (Tilley *et al.* (1996); Heinlein and Chang (2004)). Lowering androgen levels to stop them from getting into prostate cancer cells often makes tumors shrink and grow more slowly, but ADT alone can only extend a patient's life and cannot cure prostate cancer (Feldman and Feldman (2001)). The main drawback of ADT is the development of resistance due to cancer cells proliferating at castration levels of androgen (Feldman and Feldman (2001)). The development of resistance can take from a few months to more than ten years (Tsao *et al.* (2012); Hussain *et al.* (2013)), after which there is only less effective treatments and high death rate (Karantanos *et al.* (2015)). Intermittent androgen suppression (IAS) was implemented in order to delay the progression of androgen resistance and improve the quality of life of patients (Bruchovsky *et al.* (2006b)). During off-treatment periods, patients can take a vacation from the severe side effects of ADT (Klotz and Toren (2012)), and studies have suggested that IAS may not negatively affect the time to androgen resistance or survival in comparison to continuous ADT (Gleave (2014)).

1.4 Mathematical Modeling of Intermittent Androgen Suppression Therapy

The first to study the possible pathways to androgen tumor relapse during ADT was Jackson (2004a). Jackson (2004a) used a system of partial differential equations to model the mechanics of the progression to castrate resistant prostate cancer (CRPR). The main finding of Jackson's work was that ADT is prone to failure and the delay of resistance can occur for only a restricted range of parameters values (Jackson (2004a)). Then many researchers started modeling the dynamics of androgen suppression therapy. Ideta *et al.* (2008) developed a system of ordinary differential equations to study the mechanics of ADT. They considered castrate-resistant (CR) and castrate-sensitive (CS) cell populations as well as androgen levels. Their model included mutations from CS to CR cells, and their focus was on comparing continuous and intermittent therapy

and the development of resistance. Their results suggest that the mutation rates between cancer types has an influence in the time to androgen relapse (Ideta *et al.* (2008)). Hirata *et al.* (2010) considered a three cell populations using a piece-wise linear model to fit clinical prostate-specific antigen (PSA) data. Their model included CS cells that could mutate into CR cells, CR cells that could mutate into CS cells, and CR cells that do not mutate back CS cells. Several investigators using Hirata's model, have studied estimation of parameters (Guo *et al.* (2013); Tao *et al.* (2013)), optimal switching times and control in IAS (Guo *et al.* (2013); Suzuki *et al.* (2014); Hirata *et al.* (2012a)), and forecasting cancer resistant prostate cancer progression (Hirata *et al.* (2012b, 2014a)). Portz *et al.* (2012) developed a model of ADT by extending the works of Jackson (2004a) and Ideta *et al.* (2008). Their model included two cell populations as in Ideta *et al.* (2008) but also included a limited nutrient based cancer growth model by the cell quota model Droop (1973).

1.5 Thesis Overview

All the novel contributions presented in this dissertation involve the Cell Quota model (Droop (1973)) and follow from the works of Portz *et al.* (2012). The cell quota model is a two-parameter curve which maps specific growth rate to intracellular nutrient of a cell,

$$\mu\left(1-\frac{q}{Q}\right)$$

where the cell quota Q is often expressed as units per cell, or the relative mass of some nutrient per unit of biomass (Everett *et al.* (2014)). The subsistence quota q can be interpreted as the minimum Q required for life. Similarly, it can be interpreted as the conversion ratio for biomass, whereby $Q > q$ implies there is a nutrient pool available for reproduction. In this work, we shall use serum androgen concentration to approximate intracellular androgen in cancer cells. Androgen passively diffuses through

the prostate membrane via concentration gradient (Roy and Chatterjee (1995)). By assuming an equilibrium concentration of intracellular and serum levels, we use serum levels effectively as the limiting nutrient of the cell growth (Baez and Kuang (2016)).

In Chapter 2, we introduce the details of the clinical trial that is the source of data for all our predictions. We use data from Bruchovsky *et al.* (2006b), in our analysis and data fitting. Chapter 2 of this dissertation also focuses on a comparison of mathematical models of prostate cancer that are prominent in literature. A pair of novel models are presented in this chapter that aim to enhance Portz *et al.* (2012) model. We present the one population model,

$$\begin{aligned}
\frac{dx}{dt} &= \underbrace{\mu(1-\frac{q}{Q})x}_{\text{growth}} - \underbrace{(\nu\frac{R}{Q+R}+\delta x)x}_{\text{death}} \\
\frac{d\nu}{dt} &= -d\nu \\
\frac{dQ}{dt} &= \underbrace{\gamma}_{\text{production}}\ \underbrace{(Q_m-Q)}_{\text{diffusion}} - \underbrace{\mu(Q-q)}_{\text{uptake}} \\
\frac{dP}{dt} &= \underbrace{bQ}_{\text{baseline}} + \underbrace{\sigma x Q}_{\text{tumor production}} - \underbrace{\epsilon P}_{\text{clearance}},
\end{aligned}$$

and the two population model,

$$\begin{aligned}
\frac{dx_1}{dt} &= \underbrace{\mu(1-\frac{q_1}{Q})x_1}_{\text{growth}} - \underbrace{(D_1(Q)+\delta_1 x_1)x_1}_{\text{death}} - \underbrace{\lambda(Q)x_1}_{\text{CS to CR}} \\
\frac{dx_2}{dt} &= \underbrace{\mu(1-\frac{q_2}{Q})x_2}_{\text{growth}} - \underbrace{(D_2(Q)+\delta_2 x_2)x_2}_{\text{death}} + \underbrace{\lambda(Q)x_1}_{\text{CS to CR}} \\
\frac{dQ}{dt} &= \underbrace{\gamma}_{\text{production}}\ \underbrace{(Q_m-Q)}_{\text{diffusion}} - \underbrace{\frac{\mu(Q-q_1)x_1+\mu(Q-q_2)x_2}{x_1+x_2}}_{\text{uptake}} \\
\frac{dP}{dt} &= \underbrace{bQ}_{\text{baseline}} + \underbrace{\sigma(Qx_1+Qx_2)}_{\text{tumor production}} - \underbrace{\epsilon P.}_{\text{clearence}}.
\end{aligned}$$

These models aim to keep the strength of Portz *et al.* (2012) model, its biological realism, but making simplifying assumptions to facilitate mathematical analysis and parameter estimation. In this chapter, we compare our results to Hirata *et al.* (2010) since it has been used extensively in the study of intermittent androgen suppression therapy.

In Chapter 3 of this dissertation, we explore the problem of estimating parameters correctly as well as how to make predictions of androgen resistance in a quantifiable manner. First, we study the parameter identifiability of the models presented in Chapter 2. Parameter identifiability deals with the problem of uniquely inferring parameters from data (Eisenberg *et al.* (2013)). Hence, a model that has unidentifiable parameters can yield the predictions under different sets of parameters. For example, a unidentifiable model can predict that, in a patient with androgen resistant prostate cancer, the cancer cell growth parameter can have multiple values. Therefore, it is impossible to map back to the specific parameter values and learn something about individual patients. We demonstrate how the Hirata *et al.* (2010) model, a commonly used model of IAS, fails to be identifiable. Thus, multiple parameter combinations can yield the same conclusions and individual patient insights are not reliable. The figure below depicts the issues when a model is not identifiable. In addition, we use the ensemble Kalman filter for uncertainty quantification. Here we briefly present a overview of the derivation. If error is assumed to be normally distributed with mean 0 and covariance matrix $\mathbf{R}$, we can express the error as a Gaussian random variable.

$$\frac{1}{(2\pi)^{\frac{n}{2}}(R)^{\frac{1}{2}}} exp\left\{-\frac{1}{2}\left[\mathbf{y}_j - \mathbf{H}_j(\mathbf{x}(t_j))\right]^T \mathbf{R}^{-1}\left[\mathbf{y}_j - \mathbf{H}_j(\mathbf{x}(t_j))\right]\right\} \tag{1.1}$$

Then, the Maximum Likelihood Estimate is given by

$$L(\mathbf{x}(t)) = \prod_{j=1}^{n} \frac{1}{(2\pi)^{\frac{n}{2}}(\mathbf{R}_j)^{\frac{1}{2}}} exp\left\{-\frac{1}{2}\left[\mathbf{y}_j - \mathbf{H}_j(\mathbf{x}(t_j))\right]^T \mathbf{R}^{-1}\left[\mathbf{y}_j - \mathbf{H}_j(\mathbf{x}(t_j))\right]\right\} \tag{1.2}$$

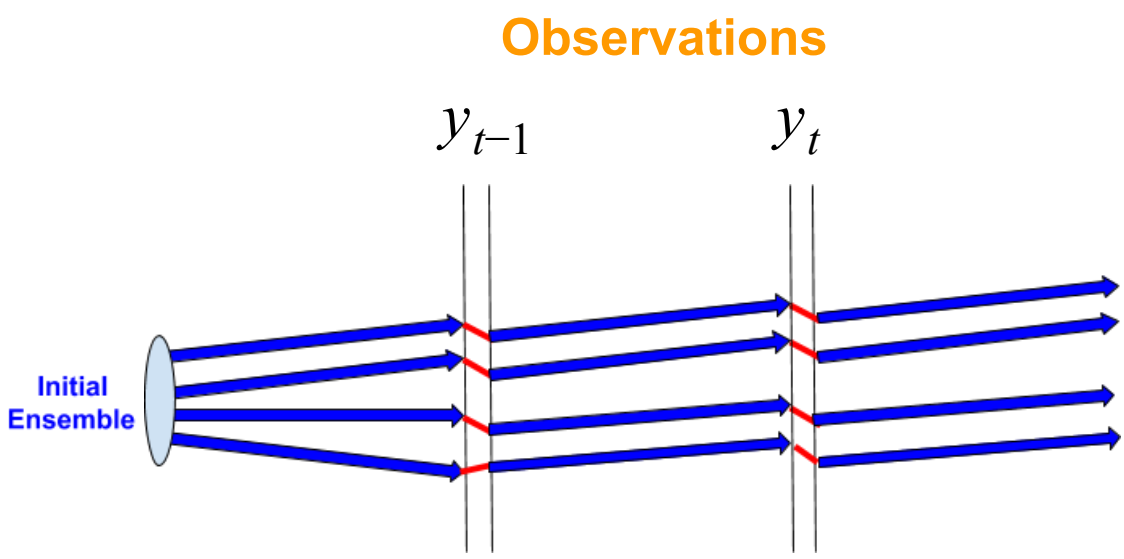

Figure 1.1: Schematic Representation of Kalman Filter Algorithm. First, We Start with an Initial Ensemble of Initial Conditions at Reasonable Time Points. Then Integrate the Model Forward to the First Forecast Time at y_{t-1}. At $t-1$ Observe PSA Levels, and Update the Forecast Ensemble with the Kalman Cost Function $J_{t_n}(\mathbf{x})$.

Then, we can take the log of the likelihood function

$$\log\left(L(\mathbf{x}(t))\right) = -\sum_{j=1}^{n} \frac{1}{2} \left[\mathbf{y}_j - \mathbf{H}_j(\mathbf{x}(t_j))\right]^T \mathbf{R}^{-1} \left[\mathbf{y}_j - \mathbf{H}_j(\mathbf{x}(t_j))\right] + C$$

Thus, the most likely trajectory minimizes the cost function

$$J(\{\mathbf{x}(t)\}) = \sum_{j=1}^{n} \frac{1}{2} \left[\mathbf{y}_j - \mathbf{H}_j(\mathbf{x}(t_j))\right]^T \mathbf{R}^{-1} \left[\mathbf{y}_j - \mathbf{H}_j(\mathbf{x}(t_j))\right]$$

$$J_{t_n}(\mathbf{x}) = \sum_{j=1}^{n} \frac{1}{2} \left[\mathbf{y}_j - \mathbf{H}_j(\mathbf{M}_{t,t_j}(\mathbf{x}))\right]^T \mathbf{R}^{-1} \left[\mathbf{y}_j - \mathbf{H}_j(\mathbf{M}_{t,t_j}(\mathbf{x}))\right]$$

We can express $J(\mathbf{x})$ as

$$\begin{aligned} J_{t_n}(\mathbf{x}) &= \sum_{j=1}^{n-1} \frac{1}{2} \left[\mathbf{y}_j - \mathbf{H}_j(\mathbf{M}_{t,t_j}(\mathbf{x}))\right]^T \mathbf{R}^{-1} \left[\mathbf{y}_j - \mathbf{H}_j(\mathbf{M}_{t,t_j}(\mathbf{x}))\right] \\ &+ \frac{1}{2} \left[\mathbf{y}_n - \mathbf{H}_n(\mathbf{M}_{t,t_n}(\mathbf{x}))\right]^T \mathbf{R}^{-1} \left[\mathbf{y}_n - \mathbf{H}_n(\mathbf{M}_{t,t_n}(\mathbf{x}))\right] \\ &= \left[\mathbf{x}_n - \bar{\mathbf{x}}_n^b\right]^T \left(\mathbf{P}_n^b\right)^{-1} \left[\mathbf{x}_n - \bar{\mathbf{x}}_n^b\right] \\ &+ \left[\mathbf{y}_n - \mathbf{H}_n(\mathbf{M}_{t,t_n}(\mathbf{x}))\right]^T \mathbf{R}^{-1} \left[\mathbf{y}_n - \mathbf{H}_n(\mathbf{M}_{t,t_n}(\mathbf{x}))\right] \\ &= \left[\mathbf{x}_n - \bar{\mathbf{x}}_n^a\right]^T \left(\mathbf{P}_n^a\right)^{-1} \left[\mathbf{x}_n - \bar{\mathbf{x}}_n^a\right] + c \end{aligned}$$

Formally, we want the analysis mean $\bar{\mathbf{x}}^a$ to minimize the Kalman filter cost function $J(\mathbf{x})$ (Hunt *et al.* (2007)):

$$\left[\mathbf{x}_n - \bar{\mathbf{x}}_n^b\right]^T \left(\mathbf{P}_n^b\right)^{-1} \left[\mathbf{x}_n - \bar{\mathbf{x}}_n^b\right] + \left[\mathbf{y}_n - \mathbf{H}_n(\mathbf{M}_{t,t_n}(\mathbf{x}))\right]^T \mathbf{R}^{-1} \left[\mathbf{y}_n - \mathbf{H}_n(\mathbf{M}_{t,t_n}(\mathbf{x}))\right]$$

In Chapter 4, we present a novel model that introduces a time delay in order to fit patient data with greater accuracy and improve its predictive power. We also work with the challenges of a time dependent delay in our system. Here we present a preview of our one population delay mode:

$$\begin{aligned} x' &= \mu \left(1 - \frac{q}{Q(t-\tau)}\right) x(t-\tau) e^{-d_m \tau} - \frac{dR}{R+Q(t)} x(t) - \delta x^2(t) \\ Q' &= \gamma \left(Q_m - Q(t)\right) - \mu \left(1 - \frac{q}{Q(t-\tau)}\right) e^{-d_m \tau} Q(t) \frac{x(t-\tau)}{x(t)} \\ P' &= bQ(t) + \sigma X(t) Q(t) - \epsilon P(t) \end{aligned}$$

In this chapter we demonstrate that the biological accuracy can produce more reliable parameter estimations that yield a Mean Square Error that is superior to the non-delay models presented in Chapter 2. With the inclusion of time delay, we finish our systematic approach to modeling prostate cancer.

Chapter 2

MATHEMATICAL MODELS OF ANDROGEN RESISTANCE IN PROSTATE CANCER PATIENTS UNDER INTERMITTENT ANDROGEN SUPPRESSION THERAPY

2.1 Introduction

Ever since the discovery of androgen dependency of prostate cells, androgen deprivation therapy (ADT) has played a vital role in the treatment of metastatic and locally advanced prostate cancer (Heinlein and Chang (2004); Shafi *et al.* (2013); Tsao *et al.* (2012)). However, controversy remains regarding its best application. Although this treatment will regress tumors in over 90% of patients Bruchovsky *et al.* (2008), after prolonged androgen depletion, patients will eventually develop castration-resistant prostate cancer (CRPC) (Feldman and Feldman (2001)). The development of CRPC can take from a few months to more than ten years (Tsao *et al.* (2012); Hussain *et al.* (2013)), after which there is a very limited number of less effective treatments and patients suffer high mortality (Karantanos *et al.* (2015)). ADT is expensive and side effects include sexual dysfunction, hot flashes, and fatigue (Klotz and Toren (2012)). For these reasons, intermittent androgen suppression (IAS) is implemented to hopefully delay the progression of CRPC and improve quality of life (Bruchovsky *et al.* (2006b)). During off-treatment periods, patients enjoy a "vacation" from the severe side effects of ADT (Klotz and Toren (2012)), and studies have suggested that IAS may not negatively affect the time to progression or survival in comparison to continuous ADT (Gleave (2014)).

Many mathematical models have studied the dynamics of prostate cancer during

ADT (Jackson (2004a); Ideta *et al.* (2008); Portz *et al.* (2012); Hirata *et al.* (2010); Swanson *et al.* (2001); Jain *et al.* (2011); Jain and Friedman (2013a,b)). A detailed review of some of these models are presented in the recent book of Kuang *et al.* (2016). Ideta *et al.* (2008) are pioneers of mathematically describing the dynamics of IAS . Ideta *et al.* (2008) developed a system of ordinary differential equations to study the mechanics of ADT. They considered castrate-resistant (CR) and castrate-sensitive (CS) cell populations as well as androgen levels. Their model included mutations from CS to CR cells, and their focus was on comparing continuous and intermittent therapy and the development of resistance. Hirata *et al.* (2010) considered a three cell populations using a piece-wise linear model to fit clinical prostate-specific antigen (PSA) data. Their model included CS cells that could mutate into CR cells, CR cells that could mutate into CS cells, and CR cells that do not mutate back CS cells. Several investigators using Hirata *et al.* (2010)'s model, have studied estimation of parameters (Guo *et al.* (2013); Tao *et al.* (2013)), optimal switching times and control in IAS (Guo *et al.* (2013); Suzuki *et al.* (2014); Hirata *et al.* (2012a)), and forecasting CRPC progression (Hirata *et al.* (2012b, 2014a)).

Built on the works of Ideta *et al.* (2008) and Jackson (2004b), Portz *et al.* (2012) developed a novel mathematical model to study the dynamics of IAS by using the cell quota model, Droop (1973), from mathematical ecology, which relates growth to an intracellular nutrient, to model the growth of both the CS and CR cell populations. The cell quota was formed as the intracellular androgen concentrations for each cell population. This model fitted clinical PSA data, and androgen data was used implicitly through the cell quota. Everett *et al.* (2014) compared Hirata *et al.* (2010), Ideta *et al.* (2008), and Portz *et al.* (2012) to asses their accuracy of fitting clinical data and predicting future PSA levels. They concluded that while a biologically-based model is important to reveal the underlying processes, a simpler model such as Hirata

et al. (2010) might be practical and useful for predicting future outcomes of individual patients.

In this work, we propose a simplification to PKN Portz *et al.* (2012), a model that is mechanistically driven but simple enough for us to perform systematical mathematical analysis of its dynamics. For simplicity, we shall use serum androgen concentration to approximate intracellular androgen. This is reasonable since androgen passively diffuses through the prostate membrane via concentration gradient Roy and Chatterjee (1995). By assuming an equilibrium concentration of intracellular and serum levels, we use serum levels effectively as the limiting nutrient of the cell growth. This approach is practical for a clinical setting, in which the data collected is applied directly to the model. The mathematical models presented shall fit PSA and androgen levels simultaneously, a novel and very desirable model feature.

2.2 Clinical Trial Data

We use data from Bruchovsky *et al.* (2006a), in our analysis and model calibration. This clinical trial admitted patients who demonstrated a rising serum PSA level after they received radiotherapy and had no evidence of metastasis (Bruchovsky *et al.* (2006a)). Treatment in each cycle consisted of cyproterone acetate for four weeks, followed by a combination of leuprolide acetate and cyproterone acetate, for an average of 36 weeks. If serum PSA is less than $4\frac{\mu g}{L}$ by the end of this period, the androgen suppression therapy is stopped. If patient's serum PSA stays above the threshold, the patient will be taken off the study. After treatment is interrupted, PSA and androgen are monitored every 4 weeks. The therapy is restarted when patient's serum PSA increases to $\geq 10\mu g/L$ (Bruchovsky *et al.* (2006a)). The data set is available at http://www.nicholasbruchovsky.com/clinicalResearch.html. Figure 2.1 shows a typical patient that undergoes IAS.

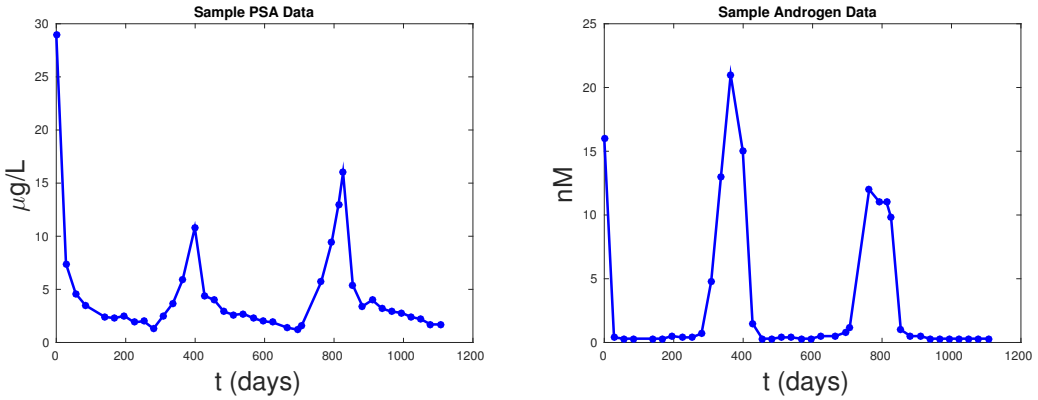

Figure 2.1: Sample Data for PSA and Androgen Data for a Patient in the Clinical Trial.

2.3 Formulation of Mathematical Models

We develop two plausible mathematical models to study the temporal dynamics of prostate cancer progression to CRPR. In Model 1, we use an average tumor model in which cancerous prostate cells are a combination of CS and CR cells. In this model, tumor cells' death rate is a monotonically decreasing exponential function, which we use to model the development of resistance. Then, we propose a two cell population model where we distinguish between CS and CR cells explicitly. To be more biologically relevant, the development of resistance is assumed to be a function of androgen levels in Model 2.

In both models, the cell growth rate is determined by the androgen *cell quota*. Specifically, we model the growth rate by a two parameter function of androgen cell quota,

$$G(Q) = \mu(1 - \frac{q}{Q}), \tag{2.1}$$

where Q is the androgen cell quota. The equation 2.1 is known as Droop equation or growth rate model. It assumes that Q is the concentration of the most limiting resource or nutrient, and q is the minimum level of Q required to prevent cell death

(Droop (1973)).

To be biologically relevant, for both models, we assume that the initial values for all variables are positive. This shall ensure all components of their solutions are positive. Accordingly, we are only interested in studying the stabilities of non-negative steady states.

2.3.1 Model 1: Single Population Model

In the following model, tumor cell volume is denoted by x (mm^3), and we assume that the total volume is a combination of CS and CR cells. Intracellular androgen cell levels are denoted by Q (nM), and PSA levels by P ($\frac{\mu g}{L}$). Droop's equations govern the growth rate of cancer cells (Droop (1973)), where μ represents the maximum cell growth rate and q the minimum concentration of androgen to sustain the tumor. Similar to Everett *et al.* (2014), we assume an androgen-dependent death rate, where R denotes the half saturation level. However, we also assume a time dependent maximum baseline death rate ν, which decreases exponentially at rate d to reflect the cell castration-resistance development due to the decreasing death rate. We also include a density-independent death rate δ that constrains the total volume of cancer cells to be within realistic ranges (Vollmer (2008)).

$$\frac{dx}{dt} = \underbrace{\mu(1-\frac{q}{Q})x}_{\text{growth}} - \underbrace{(\nu\frac{R}{Q+R}+\delta x)x}_{\text{death}} \tag{2.2}$$

$$\frac{d\nu}{dt} = -d\nu \tag{2.3}$$

$$\frac{dQ}{dt} = \underbrace{\gamma}_{\text{production}}\ \underbrace{(Q_m-Q)}_{\text{diffusion}} - \underbrace{\mu(Q-q)}_{\text{uptake}} \tag{2.4}$$

$$\frac{dP}{dt} = \underbrace{bQ}_{\text{baseline}} + \underbrace{\sigma x Q}_{\text{tumor production}} - \underbrace{\epsilon P}_{\text{clearance}} \tag{2.5}$$

where

$$\gamma = \gamma_1 u(t) + \gamma_2 \qquad u(t) = \begin{cases} 1, \text{ on treatment,} \\ 0, \text{ off treatment.} \end{cases}$$

In this model, androgen is assumed to be the most limiting nutrient. We assume that the androgen concentration in cancer cells is approximately the same as the androgen concentration in serum (Roy and Chatterjee (1995)). Parameter γ_1 denotes the constant production of androgen by the testes, and γ_2 denotes the production of androgen by the adrenal gland and kidneys. As over 95% of androgen is produced in the testes we have that $\gamma_1 >> \gamma_2$. Parameter $u(t)$ is a switch between on and off treatment cycles. Since LHRH agonists only stop testes production of androgen during treatment. During treatment, γ_2 will be the only production of androgen. $Q_m > q$ denotes the maximum androgen level in serum. The androgen uptake by prostate cells for growth is denoted by $\mu_m(Q - q)$. PSA is produced by both the regular cells in the prostate at the rate bQ and by the cancer cells at the rate $\sigma x Q$. Notice that we have assumed that cell production of PSA is assumed to be dependent on levels of androgen. Finally, PSA is cleared from serum at rate ϵ.

2.3.2 Model 2: Two Population Model

Now we present a two cell population model. In this model, we explicitly differentiate between CS and CR cells. x_1 (mm^3) and x_2 (mm^3) denote the CS and CR cell populations respectively. The proliferation of each cancer cell population is denoted by

$$G_i(Q) = \mu(1 - \frac{q_i}{Q}), i = 1, 2$$

for x_1 and x_2 respectively. For each respective population at androgen levels below q_i prostate cells do not proliferate. Since CR cell populations proliferate at lower levels

of androgen, we assume that $q_2 < q_1$. Death rates are denoted by:

$$D_i(Q) = d_i \frac{R_i}{Q + R_i}, i = 1, 2,$$

for their respective cell populations. We shall assume that $d_1 > d_2$, as CR cells are less susceptible to apoptosis by androgen deprivation than CS cells. Parameters $\delta_i, i = 1, 2$ denote the density dependent death rates and we use these parameters to keep the maximum tumor volume to biological ranges.

Mutation between cell populations takes the form of a hill equation given by:

$$\underbrace{\lambda(Q) = c\frac{K}{Q + K}}_{\text{CS to CR}}.$$

The CS to CR rate, $\lambda(Q)$, is small for normal androgen levels and high for low concentrations. We assume that when cells are experiencing androgen depletion, they have higher selective pressure to develop resistance. Likewise, in androgen rich environment CS cells are more likely to stay sensitive. IAS started under this assumption, with the intention to delay resistance (Gleave (2014)). c is the maximum rate of mutation between cells and K is the cell concentration for achieving half of the maximum rate of mutation. In this model, d_is are held constant and are not time dependent as the mechanism of the development of resistance is due to mutations from x_1 to x_2 via $\lambda(Q)$ and not by a decreasing androgen dependent death rate.

The increase of intracellular androgen levels by diffusion from the serum level is modeled by $\gamma(Q_m - Q)$. Also, the production of PSA now comes from both x_1 and x_2 cells at rate σ. For simplicity and in contrast to the Portz *et al.* (2012) model and the model in Morken *et al.* (2014) we assume the same PSA production rate for both cell populations.

$$\frac{dx_1}{dt} = \underbrace{\mu(1-\frac{q_1}{Q})x_1}_{\text{growth}} - \underbrace{(D_1(Q)+\delta_1 x_1)x_1}_{\text{death}} - \underbrace{\lambda(Q)x_1}_{\text{CS to CR}} \tag{2.6}$$

$$\frac{dx_2}{dt} = \underbrace{\mu(1-\frac{q_2}{Q})x_2}_{\text{growth}} - \underbrace{(D_2(Q)+\delta_2 x_2)x_2}_{\text{death}} + \underbrace{\lambda(Q)x_1}_{\text{CS to CR}} \tag{2.7}$$

$$\frac{dQ}{dt} = \underbrace{\gamma}_{\text{production}} \underbrace{(Q_m - Q)}_{\text{diffusion}} - \underbrace{\frac{\mu(Q-q_1)x_1 + \mu(Q-q_2)x_2}{x_1+x_2}}_{\text{uptake}} \tag{2.8}$$

$$\frac{dP}{dt} = \underbrace{bQ}_{\text{baseline}} + \underbrace{\sigma(Qx_1+Qx_2)}_{\text{tumor production}} - \underbrace{\epsilon P.}_{\text{clearence}} \tag{2.9}$$

In a biologically realistic situation, one expects that $Q_m > \max\{q_1, q_2\}$.

2.3.3 Derivation of dQ/dt

Now we provide a conservation law based derivation for the cell quota Q equations (2.4), and (2.8). Specifically, we derive (2.4) in details and leave to the readers the straightforward task of its extension to (2.8). Our formulation comes from the conservation of androgen as it moves in and out of the tumor. Let Q_x be the total androgen inside tumor x (mm^3). We assume that Q $(nM)$is uniformly distributed in x, and

$$Q_x = Q(t)x(t) \text{ nmol.}$$

The inflow of androgen to the tumor comes from the serum which can be approximated by

$$\gamma(Q_m - Q(t))x(t).$$

The outflow of androgen from the tumor is due to death which is

$$(\nu\frac{R}{Q+R} + \delta x(t))Q(t)x(t).$$

Then, the rate of change of androgen inside the tumor is:

$$(Q(t)x(t))' = \gamma(Q_m - Q(t))x(t) - (\nu\frac{R}{Q(t)+R} + \delta x(t))Q(t)x(t).$$

However,

$$\begin{aligned}(Q(t)x(t))' &= Q'(t)x(t) + Q(t)x'(t) \\ &= Q'(t)x(t) + \mu(Q(t)-q)x(t) - (\nu\frac{R}{Q(t)+R} + \delta x(t))Q(t)x(t),\end{aligned}$$

which implies that

$$Q'(t) = \gamma(Q_m - Q(t)) - \mu(Q(t)-q).$$

A similar approach can be applied to derive $Q'(t)$ for model 2.

2.3.4 Portz, Kuang, and Nagy (PKN) Model

In this section, we briefly review PKN model. For a more detailed explanation of this model the reader is refereed to Portz *et al.* (2012). PKN model assumes constant death rates for cancer cells (d_1, d_2). CS and CR cells have androgen cell quota Q_1, Q_2 respectively. A denotes the serum androgen concentration which is interpolated and is used in the model.

$$\frac{dx_1}{dt} = \underbrace{\mu_m(1-\frac{q_1}{Q_1})x_1}_{\text{growth}} - \underbrace{d_1x_1}_{\text{death}} - \underbrace{\lambda_1(Q_1)x_1}_{\text{CS to CR}} + \underbrace{\lambda_2(Q_2)x_2}_{\text{CR to CS}} \tag{2.10}$$

$$\frac{dx_2}{dt} = \underbrace{\mu_m(1-\frac{q_2}{Q_2})x_2}_{\text{growth}} - \underbrace{d_2x_2}_{\text{death}} - \underbrace{\lambda_2(Q_2)x_2}_{\text{CR to CS}} + \underbrace{\lambda_1(Q_1)x_1}_{\text{CS to CR}} \tag{2.11}$$

$$\frac{dQ_1}{dt} = \underbrace{v_m\frac{q_m-Q_1}{q_m-q_1}\frac{A}{A+v_h}}_{\text{Androgen influx to CS cells}} - \underbrace{\mu(Q_1-q_1)}_{\text{uptake}} - \underbrace{bQ_1}_{\text{degradation}} \tag{2.12}$$

$$\frac{dQ_2}{dt} = \underbrace{v_m\frac{q_m-Q_2}{q_m-q_2}\frac{A}{A+v_h}}_{\text{Androgen influx to CR cells}} - \underbrace{\mu(Q_2-q_2)}_{\text{uptake}} - \underbrace{bQ_2}_{\text{degradation}} \tag{2.13}$$

$$\frac{dP}{dt} = \underbrace{\sigma_0(x_1+x_2)}_{\text{baseline production}} + \underbrace{\sigma_1x_1\frac{Q_1^m}{Q_1^m+\rho_1^m}}_{\text{tumor production}} + \underbrace{\sigma_2x_2\frac{Q_2^m}{Q_2^m+\rho_2^m}}_{\text{tumor production}} - \underbrace{\delta P.}_{\text{clearence}} \tag{2.14}$$

2.4 Model Dynamics

Now, we study the mathematical properties and dynamics of our two models. For model 1, we shall state the results without providing proofs as they are routine. The detailed mathematical analysis for model 2 will be presented. Proposition 1 summarizes the mathematical dynamics of model 1. Since P is decoupled from the system, we shall refer only to the dynamics of (2.2)-(2.4). This proposition reveals that there is no cure for cancer. Since ADT is non-curative, this property is biologically reasonable.

Proposition 1. Solutions of the system (2.2)-(2.4) are positive and bounded. The system (2.2)-(2.4) has a cancer free steady state $E_0 = (0, 0, \frac{\gamma Q_m+\mu q}{\mu+\gamma})$ that is unstable, a steady state $E_1 = (\frac{\mu\gamma}{\delta}\frac{Q_m-q}{\gamma Q_m+\mu q}, 0, \frac{\gamma Q_m+\mu q}{\mu+\gamma})$ that is globally stable.

Next, we do a thorough mathematical analysis of model 2. First, we study boundedness and positivity of the system. Followed by the number and existence of

steady states. Finally, we analyze the local stability of the steady states. Observe that P is also decoupled from equations $(2.2)-(2.4)$ and we do not include it in the analysis.

Proposition 2. Assume $q_2 \leq q_1 < Q_m$ and $\delta_1 \geq \delta_2$, then solutions of (2.6)-(2.8) with initial conditions $x_1(0) > 0$, $x_2(0) > 0$, and $q_2 \leq Q(0) \leq Q_m$ stay in the region $\{(x_1, x_2, Q) : x_1 \geq 0, x_2 \geq 0, x_1 + x_2 \leq \frac{G_2(Q_m) - D_m(q_2)}{\delta_2}, q_2 \leq Q \leq Q_m\}$. Where $D_m = \min\{D_1(q_2), D_2(q_2)\}$.

Proof. We note that on (2.6), x_1 appears on every term ensuring its positivity. Since x_2 appears on the first two terms of (2.7) and x_1 appears on the last term the positivity of x_2 is also guaranteed.

Since $q_2 \leq q_1 < Q_m$, and

$$Q' = \gamma(Q_m - Q) - \frac{\mu(Q - q_1)x_1 + \mu(Q - q_2)x_2}{x_1 + x_2}$$

We see that $Q'(q_2) > 0$ and $Q'(Q_m) < 0$. It is thus easy to see that $q_2 \leq Q(t) \leq Q_m$ for $t > 0$ with initial conditions $q_2 \leq Q(0) \leq Q_m$.

For boundedness of x_1 and x_2, we let $N = x_1 + x_2$. Since we have that $\delta_1 \geq \delta_2$, and the growth rate $G_i(Q)$, $i = 1, 2$ are increasing functions of Q, we have

$$\begin{aligned} N' &\leq (G_2(Q) - D_m)N - \delta_2 N^2 && (2.15) \\ &\leq (G_2(Q_m) - D_m)N - \delta_2 N^2 && (2.16) \end{aligned}$$

which implies that $\limsup_{t\to\infty} N(t) \leq \dfrac{G_2(Q_m) - D_m}{\delta_2}$. □

Now we study the steady states of model 2. We seek to understand the conditions under which one population will overtake the other, and the circumstances under which they may coexist.

Proposition 3. Assume $q_2 \leq q_1 < Q_m$ and $\delta_1 \geq \delta_2$. The system (2.6)-(2.8) has a CR cell only steady state $E_1 = (0, \frac{G_2(Q^1)-D_2(Q^1)}{\delta_2}, Q^1)$, and a coexistence steady state $E_2 = (\frac{G_1(Q^*)-D_1(Q^*)-\lambda_1(Q^*)}{\delta_1}, x_2^*, Q^*)$, where $Q^1 = \frac{\gamma Q_m + \mu q_2}{\gamma+\mu}$ and $Q^* > Q^1$.

Proof. Let $E = (x_1^*, x_2^*, Q^*)$ be a steady state of the system (2.6)-(2.8). We have two mutually exclusive cases: $x_1^* = 0$ and $x_1^* > 0$.

If $x_1^* = 0$, then we have two possibilities: i) $x_2^* = 0$ or ii) $x_2^* > 0$. In the case of i), we see that $E = E_0$. In the case of ii), we see that $E = E_1$.

If $x_1^* > 0$, we see that $x_2^* > 0$ from the equation of dx_2/dt. In this case $E = E_2$. In addition, we have the following

$$\begin{aligned} 0 &= \gamma(Q_m - Q^*) - \frac{\mu(Q^* - q_1)x_1^* + \mu(Q^* - q_2)x_2^*}{x_1^* + x_2^*} \qquad (2.17) \\ &\geq \gamma(Q_m - Q^*) - \mu(Q^* - q_2) \\ Q^* &\geq \frac{\gamma Q_m + \mu q_2}{\gamma + \mu} = Q^1. \end{aligned}$$

This proves the proposition. □

Proposition 3 demonstrates that if the CS cell population survives, then the CR must also survive. Biologically, this makes sense, as the CR will always receive new mutated CR cells as ADT continues.

Next, we study the extinction of cancer cell populations and stability conditions for each of these steady states when feasible. Observe that we can not linearize at the steady state E_0 since the last term of dQ/dt is not differentiable at E_0. This prevents us from carrying out a routine local stability analysis of E_0.

Proposition 4 below simply confirms the intuition that if both cancer cell populations growth rates are too low, they will die out eventually. For ease of computations in the following propositions, we shall define $S_1(Q) = G_1(Q) - D_1(Q) - \lambda(Q)$ and $S_2(Q) = G_2(Q) - D_2(Q)$.

Proposition 4. Assume that $S_1(Q_m) < 0$, then CS population will die out. If in addition, $S_2(Q_m) < 0$, then both cancer populations will die out.

Proof. Observe that both $S_1(Q)$ and $S_2(Q)$ are strictly increasing with respect to positive values of Q. Since,

$$\frac{x_1'(t)}{x_1(t)} = G_1(Q) - D_1(Q) - \lambda(Q) - \delta_2 x_1.$$

and $S_1(Q_m) < 0$, we know that $G_1(Q) - D_1(Q) - \lambda(Q) \leq S_1(Q_m) < 0$ for any Q. Let $m = -S_1(Q_m)$, and since $x_1(t) > 0$ we have that

$$\begin{aligned} \frac{x_1'(t)}{x_1(t)} &\leq -m \\ x_1(t) &\leq ce^{-mt}. \end{aligned}$$

Therefore $\lim_{t\to\infty} x_1(t) = 0$. Applying a similar but slightly more delicate comparison argument to $x_2(t)$ with $\lim_{t\to\infty} x_1(t) = 0$ yields that $\lim_{t\to\infty} x_2(t) = 0$. This completes the proof of this proposition. □

The following proposition provides a simple set of conditions that yields the biologically realistic final outcome when sensitive cells are overtaken by resistant cells.

Proposition 5. The CR only steady state E_1 is locally asymptotically stable when $S_1(Q^1) < 0$ and $S_2(Q^1) > 0$.

Proof. The Jacobian matrix evaluated at E_1 is given by:

$$J(E_1) = \begin{pmatrix} S_1(Q^1) & 0 & 0 \\ \lambda(Q^1) & -S_2(Q^1) & (\frac{\mu q_2}{Q^2} + \frac{d_2}{(R_2+Q)^2})\frac{G_2(Q^1)-D_2(Q^1)}{\delta_2} \\ \frac{\mu\delta_2(q_1-q_2)}{G_2(Q^1)-D_2(Q^1)} & 0 & -\gamma-\mu \end{pmatrix}.$$

The eigenvalues are the diagonal elements. We see that when $G_1(Q^1) - D_1(Q^1) - \lambda_1(Q^1) < 0$ and $G_2(Q^1) - D_2(Q^1) > 0$, all diagonal elements are negative. Hence E_1 is locally asymptotically stable. □

If both CS and CI cells can proliferate under treatment, then the coexistence equilibrium maybe stable. Figure 2.2, displays the regions when this could happen. If CS cells have a high growth rate μ, they may survive under relatively low levels of androgen. Alternatively, if these cells have a very low death rate d_1, they may persist as well.

Theorem 2.4.1. *Assume that* $A\alpha < \min\{ca+cb+ab, ca+cb+B\beta, ac+\frac{aB\beta+A\lambda(Q^*)\beta}{b}\}$, $S_1(Q^1) > 0$ *and* $S_2(Q^1) > 0$, *then coexistence steady state* E_2 *is locally asymptotically stable.*

Proof. The Jacobian matrix evaluated at E_2 is given by

$$J(E_2) = \begin{pmatrix} S_1(Q^*) - 2\delta_1(x_1^*) & 0 & S_1'(Q^*)x_1^* \\ \lambda(Q^*) & S_2(Q^*) - 2\delta_2 x_2^* & S_2'(Q^*) + \lambda'(Q^*)x_1^* \\ \frac{Q^*x_1^*(G_2(Q^*)-G_1(Q^*))}{(x_1^*+x_2^*)^2} & -\frac{Q^*x_2^*(G_1(Q^*)-G_2(Q^*))}{(x_1^*+x_2^*)^2} & -(\gamma+\mu) \end{pmatrix}.$$

From (2.7) we see that x_2^* is the solution of

$$-\delta_2(x_2^*)^2 + S_2(Q^*)x_2^* + \lambda(Q^*)x_1^* = 0.$$

Thus $x_2^* = \frac{S_2(Q^*)+\sqrt{S_2(Q^*)^2+4\delta_2\lambda(Q^*)x_1^*}}{2\delta_2}$. Evaluate $J(E_2)$ at x_1^* and x_2^*, we obtain

$$J(E_2) = \begin{pmatrix} -S_1(Q^*) & 0 & S_1'(Q^*)x_1^* \\ \lambda_1(Q^*) & -\sqrt{S_2(Q^*)^2 + 4\delta_2\lambda_1(Q^*)x_1^*} & S_2'(Q^*) + \lambda'(Q^*)x_1^* \\ \frac{Q^*x_1^*(G_2(Q^*)-G_1(Q^*))}{(x_1^*+x_2^*)^2} & -\frac{Q^*x_2^*(G_1(Q^*)-G_2(Q^*))}{(x_1^*+x_2^*)^2} & -(\gamma+\mu) \end{pmatrix}.$$

We write it as

$$J(E_2) = \begin{pmatrix} -a & 0 & A \\ \lambda(Q^*) & -b & B \\ \alpha & -\beta & -C \end{pmatrix},$$

where $a = S_1(Q^*)$, $b = \sqrt{S_2(Q^*)^2 + 4\delta_2\lambda(Q^*)x_1^*}$, $C = \gamma + \mu$, $\alpha = \frac{Q^* x_1^* (G_2(Q^*) - G_1(Q^*))}{(x_1^* + x_2^*)^2}$, $\beta = -\frac{Q^* x_2^* (G_1(Q^*) - G_2(Q^*))}{(x_1^* + x_2^*)^2}$, $A = S_1'(Q^*)x_1^*$, $B = S_2'(Q^*)x_2^* + \lambda'(Q^*)x_1^*$. Then, the characteristic polynomial is given by

$$\rho(\phi) = \phi^3 + (a+b+C)\phi^2 + (Ca+Cb+ab-A\alpha+B\beta)\phi + abC + A\lambda(Q^*)\beta - Ab\alpha + aB\beta.$$

Since $Q^* > Q^1$ and a is strictly monotone increasing with respect to Q. Then, $S_1(Q^1) > 0$ which implies $a > 0$. With the same argument we have that $b > 0$. Our biological assumption that $q_1 > q_2$ ensures that $G_1(Q) - G_2(Q) < 0$ for any Q making $\alpha, \beta > 0$. Since $S_1(Q)$ and $S_2(Q)$ are monotonically increasing we also have that $A, B > 0$.

Then,

$$\rho(\phi) = \gamma_3\phi^3 + \gamma_2\phi^2 + \gamma_1\phi + \gamma_0.$$

where $\gamma_3 = 1$,$\gamma_2 = c+a+b$, $\gamma_1 = ca+cb+ab-A\alpha+B\beta$, $\gamma_0 = abc-Ab\alpha+aB\beta+A\lambda(Q^*)\beta$.

Now, we have shown that the individual components of γ_2 are positive.

The condition

$$A\alpha < \min\{ca + cb + ab, ca + cb + B\beta, ac + \frac{aB\beta + A\lambda(Q^*)\beta}{b}\} \tag{2.18}$$

guarantees that $\gamma_1 > 0$ and $\gamma_0 > 0$.

With a few routine algebraic steps, we see that

$$\begin{aligned} \gamma_2\gamma_1 - \gamma_3\gamma_0 &> 0 \\ c(ca + cb - A\alpha + B\beta) + a(ca + cb + ab - A\alpha) + b(ca + cb + ab + B\beta) &> 0 \end{aligned}$$

owing to (2.18). Therefore E_2 is locally asymptotically stable according to the Routh-Hurwitz criterion. □

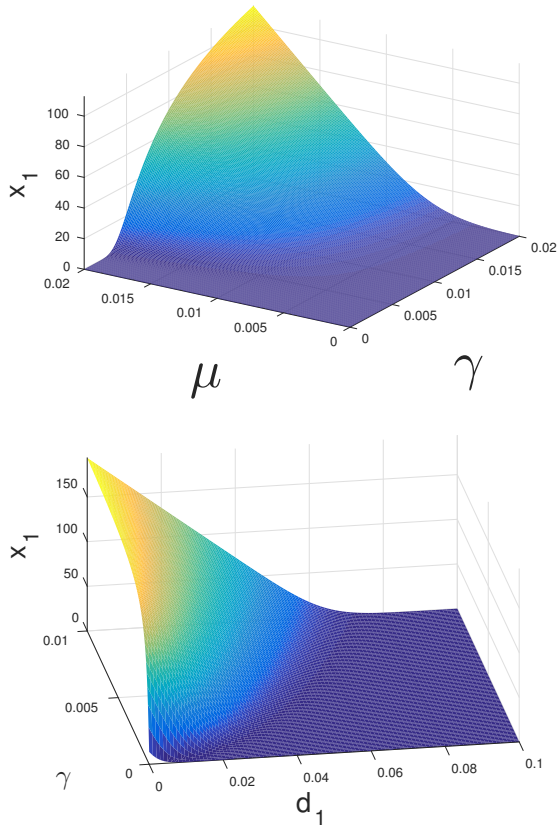

Figure 2.2: Bifurcation Diagram Displaying x_1 Cell Population Vs Parameters μ and γ (Left) and γ and d_1 (Right). This Figure Depicts the Regions in Which x_1 Can Go Extinct. This Happens When Androgen Levels γ Are Very Low, or Cancer Cells' Proliferation Rate μ Is Very Low, or Cancer Cells' Death Rate d_1 Is Very High.

2.5 Parameter Estimation

In order to perform realistic model simulations, we need to obtain reasonable parameter values and their ranges. We start by estimating the realistic ranges for each of them. Parameters $\mu,\ d_1, d_2$ are taken from Berges *et al.* (1995), where they assess the growth and death rates of prostate cells under different concentrations of androgen. In Ideta *et al.* (2008), it was shown that under continuous treatment the fastest resistance rate is $c \approx .0001$. The approximate levels at which sensitive and resistant cells proliferate was studied in Nishiyama (2013), from which we approximated q, q_1,

and q_2.

In patients with no prostate cancer, PSA levels are usually less than $5\frac{\mu g}{L}$, accounting for benign tumor hyperplasia (Klotz and Toren (2012)). This implies that when tumor volume is near zero, the steady state of PSA given by: $\frac{bQ}{\epsilon}$ shall be approximately $5\frac{\mu g}{L}$. Prostate tumor volumes are normally bounded by 80 mm in length and on average they are about 13.4 mm (Vollmer (2008)). Since all our patients have advanced prostate cancer we assumed a maximum length of 40 mm, and we compute the corresponding tumor volume assuming that tumors are spherical. Under complete androgen independence, tumor volume should not exceed 700 (mm^3). Thus, $\frac{\mu}{\delta} \approx \frac{\mu}{\delta_2} + \frac{\mu}{\delta_2} \approx 700$ (mm^3). Parameter Q_m is patient specific, and is taken from the maximum androgen serum concentration of each patient during the first 1.5 cycles of treatment. Parameter γ_1 is held constant among every patient and γ_2 has a range of $0 - .01\frac{nmol}{Lday}$. The half-saturation variables $K, R, R1$, and $R2$ are estimated from Everett *et al.* (2014). Table 4.1 shows definitions, ranges, units, and sources for each of the parameters in our models.

2.6 Comparison of Models

We use data from the Vancouver Prostate Center to validate and compare the accuracy of each model. From the 109 patients registered, 103 were eligible for interruption of treatment, with a PSA response rate of 95% (Bruchovsky *et al.* (2006b)). Using the criteria of having at least 20 data points for both androgen and PSA in the initial 1.5 cycles, we select 62 from those 109 patients. The individual PSA and androgen mean square error (MSE) are provided in Table 4.2 from these 62 selected patients. Notice that PKN model did not include an androgen equation and thus we cannot compare the fittings of androgen with PKN model.

For PKN model, we interpolated androgen serum data using a cubic spline inter-

Table 2.1: Parameter Definitions, Units, and Ranges.

Par.	Definition	Range	Units	Source
μ	Max prolif. rate	.001-.09	day^{-1}	Berges *et al.* (1995)
q	Min cell quota	.1 - .5	nM	Nishiyama (2013)
q_1	Min CS cell quota	.1 - .5	nM	Nishiyama (2013)
q_2	Min CR cell quota	.1 - .3	nM	Nishiyama (2013)
b	Prostate baseline PSA	0.1-2.5	$10^{-3}\ \frac{\mu g}{LnMday}$	Berges *et al.* (1995)
σ	Tumor PSA prod. rate	.001-.9	$\frac{\mu g}{LnMmm^3day}$	Everett *et al.* (2014)
ϵ	PSA clearance rate	.001-.01	day^{-1}	Everett *et al.* (2014)
d	Max cell death rate	.0001-.09	day^{-1}	Berges *et al.* (1995)
d_1	Max CS CDR	.001-.09	day^{-1}	Berges *et al.* (1995)
d_2	Max CR CDR	.0001-.001	day^{-1}	Berges *et al.* (1995)
δ_1	Density death rate	.1-9 10^{-5}	$1/\text{day}/mm^3$	Vollmer (2008)
δ_2	Density death rate	.01-4.5 10^{-4}	$1/\text{day}/mm^3$	Vollmer (2008)
R	CDR half-satur. level	0-3	nM	Everett *et al.* (2014)
R_1	CS CDR half-satur.	0-3	nM	Everett *et al.* (2014)
R_2	CR CDR half-satur.	0-3	nM	Everett *et al.* (2014)
c_1	Max CS to CR rate	$10^{-5} - 10^{-4}$	day^{-1}	Ideta *et al.* (2008)
K	CS to CR half-satur.	0-1	nM	Everett *et al.* (2014)
γ_1	Testes androgen prod.	20	day^{-1}	ad hoc
γ_2	Androgen production	0.001-.01	day^{-1}	ad hoc
Q	Max androgen	15-30	nM	Berges *et al.* (1995)
ν	death rate decay rate	.01	unitless	ad hoc

polation between every androgen data point. That created a function in terms of time that was utilized as A in (2.12) and (2.13). We implemented the method used by Portz *et al.* (2012) for generating future androgen levels, by generating a rectangular function based on the average off and on-treatment serum androgen values. Parameter ranges were taken from Portz *et al.* (2012) and Everett *et al.* (2014), the reader is referred to these papers for more details on forecasting serum PSA levels and parameter values of PKN model. For every patient selected we fitted 1.5 cycles of treatment and performed parameter estimation. Then, to measure the forecasting ability of every model we ran the models for one more cycle of data using the parameters estimated from the initial 1.5 cycles.

Table 2.2: Comparison of MSE for Androgen and PSA for the First 1.5 Cycles.

	PSA			**Androgen**		
	Min	**Mean**	**Max**	**Min**	**Mean**	**Max**
PKN Model	0.5119	9.4463	93.1587	N/A	N/A	N/A
Model 1	0.9735	8.6763	71.8471	5.0351	100.1071	710.2604
Model 2	0.2461	10.3993	137.4345	5.1283	101.4763	710.4412

To compare models, we conduct simulations with MATLAB's built in function fmincon, which uses the Interior Point Algorithm, to find the optimum parameters for each patient. The algorithm searches for a minimum value in a range of pre-specified

Table 2.3: Comparison of Forecast MSE for PSA.

	Min	**Mean**	**Max**
PKN Model	12.234	162.5494	1868.6394
Model 1	11.3935	141.9280	1663.0218
Model 2	2.2727	56.3478	278.4050

parameter ranges, which we estimated from various literature sources. We use this algorithm to minimize the MSE for PSA and androgen data. The MSE is calculated with the following equations

$$P_{error} = \frac{\sum_{i=1}^{N}(P_i - \hat{P}_i)^2}{NP_i},$$

$$Q_{error} = \frac{\sum_{i=1}^{N}(Q_i - \hat{Q}_i)^2}{NQ_i},$$

where N represents the total number of data points, P_i represents the PSA data value, and $\hat{P}_i$ the value from the model. Likewise, Q_i represents the androgen data value, and $\hat{Q}_i$ the value from the model. We then use an equally weighted combination of both errors

$$error = P_{error} + Q_{error},$$

as our objective function which is then minimized with fmincon.

Figure 2.3 shows PSA fitting and forecasting simulations for patients 1, 15, 17, and 63. We selected these patients to display the typical behavior shown in all 62 patients. Patient 1 shows that models 1, 2, and PKN fit data with about the same accuracy. However, PKN overshoots in forecasting and model 2 outperforms model 1 in forecasting. Patient 17 shows that PKN underestimates future PSA levels but model 1 and 2 both perform well. Patients 15 and 63 provide the cases where PKN does a better forecast while models 1 and 2 still do better. The rest of the patients can be classified similarly.

Table 4.2 documents the error of fitting 1.5 cycles of treatment and Table 2.3 displays the errors in forecasting one more cycle of treatment. On average, PKN and model 1 perform prediction at the same level of accuracy. However, model 2 performs prediction on average about three times better than PKN model and model 1.

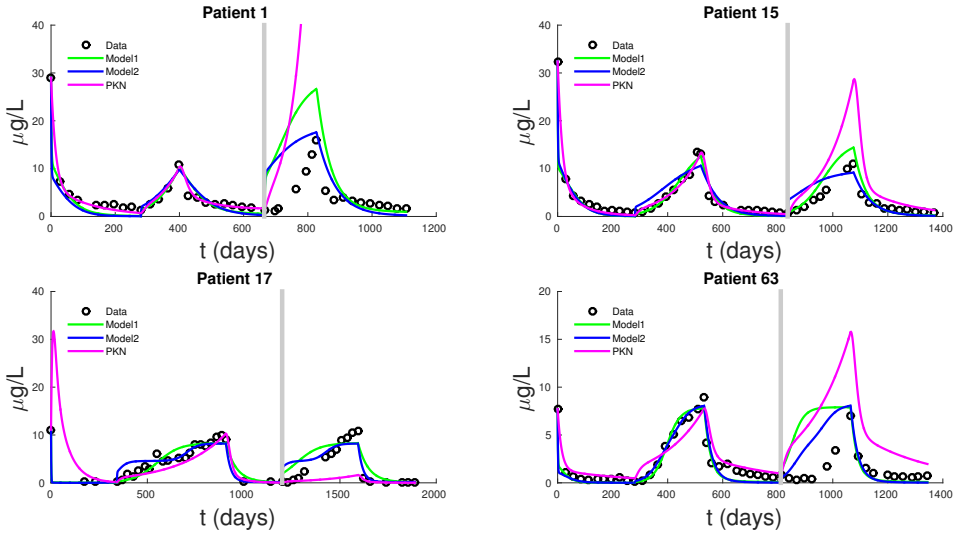

Figure 2.3: Simulations of Fittings for Every Model for 1.5 Cycles of Treatment (Left of Gray Line), and One Cycle of Forecast (Right of Gray Line). For These Four Patients We Can See That Models Fit Data at Comparable Accuracy but Model 2 Perform Much Better in PSA Forecasting.

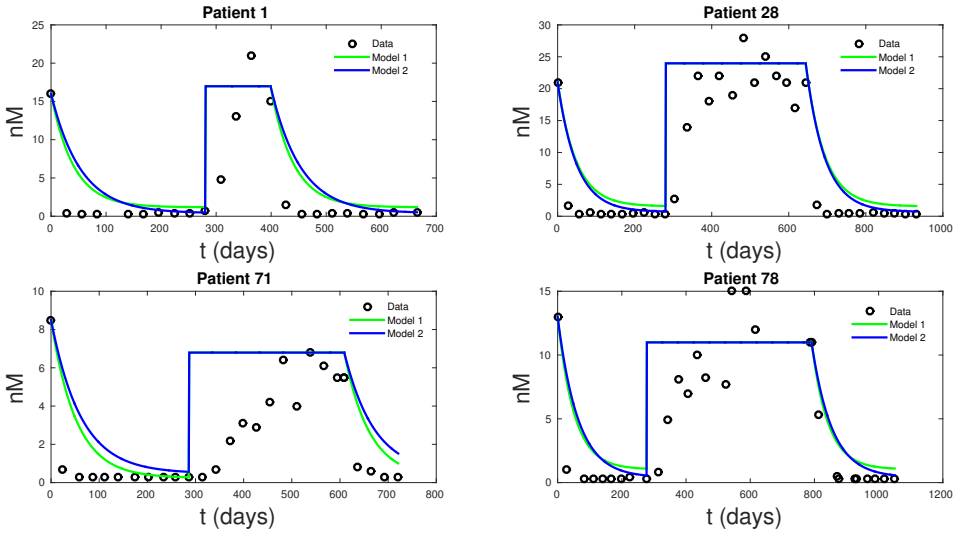

Figure 2.4: Simulations of Fittings of Androgen Levels for Models 1 and 2. These Two Models Have Comparable Goodness in Fitting Androgen Data as Their Derivations Are Very Similar.

2.7 Discussion

The main goal of this research is to produce a model that is simple enough to be used by physicians as a treatment tool and has enough biological mechanisms to capture the individual characteristics of each patient in order to provide personalized accurate forecasts of PSA dynamics. To this end, we presented two models that can accurately fit clinical PSA and androgen data simultaneously. Existing models can only fit the PSA data. While these models are simplifications of PKN, they are just as accurate in data fitting and even better at forecasting future PSA levels. Model 1 had the lowest mean MSE for data fitting of all the models, followed by PKN, and Model 2. Not surprisingly, due to its more biologically realistic model assumptions, Model 2 had the lowest forecast MSE, with PKN doing the worst. The unreliability of PKN's forecasts stems from its dependence on androgen data and hence lacks the ability to predict androgen dynamics. For this reason, the androgen cell quota values which are not directly measurable from data and are a significant source of uncertainty for PKN model. For Models 1 and 2, Q is directly computable from clinical data.

The dynamics of Model 1 is simple and its mathematical analysis is straightforward. While the mathematical analysis of Model 2 is partially tractable, the stability and global stability of the cancer cell coexistence steady state remain unsettled. However, with our bifurcation analysis, we observe that under ADT, x_2 cells may drive x_1 cells to extinction. In Figure 2.2, we see that with lower and realistic levels of androgen production when the patient is under ADT, x_1 cells will eventually become extinct even at higher level of proliferation compares to x_2 cells. Thus, we concluded that under continuous treatment, almost all patient will eventually become androgen resistant. However, it is still not clear if IAS delays the speed at which this occurs. With the models presented in this work, we have moved closer to the ultimate goal of modeling

the androgen resistance of prostate cancer.

Our work is limited by the small number of patients considered. We selected 62 patients that had at least 20 data points in the first 1.5 cycles of treatment. Using a larger time interval and more patients to calibrate models might reveal more subtle differences in the models' ability to fit data. Also, identifiability analysis to determine if our parameter values can be represented uniquely by clinical data is essential if these models are to be used in a clinical setting to reliably and accurately predict PSA dynamics. By allowing parameters to vary as treatment progresses and by studying the changes in key parameter values such as proliferation and death rates as functions of time might be useful to describe and predict resistance mechanisms as suggested in the work of Morken *et al.* (2014).

Chapter 3

ARE MATHEMATICAL MODELS RELIABLE TOOLS FOR PREDICTING ANDROGEN RESISTANCE IN PROSTATE CANCER PATIENTS?

3.1 Introduction

In the 1930s and '40s, Charles Huggins and his co-workers demonstrated that surgical castration usually caused a dramatic regression of prostate cancer; he shared the Nobel Prize in Medicine and Physiology in 1966 for this discovery (Denmeade and Isaacs (2002)). Today, androgen suppression therapy accomplishes the same goal without surgery. However, the therapy is expensive and has many adverse side effects such as sexual dysfunction and dementia (Bruchovsky *et al.* (2006a)).

Continuous androgen suppression therapy is the standard of care of patients with localized advanced prostate cancer after initial radiation treatment fails (Bruchovsky *et al.* (2006a); Nishiyama (2013); Crook *et al.* (2012); Bryce and Antonarakis (2016)). Androgen suppression therapy is expensive, and it has significant adverse side effects. Most patients eventually develop resistance to the treatment, after which the disease becomes more aggressive and prognosis is poor (Feldman and Feldman (2001); Deaths (2011)). Therefore, predicting when resistance will occur in a patient is critical to improving quality of life and avoid futile treatment. Intermittent androgen suppression therapy aims to reduce the side effects and delay the development of resistance by giving patients breaks from treatment, but the extent to which resistance is delayed is the subject of debate; continuous androgen suppression therapy remains the standard of care (Crook *et al.* (2012)).

Differential equation models of tumor dynamics usually contain many parameters

whose values may be difficult to estimate and usually are not measurable directly. Instead, they are estimated indirectly from clinical data. Identifiability analysis is a necessary step in a parameter estimation procedure, because it addresses whether it is possible to recover the model parameters uniquely from a given set of measurements (Eisenberg *et al.* (2013)). Mathematical models that are not identifiable may yield the same output for distinct parameter values (Audoly *et al.* (2001)). Furthermore, It is not possible to quantify the uncertainty in parameters that are unidentifiable.

Clinical trials of androgen suppression therapy typically include measurements of prostate specific antigen (PSA), the bio-maker used by physicians to stop and resume treatment cycles. Testosterone levels in the blood also can be obtained clinically. Testosterone drives the growth of healthy prostate cells and of castration sensitive cancer cells. Measurement of tumor volume such as by computer tomography or magnetic resonance imaging usually are not available. Thus, to quantify the uncertainty in estimates of model parameters, it is necessary to be able to associate unique values of parameters with a limited set of clinical measurements.

Many authors have proposed mathematical models to study the dynamics of prostate cancer during androgen suppression therapy (Jackson (2003); Ideta *et al.* (2008); Portz *et al.* (2012)). A review of some of these models is presented in the recent book of Kuang *et al.* (2016). Hirata *et al.* (2010) consider a three-cell population using a piece-wise linear model to fit clinical PSA data. Several investigators using Hirata *et al.* (2010)'s model have studied estimation of parameters (Guo *et al.* (2013); Tao *et al.* (2013)), optimal switching times and control in intermittent androgen suppression (Guo *et al.* (2013); Hirata *et al.* (2012a)), and forecasting castration resistant prostate cancer progression (Hirata *et al.* (2014b)). Portz *et al.* (2012) included androgen as a limiting nutrient for cancer growth. Many models have been developed based on the frameworks of the PKN model (Morken *et al.* (2014); Everett *et al.* (2014); Baez and

Kuang (2016)). More recently, Baez and Kuang (2016) proposed two simplifications to PKN model in order to have a more tractable model for mathematical analysis. Both models fit clinical PSA data with the same accuracy, and in addition can fit clinical testosterone data simultaneously. Several of these models postulate the existence of a population of castration-sensitive cells, that is, cells that respond to androgen suppression therapy, and a population of castration-insensitive cells that does not. Moreover, cells are assumed to be able to mutate from one type to the other.

In this paper, we review the Hirata *et al.* (2010) model, Portz *et al.* (2012) model, and both models presented in Baez and Kuang (2016). We study the *parameter identifiability* of each model. Since only predictions produced with an identifiable model can be trusted, we focus only on the Baez-Kuang model by Baez and Kuang (2016), the only model that has all of its parameters identifiable. For the Baez-Kuang model we perform uncertainty quantification using an ensemble Kalman filter (Hunt *et al.* (2007). Using an augmented state vector approach, we estimate both the states of the system and parameter values of the model (Moradkhani *et al.* (2005)). Using synthetic data, we compare our augmented state approach for parameter estimation to the widely used Nelder-Mead algorithm implemented in MATLAB. Using clinical data, we estimate parameters and confidence intervals to show that it is possible to estimate correct parameter values and future levels of PSA for individual patients. Then, we diagnose each patient for resistance in the next cycles of therapy.

3.2 Problem Definition

We consider the ordinary differential equation model of the form

$$\frac{d\mathbf{x}}{dt} = F(\mathbf{x}(t), \mathbf{p}) \tag{3.1}$$

$$\mathbf{y}(t) = \mathbf{H}(\mathbf{x}(\mathbf{t}), \mathbf{p}) + \boldsymbol{\epsilon}(\mathbf{t}) \tag{3.2}$$

where $\mathbf{x}(t)$ is an m-dimensional state vector, $\mathbf{p}$ is a n-dimensional vector of parameters, and $\mathbf{H}(\mathbf{x}(\mathbf{t}), \mathbf{p})$ is a mapping from the state space to the set of observables. (In principle, the set of observables may change from one measurement time to another, but in this paper, we assume that the set of available clinical measurements does not change.) The measurement noise $\boldsymbol{\epsilon}(t)$ is assumed to be normally distributed with mean zero and a constant covariance matrix.

The degree of agreement to experimental measurements, $\mathbf{y}(t_i)$, with those predicted by the model, $\mathbf{H}(\mathbf{x}(\mathbf{t}), \mathbf{p})$ is described by an objective function. We use the mean-squared error (MSE), defined as

$$E(\mathbf{x}_0; \mathbf{p}) = \sum_{k=1}^{m} \sum_{i=1}^{N} \frac{\left(H(x_k(t_i), \mathbf{p}) - y_k(t_i)\right)^2}{n}, \tag{3.3}$$

which measures the difference between a model and the data.

Structural identifiability refers to the question of whether the components of $\mathbf{p}$ can be inferred uniquely from a given set of measurements under the assumption that $\epsilon(\mathbf{t}) = \mathbf{0}$ (i.e., in the noise-free case). *Structural identifiability* is a necessary condition for finding solutions to the real data problem that includes noisy measurements (Saccomani and D'Angiò (2009); Audoly *et al.* (2001); Wu *et al.* (2008); Eisenberg *et al.* (2013)). *Structural identifiability* can be approached *globally* or *locally*. *Global identifiability* holds for all possible parameter values, i.e. independently of the actual parameter values, and local identifiability holds around a specific point in the parameter space. We follow the definition of Eisenberg *et al.* (2013) for global structural identifiability of parameters.

Definition 3.2.1. For a given ODE model $\dot{\boldsymbol{x}} = \mathbf{H}(\mathbf{x}(t), \mathbf{p})$ and output $\mathbf{y}(t)$, an individual parameter p is *globally structurally identifiable* if for almost every value p^* and almost all initial conditions, the equation $\mathbf{y}(\mathbf{x}(t), p^*) = \mathbf{y}(\mathbf{x}(t), p)$ implies $p = p^*$.

Achieving global structural identifiability is possible only for simple models (Audoly *et al.* (2001); Quaiser and Monnigmann (2009)). *Global structural identifiability* becomes unfeasible for complex non-linear models. Thus, in this paper, we limit this approach to the only linear model, the Hirata model (3.8-3.9). For more complex models we perform *local structural identifiability*. We describe the details of the method used on Appendix A.

Practical identifiability refers to the question of whether the components of $\mathbf{p}$ can be estimated (with confidence bounds) from noisy measurements using a Kalman filter or other scheme. *Structural identifiability* is necessary for *practical identifiability*. We address the *practical identifiability* of the Baez-Kuang model as is the only model with all *structurally identifiable* parameters. We use synthetic data in section 3.5.2 to estimate confidence intervals for each parameter. Parameters with large confidence intervals indicate practical identifiability problems to determine the correct parameter values.

Fisher Information Matrix Method

For complex systems with many parameters, we can detect any unidentifiable parameter combinations and unobservable parameters using the Fisher Information Matrix (FIM) (Jacquez and Greif (1985); Raue *et al.* (2014)). The FIM has been used as part of methods developed by many researchers to study identifiability (Quaiser and Monnigmann (2009); Miao *et al.* (2011); Eisenberg and A.L. Hayashi (2014); Jacquez and Greif (1985)). The FIM uses the sensitivity of the model outputs at discrete time points t_i, with respect to the parameters. The sensitivity information is stored in the sensitivity matrix S, which is a block matrix that consists of $m \times n$ time dependent

blocks $\beta(t_i)$.

$$S = \begin{pmatrix} \beta(t_1) \\ \beta(t_2) \\ \vdots \\ \beta(t_i) \end{pmatrix}$$

The entries of $\beta(t_i)$ are called sensitivity coefficients. For a parameter $p_j \in \mathbf{p}$, and fixed time t_k, the sensitivity of a state variable $x_i(t) \in \mathbf{x}(t)$ is given by

$$\beta_{ij}(t_k) = \frac{\partial H(x_i(t), \mathbf{p})}{\partial p_j}. \tag{3.4}$$

Using the sensitivity matrix, we compute $FIM = S^T S$, which represents the amount of information contained in the model (Eisenberg and A.L. Hayashi (2014)). The rank of the FIM corresponds to the number of *observable parameters* in $\mathbf{p}$. Observability is a measure for how well internal states of a system can be inferred by knowledge of its external outputs (Wu *et al.* (2008)). A parameter that is not observable by definition cannot be identifiable, but an observable parameter might not be identifiable either. Thus, a rank deficient FIM indicates the presence of unobservable parameters, and a full rank FIM indicates that all parameters are observable. After we determine *parameter observability* we then look for parameter dependencies that might indicate that a pair of parameters that are not distinguishable from each other.

According to the Cramr-Rao theorem, $C = FIM^{-1}$ represents the error covariance matrix of the minimum variance unbiased estimator Rodriguez-Fernandez *et al.* (2006). The correlation matrix (CM) which elements are the approximate correlation coefficients between the i-th and the j-th parameter, is defined by:

$$CM_{ij} = \frac{C_{ij}}{\sqrt{C_{ii} C_{jj}}} \tag{3.5}$$

$$CM_{ij} = 1, i = j \tag{3.6}$$

Locally identifiable parameters will have correlations with all parameters between -1 and 1, but usually non-zero because they are typically not orthogonal (Jacquez and Greif (1985)).

Profile Likelihood Method

The identifiability of a parameter might be determined by the higher order terms ignored in the linearization of the FIM method. Therefore, we apply the identifiability method introduced by Raue *et al.* (2009) known as the profile likelihood (PL) method to check identifiability of parameter pairs using the full system. PL approach determines the identifiability of the model parameters by posing a parameter estimation problem, with perfect data to address structural identifiability or with noisy data to address practical identifiability. The profile likelihood function takes the form

$$L(p_i) = \min_{p_{j\neq i}}(E(x_0; \mathbf{p})) \tag{3.7}$$

which 'profiles' an element p_i of the parameter vector $\mathbf{p}$ by fixing its value across a range of values, and fitting all remaining parameters $p_{j\neq i}$ for each fixed value of p_i, using the likelihood function L as the objective function. The minimum value of the likelihood function for each parameter value constitutes the likelihood profile for the fixed parameter. A parameter is structurally unidentifiable when its likelihood profile is flat across its range. For unidentifiable parameters, the best fit values of the other parameters may indicate the functional form of pairwise parameter dependencies (Raue *et al.* (2009); Eisenberg and A.L. Hayashi (2014)). We call parameter dependencies identifiable parameter combinations, which are combinations of parameters that are not identifiable by themselves but their combination is identifiable. These parameters will appear in the correlation matrix as having either 1 or -1.

3.3 Structural Identifiability of Prostate Models

In this section we present several mathematical models from literature to test their structural identifiability.

3.3.1 Unidentifiability of Hirata Model

First, we study the structural identifiability of the Hirata model (Hirata *et al.* (2012a,b, 2010, 2014b)). This model considered a castration sensitive cell population (x_1), a reversible castration resistant cell population (x_2), and an irreversible castration resistant cell population (x_3), modeled by the following:

$$\frac{d}{dt}\begin{pmatrix} x_1(t) \\ x_2(t) \\ x_3(t) \end{pmatrix} = \begin{pmatrix} w_{1,1}^{on} & 0 & 0 \\ w_{2,1}^{on} & w_{2,2}^{on} & 0 \\ w_{3,1}^{on} & w_{3,2}^{on} & w_{3,3}^{on} \end{pmatrix} \begin{pmatrix} x_1(t) \\ x_2(t) \\ x_3(t) \end{pmatrix} \tag{3.8}$$

for the on-treatment period and

$$\frac{d}{dt}\begin{pmatrix} x_1(t) \\ x_2(t) \\ x_3(t) \end{pmatrix} = \begin{pmatrix} w_{1,1}^{off} & w_{1,2}^{off} & 0 \\ 0 & w_{2,1}^{off} & 0 \\ 0 & 0 & w_{3,3}^{off} \end{pmatrix} \begin{pmatrix} x_1(t) \\ x_2(t) \\ x_3(t) \end{pmatrix} \tag{3.9}$$

for the off-treatment periods. PSA levels P are modeled by

$$P = x_1(t) + x_2(t) + x_3(t). \tag{3.10}$$

This model incorporates three different cancer cell populations and tries to understand the mechanism of resistance by estimating the transition parameters (Hirata *et al.* (2010)). Since this model looks at specific parameters to predict resistance, we need to address whether parameters can be determined from data (*observable*), and if the values determined are unique (*identifiable*). Since this model is piece-wise

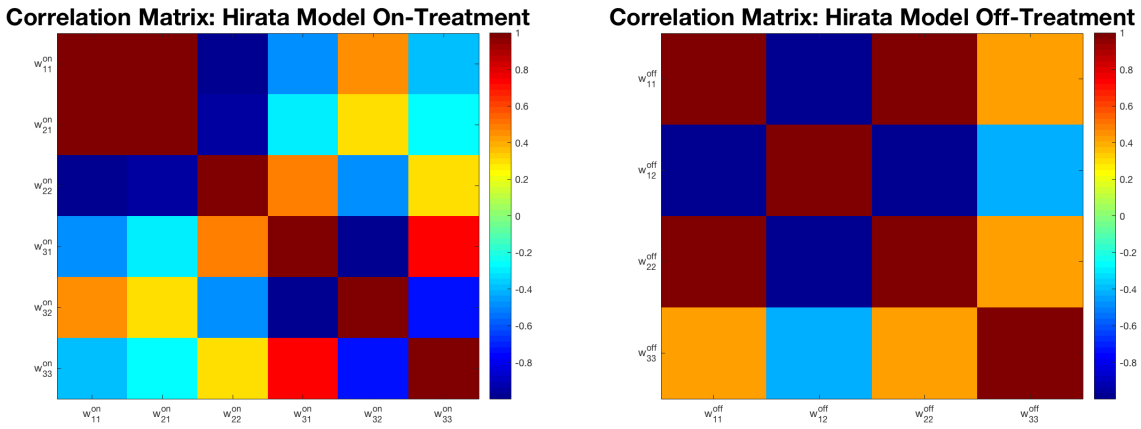

Figure 3.1: Correlation Matrix for Hirata On-treatment and Off-treatment Phases.

linear, we can perform identifiability analysis both globally and locally. The details of global identifiability for the Hirata model are in Appendix B. We separate Hirata model into two models for identifiability purposes, we refer to Hirata on-treatment and off-treatment. We show that the off-treatment Hirata model is not identifiable globally, since it is the simplest case with the least number of parameters. In Appendix B, we see that parameters w_{11}^{off} and w_{22}^{off} are not identifiable from each other globally. Since all parameters appear in the transfer function, all parameters are observable. We see from Figure 3.1, that indeed parameters w_{11}^{off} and w_{22}^{off} have a correlation of exactly 1. Therefore, a change in one of them can be compensated a change in the other without modifying the output. The FIM generated is full rank, agreeing with the transfer function method that all parameters are observable. Now, we can use the profile likelihood method to show the type of functional relationship of these parameters, this is illustrated in Figure 3.2. In this case, we know the global identifiability from the transfer function method. However, in cases where this information is not available we can use the PL method to check if the identifiability of parameters could be obtained by using the full system over a range of values.

Hirata model has been tested and can fit clinical data remarkably well using a

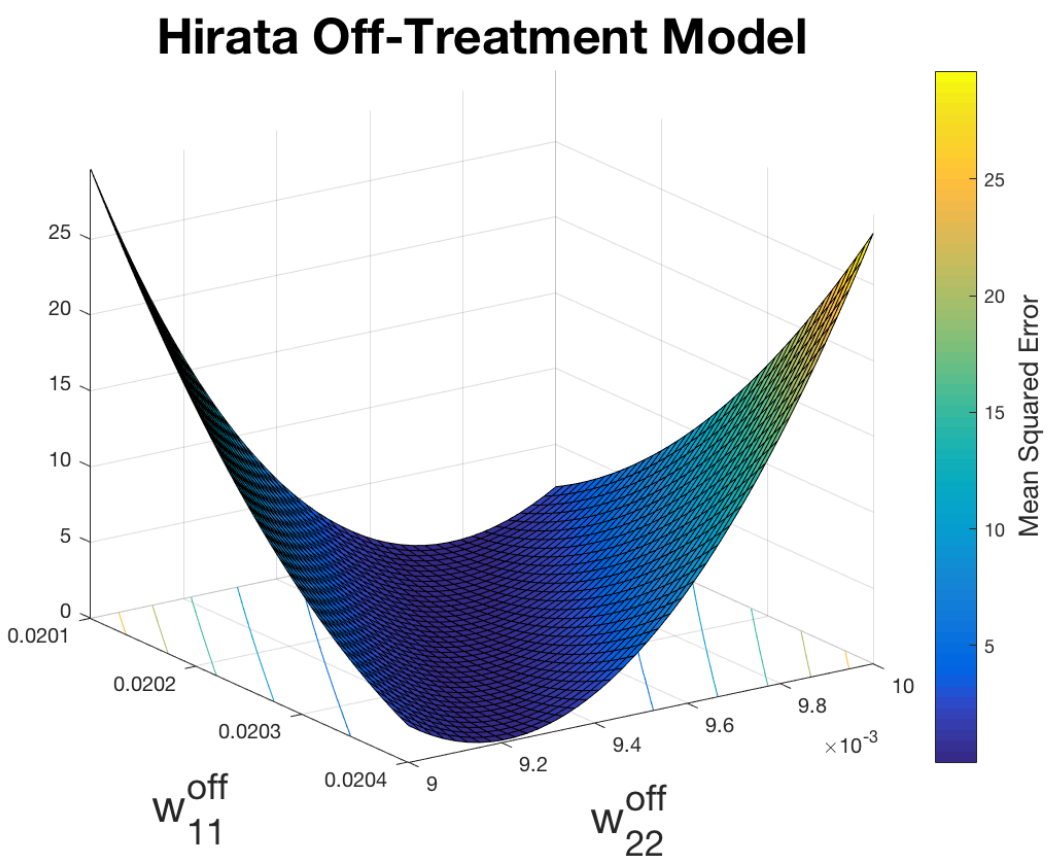

Figure 3.2: Profile Likelihood Function Values (Eq 3.7) for the for Hirata Off-treatment Model (3.9) with Parameters w_{11}^{off} and w_{22}^{off}, Using Eq 3.10 as the Observation Function for PSA.

penalty method. However, since two of its main parameters that the model depends for forecasting cannot be validated as multiple values will produce the same results. We understand that if a model is relatively insensitive to a particular parameter, we can simply fix w_{11}^{off} and extract w_{22}^{off} from the data. However, in Figure 3.6 we see that when we fix w_{11}^{off} we get widely varying outputs for future PSA data while having the same fittings for previous data. Therefore, this model is not reliable to make predictions on future levels of PSA.

3.3.2 *Unidentifiability of PKN Model*

The PKN model assumes constant death rates for cancer cells (d_1, d_2). Castration sensitive,(x_1) and castration resistant cells (x_2), have androgen cell quota Q_1, Q_2 respectively. The function $\lambda_1(Q_1)$ is the transition rate of x_1 cells to x_2 cells and and $\lambda 2(Q_2)$ is the transition from x_2 to x_1. A denotes the serum androgen concentration which is interpolated from the data. PSA is denoted by P. This model only has P as an observable output and A as an observable input. For a more detailed explanation of this model the reader is referred to Portz *et al.* (2012).

$$\frac{dx_1}{dt} = \left(\mu_m\left(1 - \frac{q_1}{Q_1}\right) - d_1 - \lambda_1(Q_1)\right)x_1 + \lambda_2(Q_2)x_2 \tag{3.11}$$

$$\frac{dx_2}{dt} = \left(\mu_m\left(1 - \frac{q_2}{Q_2}\right) - d_2 - \lambda_2(Q_2)\right)x_2 + \lambda_1(Q_1)x_1 \tag{3.12}$$

$$\frac{dQ_1}{dt} = v_m\frac{q_m - Q_1}{q_m - q_1}\frac{A}{A + v_h} - \mu(Q_1 - q_1) - bQ_1 \tag{3.13}$$

$$\frac{dQ_2}{dt} = v_m\frac{q_m - Q_2}{q_m - q_2}\frac{A}{A + v_h} - \mu(Q_2 - q_2) - bQ_2 \tag{3.14}$$

$$\frac{dP}{dt} = \sigma(x_1 + x_2) + \frac{\sigma_1 x_1 Q_1^m}{Q_1^m + \rho_1^m} + \frac{\sigma_2 x_2 Q_2^m}{Q_2^m + \rho_2^m} - \delta P \tag{3.15}$$

Since the PKN model is very complex with many parameters, we perform only *local identifiability* via FIM method. The FIM for this model is rank 17. Since this model has 21 total parameters, at least 4 of them are not observable from data, and thus cannot be identified. The unobservable and unidentifiable parameters are probably due to having only PSA as an observable output. From the correlation matrix in Figure 3.3, we see that there are a total of 8 unidentifiable parameter combinations. That is, pairs of parameters that have correlations 1 or -1. In Figure 3.6, we visualize the effect of the unidentifiability. We fix μ_m at different values and fit all remaining parameters for two cycles of treatment, for the first two cycles we have the exact same

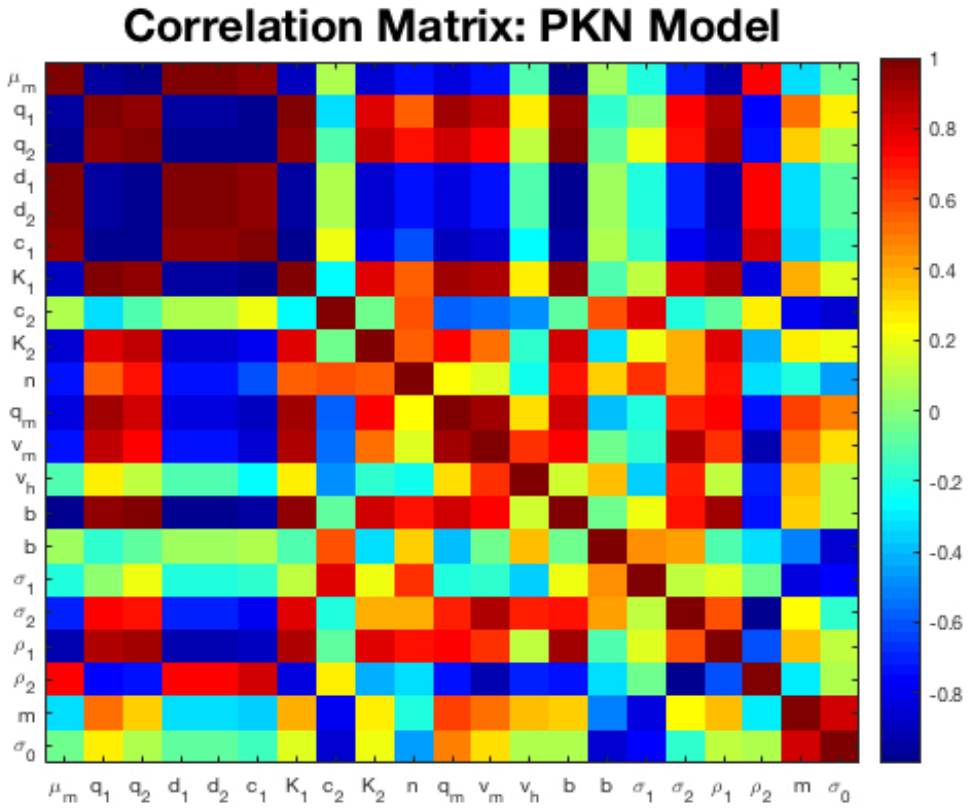

Figure 3.3: Correlation Matrix of PKN Model

fit for each fixed value of μ_m but we get different predictions afterwards. Even thou this model is useful for the understanding of the mechanisms of prostate cancer it is not a reliable model to make predictions on future PSA levels. Everett *et al.* (2014) and Morken *et al.* (2014) have used this model to study predictability of resistance and the pathways that lead to androgen resistance.

3.3.3 Unidentifiability of the Two-Population Model

The two-population model introduced in Baez and Kuang (2016) is a modification of PKN model. The aim is to take advantage of the free diffusion of androgen through the prostate membrane and use the serum androgen levels as the limiting nutrient. The

two-population model (3.16-3.19) explicitly differentiates between castration sensitive and castration resistant cells. x_1 and x_2 denote the castration sensitive and castration resistant cell populations respectively. The proliferation of each cancer cell population is denoted by

$$\mu\left(1-\frac{q_i}{Q}\right), i=1,2$$

for x_1 and x_2 respectively. For each respective population at androgen levels below q_i prostate cells do not proliferate. Since castration resistant cell populations proliferate at lower levels of androgen, it is assumed that $q_2 < q_1$. Death rates are denoted by:

$$d_i\frac{R_i}{Q+R_i}, i=1,2,$$

for their respective cell populations. It is assumed that $d_1 > d_2$, as castration resistant cells are less susceptible to apoptosis by androgen deprivation than castration sensitive cells. Parameters $\delta_i, i=1,2$ denote the density dependent death rates and are used to keep the maximum tumor volume to biological ranges.

Mutation between cell populations takes the form of a hill equation given by:

$$\underbrace{\lambda(Q)=c\frac{K}{Q+K}}_{\text{Castrate Sensitive to Castrate Resistant}} .$$

The castration sensitive to castration resistant rate, $\lambda(Q)$, is small for normal androgen levels and high for low concentrations. It is assumed that when cells are experiencing androgen depletion, they have higher selective pressure to develop resistance. Likewise, in androgen rich environment castration sensitive cells are more likely to stay sensitive. For specific details on the model and parameter definitions, the reader is referred to Baez and Kuang (2016). Similar to Morken *et al.* (2014), we can study this model to understand the mechanisms of resistance but we need to make sure it is identifiable to make accurate predictions.

The FIM for this system has rank 15, the model has a total of 17 parameters, which implies two are unobservable. Figure 3.4, shows that there are a total of 6 parameters pairs that have correlation 1 or -1. These parameter are indistinguishable from each other. Thus, there are at least 6 unidentifiable parameters in the model. We see that taking advantage of the free diffusion through the prostate membrane improves the identifiability of model parameters by reducing the number of *unobservable parameters*. However, due to the inability to observe tumor volume, we still cannot identify the transition rates between the two types of tumor cells. Figure 3.5, shows that parameter c and K have multiple minimum values in the profile likelihood function.

$$\frac{dx_1}{dt} = \left(\mu\left(1 - \frac{q_1}{Q}\right) - d_1\frac{R_1}{Q + R_1} + \delta_1 x_1\right)x_1 - \lambda(Q)x_1 \tag{3.16}$$

$$\frac{dx_2}{dt} = \left(\mu\left(1 - \frac{q_2}{Q}\right) - d_2\frac{R_2}{Q + R_2} + \delta_2 x_2\right)x_2 + \lambda(Q)x_1 \tag{3.17}$$

$$\frac{dQ}{dt} = \gamma(Q_m - Q) - \frac{\mu(Q - q_1)x_1 + \mu(Q - q_2)x_2}{x_1 + x_2} \tag{3.18}$$

$$\frac{dP}{dt} = bA + \sigma(Qx_1 + Qx_2) - \epsilon P \tag{3.19}$$

3.3.4 Identifiability of Baez-Kuang Model

The Baez-Kuang model is the second model introduced in Baez and Kuang (2016), where the mechanism of resistance is simplified and estimated using a monotonically decreasing androgen dependent death rate function. In this model, tumor cell volume is denoted by x, and it is assumed that the total volume is a combination of castration sensitive and castration resistant cells. Intracellular androgen cell levels are denoted by Q,and PSA levels by P. An androgen-dependent death rate is assumed, where R denotes the half saturation level. The time dependent maximum baseline death rate ν, which decreases exponentially at rate d reflects the cell castration-resistance

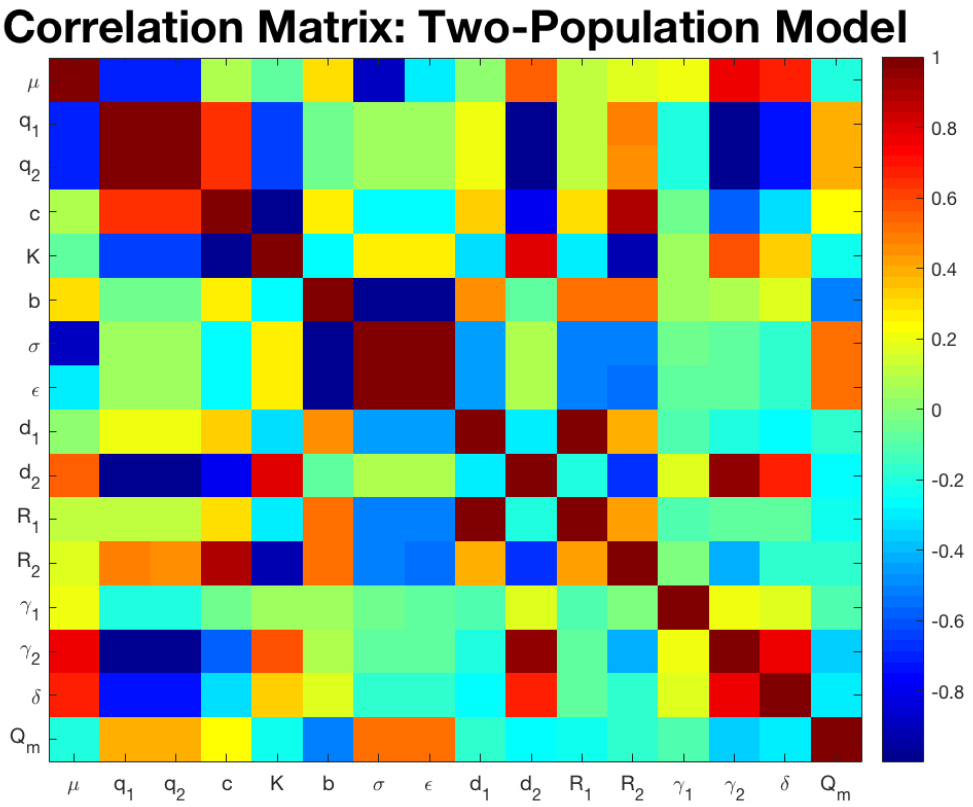

Figure 3.4: Correlation Matrix of the Two-Population Matrix

development due to the decreasing death rate.

$$\frac{dx}{dt} = \underbrace{\mu\left(1-\frac{q}{Q}\right)x}_{\text{growth}} - \underbrace{\left(\nu\frac{R}{Q+R}+\delta x\right)x}_{\text{death}} \tag{3.20}$$

$$\frac{d\nu}{dt} = -d\nu \tag{3.21}$$

$$\frac{dQ}{dt} = \underbrace{\gamma}_{\text{production}}\ \underbrace{(Q_m - Q)}_{\text{diffusion}} - \underbrace{\mu\,(Q-q)}_{\text{uptake}} \tag{3.22}$$

$$\frac{dP}{dt} = \underbrace{bQ}_{\text{baseline}} + \underbrace{\sigma x Q}_{\text{tumor production}} - \underbrace{\epsilon P}_{\text{clearance}} \tag{3.23}$$

We have 11 parameters, and the corresponding FIM is rank 11, which indicates that all parameters are observable with perfect data. Since this model does not have transition of prostate cell types, and the death rate follows a separate dynamic, this model does

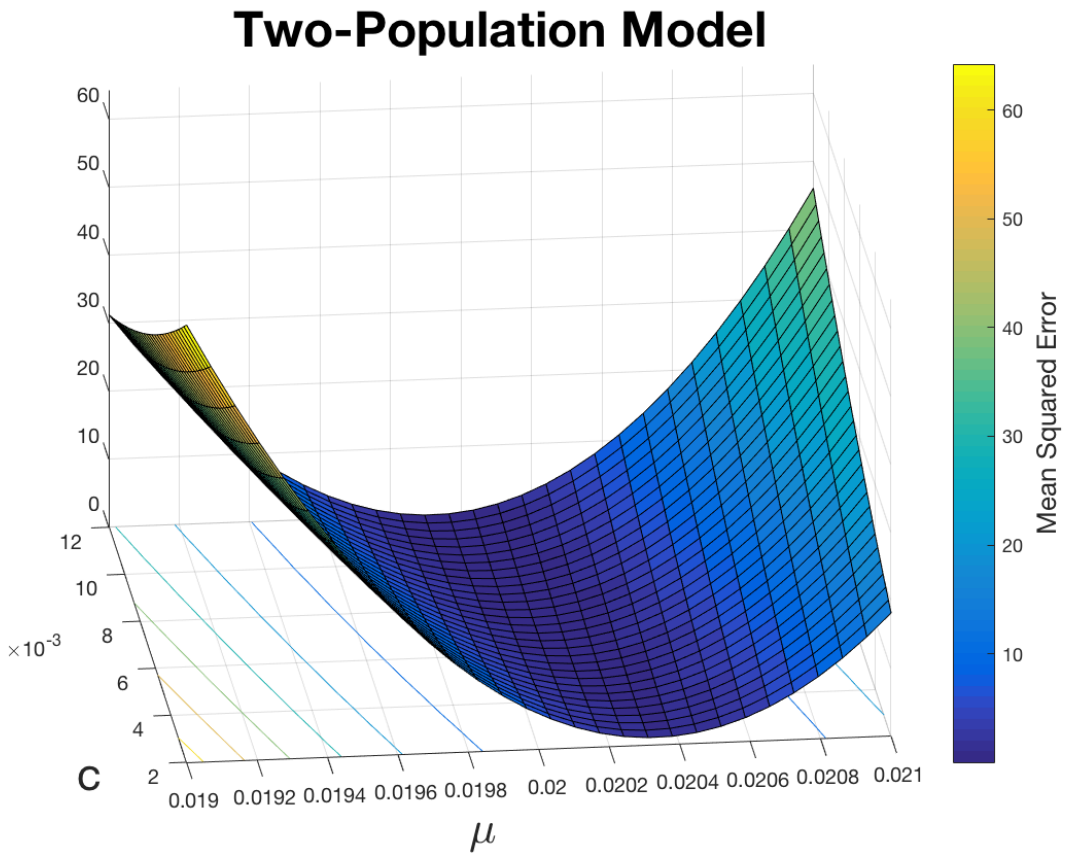

Figure 3.5: Profile Likelihood Function Values (Eq 3.7) for the Two-population Model (3.16-3.19) for Parameters c and μ, Using Psa and Androgen as the Observable Outputs.

not exhibit any dependencies on its parameters. Figure 3.8, shows that there are no parameter correlations in the model that are 1 or -1. We apply the profile likelihood method to see if the full model is identifiable within a given range of values. Figure 3.7 shows a representative example of the profile likelihood of two parameters for the Baez-Kuang Model, the graph of MSE, equation (3.7), has a bounded region where MSE is minimized as a function of parameters μ and c at a single point. Therefore, all parameters in the Baez-Kuang model are identifiable.

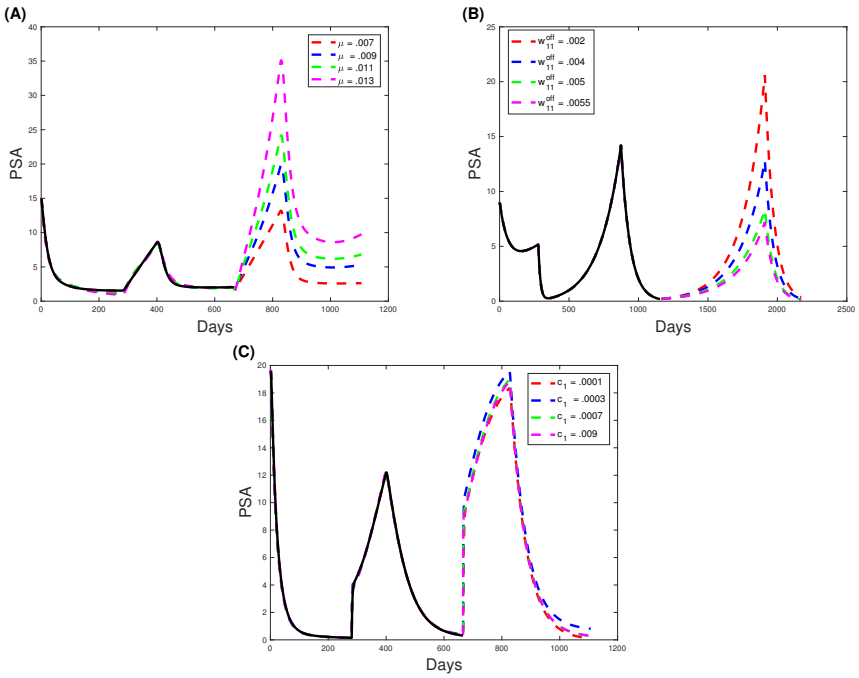

Figure 3.6: The Solid Black Curve in Each Plot Represents the Model Output after Fitting the Parameters Using Matlab's Fminsearch. The Dashed Line Represent Predictions Generated from the Same Parameters as the Solid Line. (A) Pkn Model Equations 3.11-3.15 (B) Hirata Model Equations 3.8-3.9 (C) Two-population Model Equations 3.16-3.19.

3.4 Sensitivity Analysis

Sensitivity analysis is used to understand which parameters play an important role in the model, as well as to determine points in time at which data collection is more beneficial, which are displayed as peaks in the sensitivity function (Banks *et al.* (2007); Gonnet *et al.* (2012)). A way to compare parameter influences on state variables is to use the normalized sensitivities. This approach was briefly presented in Baez and Kuang (2016), which gives a snapshot of the relative parameter sensitivities at a single time point. However, if we want to study the sensitivity over a time interval we need time dependent sensitivities.

Parameter sensitivities' time evolution follows a system of ODEs given by differen-

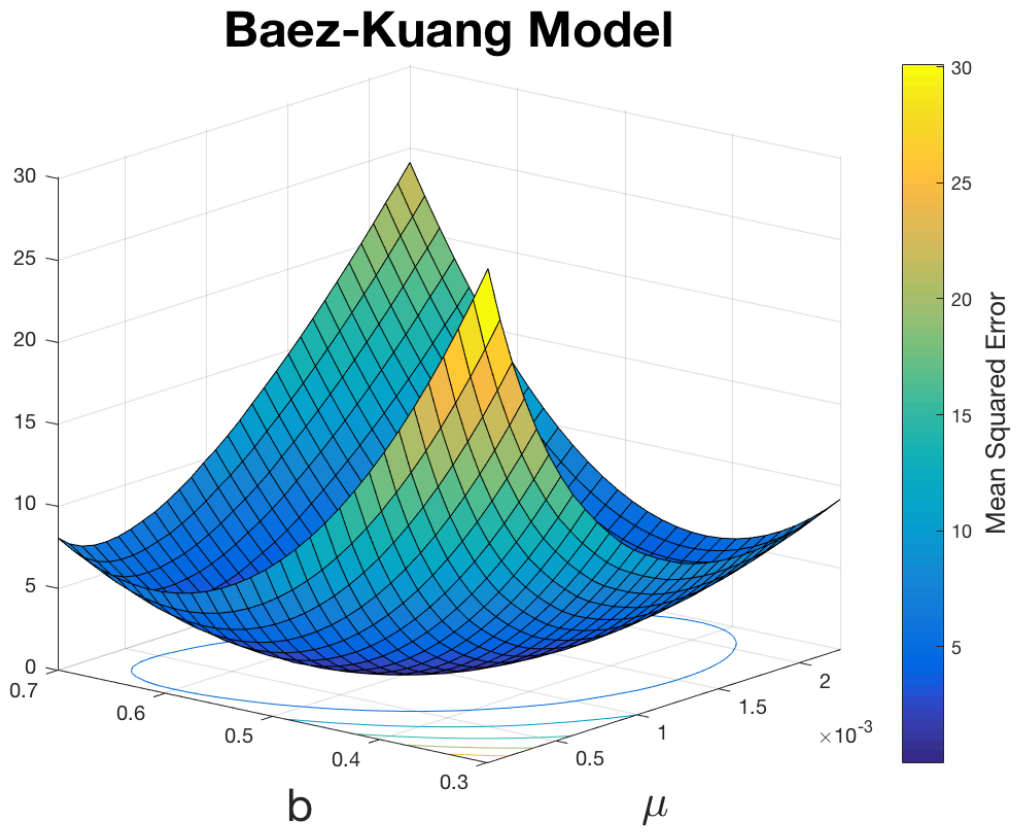

Figure 3.7: Profile Likelihood Function Values (Eq 3.7) for the Baez-Kuang Model (4.1-3.23) for for Maximal Tumor Growth μ and Prostate Baseline PSA Production b, Using PSA and Androgen as the Observable Outputs.

tiating Eq B.1 with respect to t.

$$\dot{s_k}(t, p_k) = \frac{\partial^2 x(t, \mathbf{p})}{\partial p_k \partial t} = J(\mathbf{x}(t), \mathbf{p}) s_k(t, p_k) + \frac{\partial F(t, \mathbf{p})}{\partial p_k}$$

where $J(\mathbf{x}(t), \mathbf{p})$ is the Jacobian matrix of $F(\mathbf{x}(t), \mathbf{p})$ with respect to $\mathbf{x}(t)$. Thus, for a given parameter, the linear tangent model yields a corresponding set of sensitivity equations that we solve with trivial initial conditions (Banks *et al.* (2007); Yue *et al.* (2006)). For the Baez-Kuang model (4.1-3.23), system 3.24 provides an illustrative example of the sensitivity equations with respect to parameter μ.

We solve the original the Baez-Kuang model system of equations (4.1-3.23) for

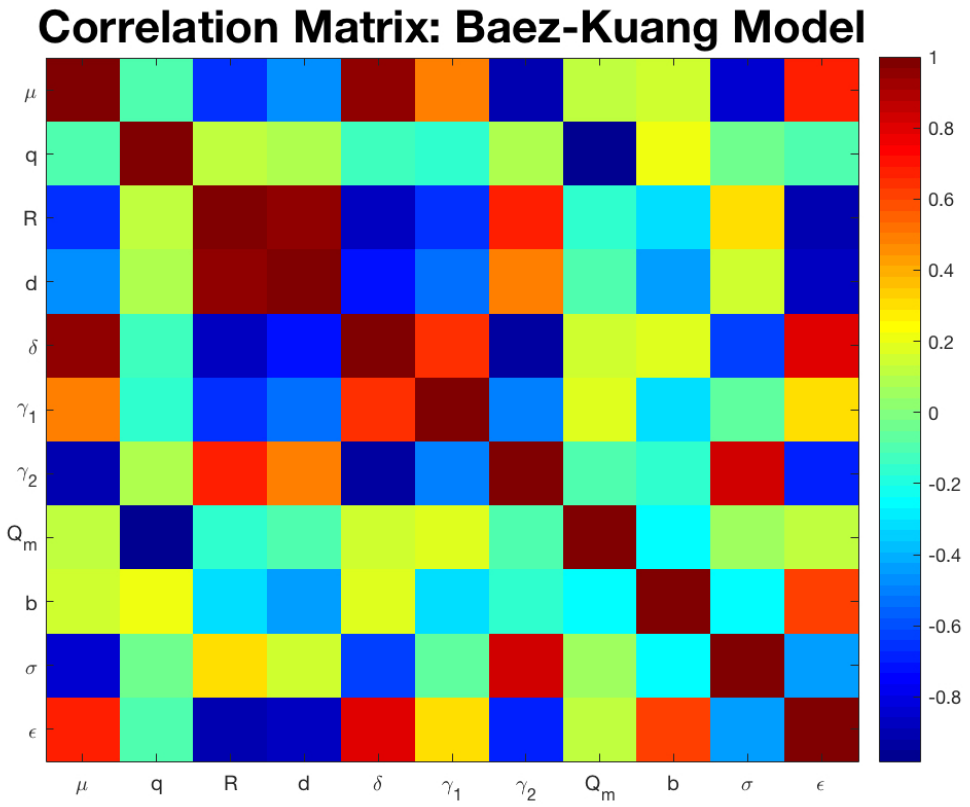

Figure 3.8: Correlation matrix of the Baez-Kuang Model.

specific parameter values. We generate those parameters from a patient by fitting results within the parameter ranges given in Baez and Kuang (2016) using a Nelder-Mead algorithm. Then we solve the non-autonomous linear system of sensitivity equations for parameters μ and d. In Figure 3.9c, we observe a spike in the sensitivity function after the off-treatment phase. Thus, parameter μ holds the most information about PSA in the second cycle of treatment and less during the first treatment cycle. In order to capture the information on the growth rate of cancer cells we need to observe its dynamics when they are not subject to androgen suppression. Figure 3.9f shows that for parameter d, there is a spike in the sensitivity function for cancer cells during the on-treatment phase. Therefore, it is crucial for a parameter estimation problem to have both the initial on-treatment and off-treatment periods so that more

information is captured. Since intermittent androgen suppression has not been shown to be detrimental to patients compared to continuous androgen suppression therapy, we see that from the sensitivity analysis it is favorable to have an intermittent schedule. In order to capture more dynamics from the model which is not be possible during continuous treatment.

$$\dot{S_\mu} = \begin{pmatrix} -c\gamma_1 - \gamma_2 - \mu & 0 & 0 & 0 \\ \frac{\mu q X(t)}{Q(t)^2} + \frac{RV(t)X(t)}{(Q(t)+R)^2} & \mu\left(1 - \frac{q}{Q(t)}\right) - \frac{RV(t)}{Q(t)+R} - 2\delta X(t) & 0 & -\frac{RX(t)}{Q(t)+R} \\ b + \sigma X(t) & \sigma Q(t) & -\epsilon & 0 \\ 0 & 0 & 0 & -d \end{pmatrix} \begin{pmatrix} S_\mu^Q \\ S_\mu^x \\ S_\mu^P \\ S_\mu^V \end{pmatrix} + \begin{pmatrix} -(Q(t) - q) \\ \left(1 - \frac{q}{Q(t)}\right) X(t) \\ 0 \\ 0 \end{pmatrix} \tag{3.24}$$

3.5 Baez-Kuang model Data Assimilations

3.5.1 Data Used

We use data from the Vancouver Prostate Center to validate and compare the accuracy of each model. From the 109 patients registered, 103 were eligible for interruption of treatment, with a PSA response rate of 95% (Bruchovsky *et al.* (2006a)). From the 103 patients we select a subset of 38, using the criteria of having at least 20 data points for both androgen and PSA in the initial 1.5 cycles. Also, patients did not exhibit resistance in the first 2 complete cycles of treatment. We shall compare the data assimilation approach for parameter estimation to the method used in Baez and Kuang to address the effectiveness of this technique.

3.5.2 Parameter Estimation

There is a straight forward theory for the estimation of parameters Jazwinski (2007); Carrassi and Vannitsem (2011); Yang and Delsole (2009); Lahoz *et al.* (2010); Baek *et al.* (2006); Moradkhani *et al.* (2005) using the augmented state space approach. We define, the augmented state vector x^* with dimension $m + n$ as

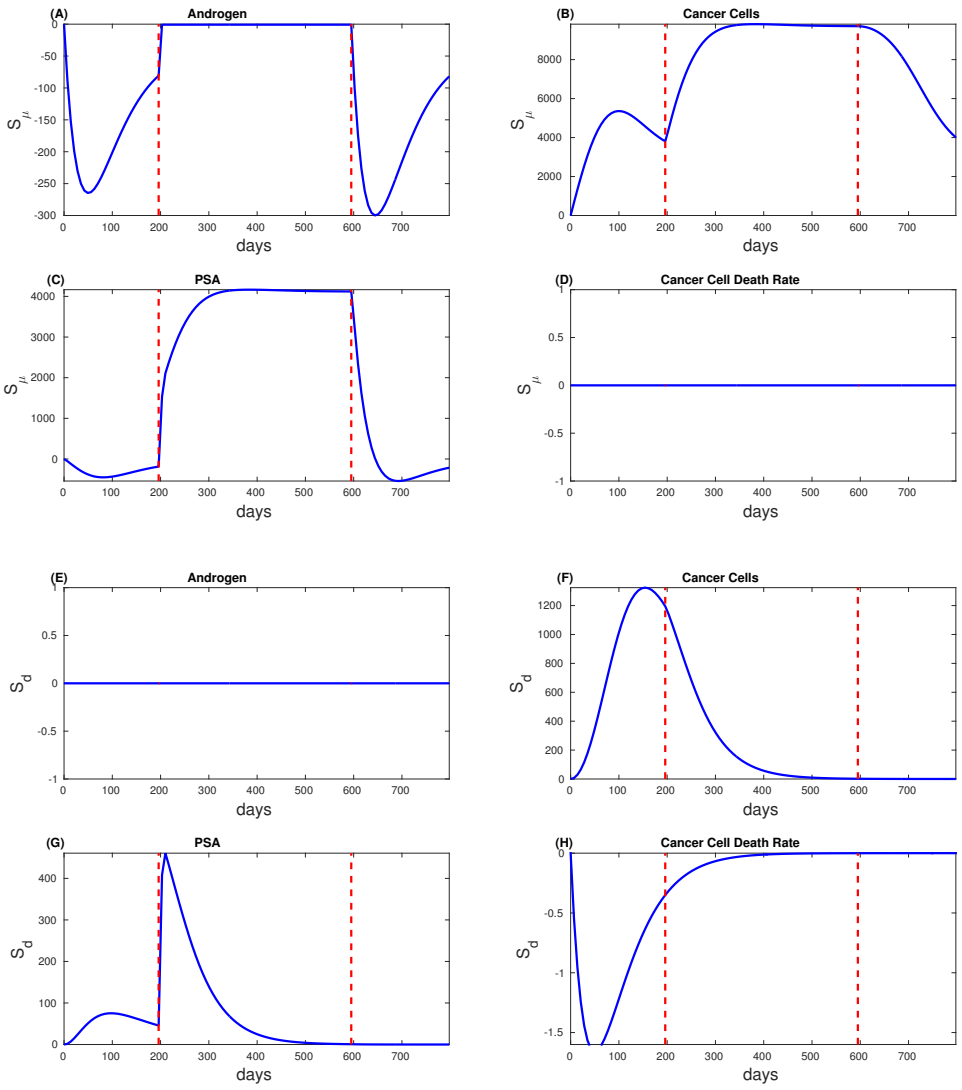

Figure 3.9: The Parameter Sensitivities, s_μ, of Each Component of the Baez-kuang Model (4.1-3.23), as a Function of Time. (A)-(D)Functions of Each Model Component with Respect to the Rate μ. (E)-(H) Similarly, but for the Cell Death Component d.

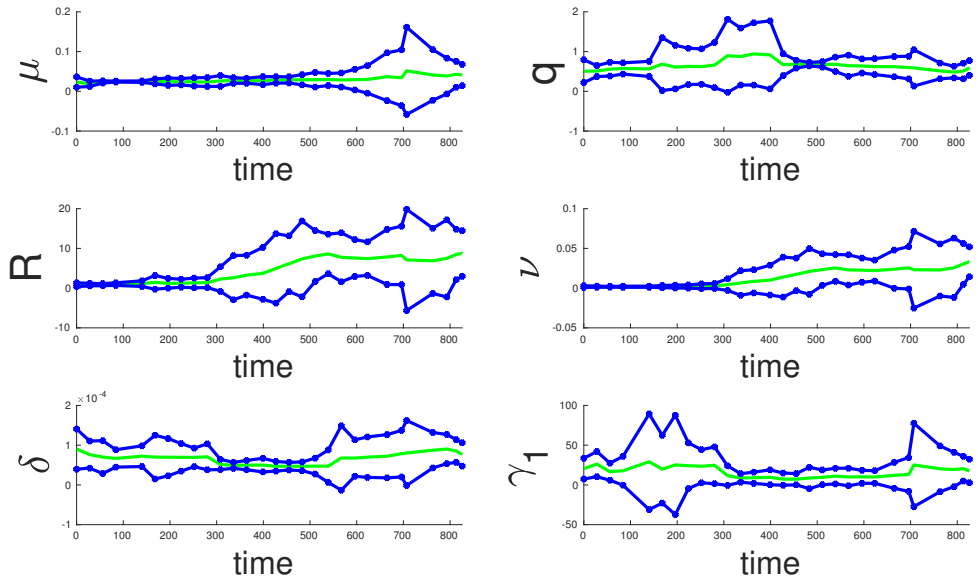

Figure 3.10: Blue Lines Denote the Maximum and Minimum Values. The Green Line Denotes the Most Likely Value.

$$\mathbf{x}^* = \begin{bmatrix} \mathbf{x} \\ \mathbf{p} \end{bmatrix}.$$

Because model parameters are not observed, the observation operator for the augmented model is

$$\mathbf{H}^* = \begin{bmatrix} \mathbf{H} \\ 0 \end{bmatrix},$$

where 0 is a n by m zero matrix. Then, an ensemble Kalman Filter to this new augmented system. For an overview of the details of the ensemble Kalman Filter the reader is referred to Hunt *et al.* (2007). Figure (3.10) shows how we estimate the parameters over time and keep track of the ranges as a confidence interval.

Synthetic Data

We generate synthetic data for the Baez-Kuang model using parameters in the ranges given in Baez and Kuang (2016) at various noise levels. Thus, we are testing how the model fits data when the only source of error comes from the data measurement. In a sequel paper, the authors shall address the problem of model bias, but for this work we only address measurement error. We run 100 simulations at %5 and %20 noise, and estimate parameters using the augmented state approach and also using MATLAB's built in function fminsearch. We see that for low levels of noise, %5, fminsearch can approximate parameters better than the augmented state approach. We believe that when noise is so low simply finding the best fit is sufficient. However, for higher levels of noise, the augmented space produces a tighter and more accurate range of values. Figure 3.12 shows the distributions of parameter μ for %5 and %20 percent noise. We use μ and d since Baez and Kuang (2016) show that those parameters are the most sensitive in the system. The results of parameter estimates is summarized in Table 3.1 for fminsearch method and in Table 3.2 for the augmented state method. We see that we have small standard deviations for our estimated parameter values.

Clinical Data

The goal of our modeling of prostate cancer under androgen suppression is to predict androgen resistance. In order to accomplish this goal we must use real clinical data. Using our subset of 38 patients we perform parameter estimations with the augmented state approach for 1.5 cycles and 2 cycles of treatment. Based on our results with synthetic data, the augmented state approach is more suitable to estimate parameters at higher noise levels. Since PSA data has error closer to %20, we use the augmented state approach. After estimation, we use the ensemble of parameter values to predict

the future levels of PSA.

Par.	**Min**	**Mean**	**Max**	**Abs. Error**	**Rel. Error**
μ	1.712×10^{-2}	2.094×10^{-2}	2.881×10^{-2}	9.365×10^{-4}	4.682×10^{-2}
q	2.646×10^{-5}	3.717×10^{-1}	.9	.1283	.2567
R	.0123	4.557×10^{-1}	.8	4.432×10^{-2}	8.864×10^{-2}
d	1.199×10^{-8}	2.351×10^{-2}	8.999×10^{-2}	3.508×10^{-3}	.1754
δ	7.02×10^{-5}	9.706×10^{-5}	2.999×10^{-4}	2.941×10^{-6}	2.941×10^{-2}
γ_1	15.01	18.93	25.00	1.073	5.364×10^{-2}
γ_2	5.001×10^{-6}	1.310×10^{-3}	2.959×10^{-2}	3.103×10^{-4}	.3103
Q_m	12.36	16.92	21.41	7.683×10^{-2}	4.519×10^{-3}
b	.2019	5.464×10^{-1}	.9000	4.636×10^{-2}	9.273×10^{-2}
σ	4.073×10^{-4}	1.288×10^{-2}	2.846×10^{-2}	7.121×10^{-3}	.3561
ϵ	.1455	5.783×10^{-1}	1.032	.2217	.2771

Table 3.1: Table Fminsearch Parameters at %20 Noise.

3.6 Conclusion

In this work, we proposed an alternative approach to the estimation of parameters and proposed a method for making predictions. With our approach, we are able to have a measure of uncertainty and also fit data to the same accuracy than the standard Nelder-Mead algorithm in MATLAB using synthetic data. Table 3.1 shows the parameter ranges and mean values for the parameters estimated using the Fminsearch algorithm and Table 3.2 shows how the results for the ensemble Kalman filter approach. There were a total of 9 patients that developed resistance after the fifth cycle of treatment. Forecasting one cycle of data resulted in the prediction of 4 patients with

Par.	**Min**	**Mean**	**Max**	**Abs. Error**	**Rel. Error**
μ	1.985×10^{-2}	2.213×10^{-2}	2.730×10^{-2}	2.096×10^{-3}	.1048
q	1.057	1.883	2.349	1.393	2.786
R	.5411	1.871	3.199	1.371	2.743
d	.1825	.3372	.4774	.3188	1.594
δ	1.243×10^{-4}	1.326×10^{-4}	1.533×10^{-4}	3.261×10^{-5}	.3261
γ_1	3.840	4.796	6.090	15.20	.7602
γ_2	5.508×10^{-6}	2.072×10^{-4}	9.063×10^{-4}	8.273×10^{-4}	.8273
Q_m	17.61	17.91	18.89	.8991	5.289×10^{-2}
b	2.845	3.471	4.276	2.954	5.909
σ_1	7.489×10^{-2}	8.299×10^{-2}	9.287×10^{-2}	6.281×10^{-2}	3.141
ϵ	2.813	3.049	3.367	2.243	2.804

Table 3.2: Table Kalman Filter Parameters at %20 Noise

resistance and one with false positive resistance. Predicting two cycles resulted in predicting correctly 3 patients with resistance and no false positives. That is a 100 perfect accuracy in predicting non resistance for the two cycle prediction and 97 percent for the one cycle prediction. In Figure 3.11 we summarize the different cases of forecasts, and Table 3.3 gives the details for the forecast for every patient. We see that when forecasting a single cycle of treatment we produced a single false positive and we were successful in predicting %44 of the resistant cases. Since we did not produce a single false positive when using less data we can infer that we have some model bias that needs to be address, however, we have high accuracy when predicting non resistance in both cases. Our model bias could be in the growth/death rate of cancer cells and we might be underestimating their actual size. This work is the first step in producing a more reliable mathematical framework for use in a clinical setting

		One Cycle Predicted				Two Cycles Predicted			
	Patient	Ensemble MSE			Resistance	Ensemble MSE			Resistance
P#	Resistant?	Min	Mean	Max	Predicted?	Min	Mean	Max	Predicted?
1	NO	5.39	5.719	6.245	NO	8.83	12.30	32.33	NO
6	NO	14.1	24.15	41.32	NO	30.1	32.24	36.34	NO
14	NO	17.7	17.74	17.82	NO	27.4	36.07	42.3	NO
15	NO	.797	1.239	2.536	NO	3.50	9.174	17.12	NO
17	NO	17.2	51.16	85.74	NO	4.15	17.03	238.9	NO
19	YES	10.6	46.63	114.7	YES	13.9	18.72	24.58	NO
24	NO	9.96	11.37	13.2	NO	8.71	12.87	18.04	NO
25	NO	38.3	50.07	60.38	NO	48.7	58.58	67.63	NO
28	NO	46.8	57.55	75.93	NO	14.02	25.39	39.68	NO
29	NO	7.93	9.453	12.29	NO	33.2	33.78	34.60	NO
30	NO	1.60	3.419	5.609	NO	24.8	30.06	35.42	NO
32	NO	6.48	7.171	8.667	NO	4.55	5.169	6.783	NO
36	YES	.604	.6765	1.481	YES	44.3	117.1	304.7	YES
37	NO	1.80	3.374	6.277	NO	14.3	247.9	5021.2	NO
39	NO	4.40	5.836	7.891	NO	7.79	11.58	19.37	NO
44	NO	29.2	32.14	36.18	NO	23.6	28.23	32.86	NO
51	NO	7.77	33.9	111.8	NO	18.4	20.1	22.93	NO
52	YES	11.2	15.34	19.63	NO	45.2	54.42	84.28	NO
54	YES	122.1	130.9	141.2	NO	467.2	498.2	546.2	NO
55	NO	7.09	8.310	10.20	NO	10.7	11.49	12.57	NO
58	NO	11.2	19.32	28.89	NO	6.86	7.952	10.28	NO
60	NO	32.02	48.09	77.21	NO	75.3	88.24	107.1	NO
62	NO	25.7	51.94	192.3	YES	29.0	90.82	218.9	NO
63	NO	2.67	2.917	6.481	NO	3.81	8.688	13.31	NO
64	YES	19e3	21e3	23e3	YES	8e+03	8e+03	8e+03	YES
66	NO	23.5	29.58	37.07	NO	24.1	28.28	32.67	NO
75	NO	4.38	7.128	24.78	NO	6.03	6.685	8.846	NO
77	NO	34.4	34.79	35.26	NO	25.1	28.31	40.10	NO
79	NO	7.08	7.782	8.831	NO	7.13	9.517	13.76	NO
83	YES	39.4	42.48	47.70	NO	30.9	37.52	53.83	NO
87	NO	12.8	13.10	14.01	NO	17.6	21.78	33.38	NO
88	YES	8.08	10.07	12.67	NO	8.26	10.00	15.85	NO
91	NO	3.55	3.696	3.887	NO	3.81	4.389	5.195	NO
93	NO	7.55	8.540	9.593	NO	23.4	26.33	30.94	NO
100	NO	8.93	12.14	29.80	NO	12.6	17.85	19.78	NO
101	YES	4.75	5.306	6.418	NO	7.23	8.524	11.79	NO
102	NO	20.91	21.26	21.63	NO	19.3	21.49	23.73	NO
105	YES	5.73	28.60	172.9	YES	622.1	2e+03	4e+03	YES

Table 3.3: Table of Patient Statistics. A Patient Is Resistant If PSA Does Not Fall below 4 $\frac{Ng}{L}$ on Treatment.

and in future work we shall address the problems of model bias to see if the percentage of resistance predicted improves.

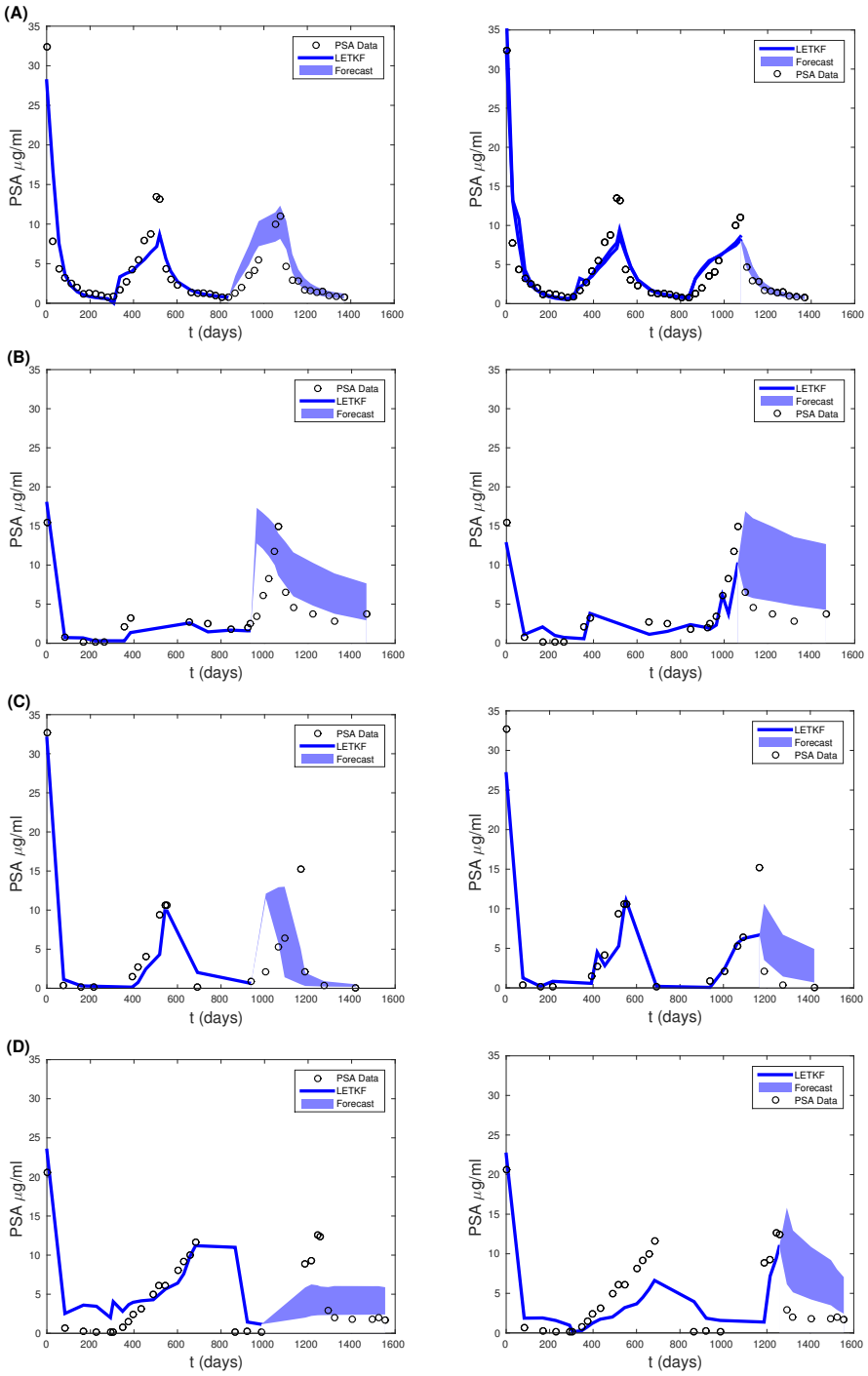

Figure 3.11: Ensemble Forecasts of Psa Levels on Four Representative Patients. Using the Baez-Kuang Model Eqs (4.1-3.23). Panel (a)-(D) on the Left Show Predictions of PSA Values Immediately Following Cessation of Treatment after the Second Cycle and on the Right Show Forecast of PSA Levels Immediately after the Third Cycle of Treatment.

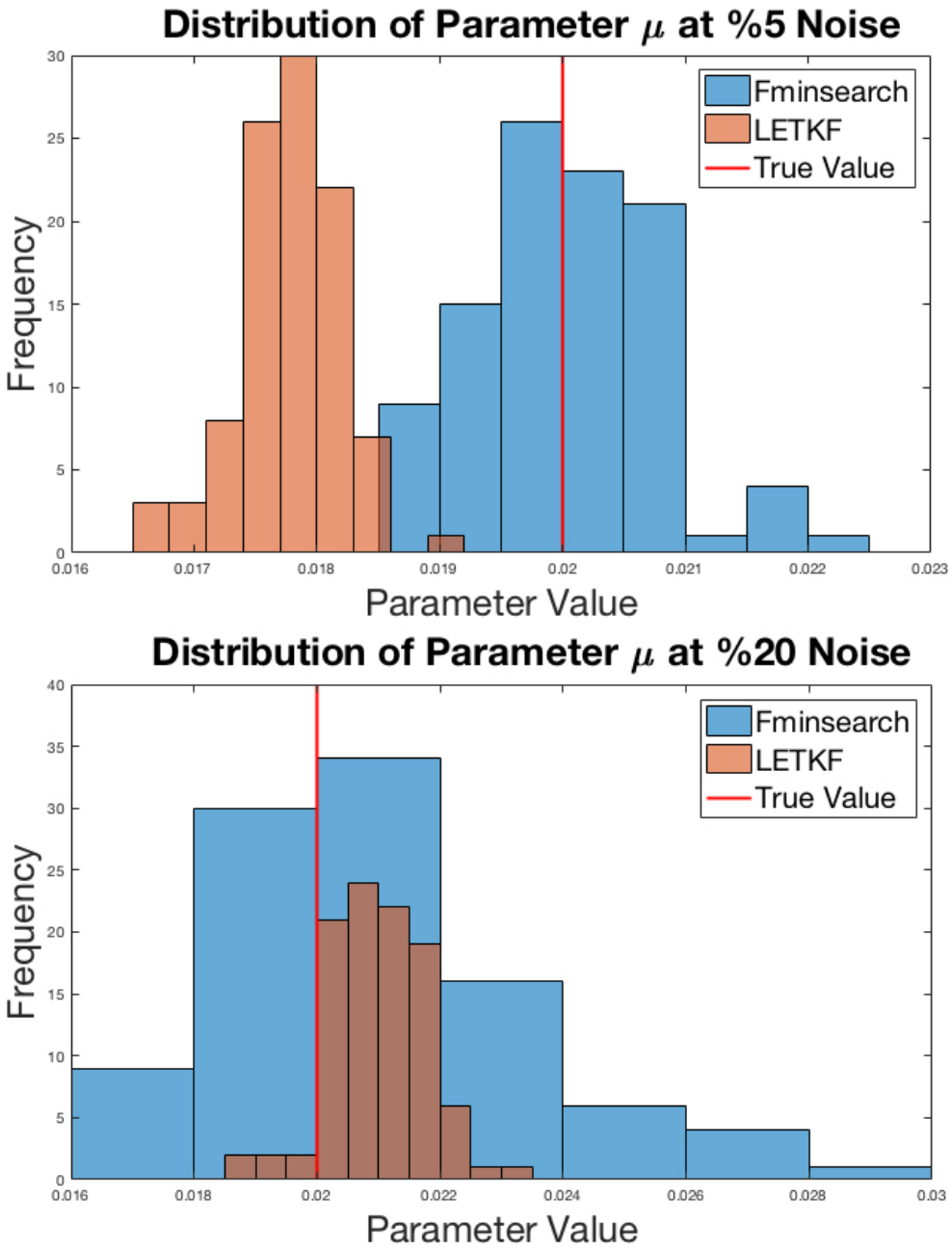

Figure 3.12: Distributions of Parameter Values Approximated with Fminsearch Algorithm Vs Augmented Ensemble Kalman Filter for %5 and %20 Percent Noise Levels.

Chapter 4

MATHEMATICAL MODEL FOR ANDROGEN SUPPRESSION THERAPY WITH TIME DELAY

4.1 Introduction

There have been several mathematical models that study the dynamics of prostate cancer under androgen deprivation therapy(Baez and Kuang (2016); Hirata *et al.* (2010); Portz *et al.* (2012); Jackson (2003); Everett *et al.* (2014)). In Chapter 2, we proposed two mathematical models that are more reliable in predicting prostate cancer resistance than the current models in literature. In Chapter 3, we utilized the models in Baez and Kuang (2016) to perform data assimilation and forecasts using an ensemble Kalman filter. For this chapter, we attempt to create a more biologically realistic model, by incorporating a time delay τ that denotes the time it takes for prostate cells to use androgen for growth. Also, we incorporate a delay dependent parameter since there is not time delay in the death rate of prostate cells due to androgen deprivation. The inclusion of a delay dependent parameter to balance growth and death is many times neglected. Since, it is very complicated to analytically study models with delay dependent parameters even if there is only a single discrete delay, and it is common to use computer software to perform numerical analysis (Beretta and Kuang (2002)). In this work, we combine graphical information with analytical results to study the local stability of steady states that involves delay dependent parameters by applying the theory developed in Beretta and Kuang (2002) and Beretta and Kuang (2001). Furthermore, we seek to justify the inclusion of the delay dependent parameter by analyzing an alternative model without it. If we exclude delay dependent parameters,

it is often possible to analyze models more extensively. Therefore, we compare a models' ability to fit clinical data in Section 4.6.

4.2 Proposed Prostate Cancer Model

In the following model we denote the time delay as τ (d). Tumor cell volume is denoted by x (mm^3). Intracellular androgen cell levels are denoted by Q (nM), and PSA levels by P ($\frac{\mu g}{L}$).

$$\begin{aligned} x' &= f_1\left(Q(t-\tau)\right)x(t-\tau) - D_1(Q(t))x(t) - \delta x^2(t) \\ Q' &= \gamma\left(Q_m - Q(t)\right) - f_1\left(Q(t-\tau)\right)Q(t)\frac{x(t-\tau)}{x(t)} \\ P' &= bQ(t) + \sigma X(t)Q(t) - \epsilon P(t) \end{aligned} \tag{4.1}$$

where,

$$f_1\left(Q(t-\tau)\right) = \mu\left(1 - \frac{q}{Q(t-\tau)}\right)e^{-d_m\tau},$$

$$D_1(Q(t)) = \frac{dR}{R+Q(t)},$$

and

$$\gamma = \gamma_1 u(t) + \gamma_2 \qquad u(t) = \begin{cases} 1, \text{ on treatment,} \\ 0, \text{ off treatment.} \end{cases}$$

Similarly to model (2.2-2.5), it is assumed that the androgen concentration in cancer cells is approximately the same as the androgen concentration in serum. Parameter γ_1 denotes the constant production of androgen by the testes, and γ_2 denotes the production of androgen by the adrenal gland and kidneys. We include a delay dependent parameter in $f_1\left(Q(t-\tau)\right)$ since a cancer cell had to survive from time $t-\tau$ to t with the given mortality $e^{-d_m\tau}$ where $d_m = \frac{dR}{R+Q_m}$. We chose the death rate d_m since it is the lowest possible death rate of cancer cells at the highest androgen concentration Q_m.

4.2.1 Derivation of Q Equation

Now we provide a balance equation based derivation for the cell quota Q equation (4.1). Our formulation comes from the conservation of androgen as it moves in and out of the tumor. Let Q_x be the total androgen inside tumor x (mm^3). We assume that Q (nM) is uniformly distributed in x, and

$$Q_x = Q(t)x(t) \text{ nmol.}$$

The inflow of androgen to the tumor comes from the serum which can be approximated by

$$\gamma(Q_m - Q(t))x(t).$$

The outflow of androgen from the tumor is due to death which is

$$(D_1(Q(t)) + \delta x(t))Q(t)x(t).$$

Then, the rate of change of androgen inside the tumor is:

$$(Q(t)x(t))' = \gamma(Q_m - Q(t))x(t) - (D_1(Q(t)) + \delta x(t))Q(t)x(t).$$

However,

$$\begin{aligned}(Q(t)x(t))' &= Q'(t)x(t) + Q(t)x'(t) \\ &= Q'(t)x(t) + f_1\left(Q(t-\tau)\right)x(t-\tau)Q(t) - (D_1(Q(t)) + \delta x(t))Q(t)x(t),\end{aligned}$$

which implies that

$$Q'(t) = \gamma(Q_m - Q(t)) - f_1\left(Q(t-\tau)\right)Q(t)\frac{x(t-\tau)}{x(t)}.$$

4.3 Mathematical Analysis: Model With Delay Dependent Parameter

Now we proceed to analysis our full model with delay dependent parameters. Our results are based on the work of Beretta and Kuang (2002). We study the occurrence

of stability switches that occur from increasing the value of the time delay τ. The characteristic equation evaluated at the steady state (x^*, Q^*) is given by

$$P(\lambda, \tau) + Q(\lambda, \tau)e^{-\lambda\tau} = 0 \tag{4.2}$$

where

$$P(\lambda, \tau) = \lambda^2 + \lambda a(\tau) + c(\tau),$$

$$Q(\lambda, \tau) = \lambda b(\tau) + d(\tau),$$

and

$$\begin{aligned}
a(\tau) &= \frac{\gamma\left(\gamma Q_m e^{d\tau} - 2\mu q + 3\mu Q_m\right)}{\gamma Q_m e^{d\tau} + \mu q} - \frac{dR\left(\gamma e^{d\tau} + \mu\right)}{\gamma e^{d\tau}(Q_m + R) + \mu(q + R)} \\
b(\tau) &= \frac{\mu\left(\mu q e^{-d\tau} + 2\gamma q - \gamma Q_m\right)}{\gamma Q_m e^{d\tau} + \mu q} \\
c(\tau) &= \frac{2\gamma^2\mu^2(Q_m - q)^2}{\left(\gamma Q_m e^{d\tau} + \mu q\right)^2} + \frac{(Q_m - q)\left(2\gamma^2\mu - \gamma d\mu\right)}{\gamma Q_m e^{d\tau} + \mu q} \\
&- \frac{\gamma d\mu^2 R(Q_m - q)^2}{(Q_m + R)\left(\gamma Q_m e^{d\tau} + \gamma R e^{d\tau} + \mu q + \mu R\right)^2} \\
&+ \frac{(Q_m - q)(\gamma d\mu Q_m - \gamma d\mu R)}{(Q_m + R)\left(\gamma Q_m e^{d\tau} + \gamma R e^{d\tau} + \mu q + \mu R\right)} - \frac{\gamma dR}{Q_m + R} \\
d(\tau) &= -\frac{\mu e^{-d\tau}\left(\gamma e^{d\tau} + \mu\right)}{\left(\gamma Q_m e^{d\tau} + \mu q\right)^2\left(\gamma e^{d\tau}(Q_m + R) + \mu(q + R)\right)^2} - \frac{2\gamma\mu q(q - Q_m)}{\left(\gamma Q_m e^{d\tau} + \mu q\right)^2} \\
&+ \frac{-dq + \gamma q - \gamma Q_m}{\gamma Q_m e^{d\tau} + \mu q} + \frac{Q_m(dq + dR)}{(Q_m + R)\left(\gamma Q_m e^{d\tau} + \gamma R e^{d\tau} + \mu q + \mu R\right)} \\
&+ \frac{d\mu q^2 R - d\mu q Q_m R + d\mu q R^2 - d\mu Q_m R^2}{(Q_m + R)\left(\gamma Q_m e^{d\tau} + \gamma R e^{d\tau} + \mu q + \mu R\right)^2}
\end{aligned}$$

It is important to notice that,

$$P(0, \tau) + Q(0, \tau) = c(\tau) + d(\tau) \neq 0, \forall\tau \in \mathbf{R}_{+0}. \tag{4.3}$$

Equation (4.3) guarantees that $\lambda = 0$ is not a characteristic root of (4.2). That is, we cannot cross the imaginary axis at $\lambda = 0$. Then, we assume the following,

1. If $\lambda = i\omega$, $\omega \in \mathbf{R}$, then $P(i\omega, \tau) + Q(i\omega, \tau) \neq 0, \tau \in \mathbf{R}$

2. $\limsup\{\frac{|Q(\lambda,\tau)|}{P(\lambda,\tau)} : |\lambda| \to \infty, \Re\lambda \geq 0\} < 1$ for any τ.

3. $F(\omega,\tau) = |P(i\omega,\tau)|^2 - |Q(i\omega,\tau)|^2$ for each τ has at most finite number of real zeros.

4. Each positive root $\omega(\tau)$ of $F(\omega,\tau) = 0$ is continuous and differentiable in τ whenever it exists.

We need condition (1) to ensure that $P(\lambda,\tau)$ and $Q(\lambda,\tau)$ have no common imaginary roots, and that threshold time delays can be expressed analytically. We need condition (2) to guarantee that there are no roots bifurcating from infinity. Assumption (3) is needed to ensure that there are only finite ways for roots to cross the imaginary axis for any given τ. Assumption (4) is needed to compute the derivative of the imaginary roots with respect to τ. If we increase τ, then the imaginary axis cannot be crossed at $\lambda(\tau) = 0$ for some $\tau > 0$, as guaranteed by 4.3. Therefore, we look for the crossing of the imaginary axis at the imaginary roots $\lambda = \pm i\omega(\tau)$, for $\omega(\tau)$ that is real and positive at some positive τ. $\omega(\tau)$ should also satisfy (4.2) and

$$\begin{aligned} \sin(\omega\tau) &= \frac{-(c(\tau) - \omega^2)\omega b(\tau) + \omega a(\tau) d(\tau)}{\omega^2 b(\tau)^2 + d(\tau)^2} \\ \cos(\omega\tau) &= -\frac{(c(\tau) - \omega^2) d + \omega^2 a(\tau) b(\tau)}{\omega^2 b(\tau)^2 + d(\tau)^2}. \end{aligned} \tag{4.4}$$

Again, condition (4.3) guarantees that $\omega^2 b(\tau)^2 + d(\tau)^2 \neq 0$. We assume that $I \subseteq \mathbf{R}_{+0}$ is the set where $\omega(\tau)$ is a positive root and for $\tau \notin I$, $\omega(\tau)$ is not definite. We can rewrite (4.4) as

$$\sin(\omega\tau) = \mathrm{Im}\left(\frac{P(i\omega,\tau)}{Q(i\omega,\tau)}\right) \quad \cos(\omega\tau) = -\mathrm{Re}\left(\frac{P(i\omega,\tau)}{Q(i\omega,\tau)}\right) \tag{4.5}$$

which implies that

$$|P(i\omega,\tau)|^2 = |Q(i\omega,\tau)|^2.$$

If $\omega(\tau)$ satisfies (4.4) then it also must satisfy.

$$\begin{aligned} F(\omega,\tau) &= |P(i\omega,\tau)|^2 - |Q(i\omega,\tau)|^2 \\ &= (c\,(\tau) - \omega^2)^2 + \omega^2 a\,(\tau)^2 - (\omega^2 b\,(\tau)^2 + d\,(\tau)^2) \\ &= 0 \end{aligned}$$

Then, $F(\omega,\tau) = 0$ implies

$$\omega^4 - \omega^2(b\,(\tau)^2 + 2c\,(\tau) - a\,(\tau)^2) + (c\,(\tau)^2 - d\,(\tau)^2) = 0,$$

and its roots are given by

$$\omega_+^2 = \frac{1}{2}\{(b\,(\tau)^2 + 2c\,(\tau) - a\,(\tau)^2) + \Delta^{\frac{1}{2}}\}, \omega_-^2 = \frac{1}{2}\{(b\,(\tau)^2 + 2c\,(\tau) - a\,(\tau)^2) - \Delta^{\frac{1}{2}}\},$$

where,

$$\Delta = (b^2 + 2c - a^2)^2 - 4(c^2 - d^2).$$

We have explored the biologically relevant parameter values and we have found that $d(\tau)^2 > c(\tau)^2$ always holds, and that only ω_+ is a feasible root of the characteristic equation. For any $\tau \in I$ where $\omega(\tau)$ is a positive solution, we can define the angle $\theta(\tau) \in [0, 2\pi]$ as the solution of (4.4).

$$\begin{aligned} \sin(\theta(\tau)) &= \frac{-(c\,(\tau) - \omega^2)\omega b\,(\tau) + \omega a\,(\tau)\, d\,(\tau)}{\omega^2 b\,(\tau)^2 + d\,(\tau)^2} \\ \cos(\theta(\tau)) &= -\frac{(c\,(\tau) - \omega^2)d + \omega^2 a\,(\tau)\, b\,(\tau)}{\omega^2 b\,(\tau)^2 + d\,(\tau)^2} \end{aligned} \tag{4.6}$$

Then relationship between $\theta(\tau)$ and $\omega(\tau)\tau$ is

$$\omega(\tau)\tau = \theta(\tau) + n2\pi, \quad n \in \mathbf{N}_0 \tag{4.7}$$

Then we can define the maps $\tau_n : I \to \mathbf{R}_{+0}$ given by

$$\tau_n(\tau) = \frac{\theta(\tau) + 2\pi n}{\omega_+(\tau)} \tag{4.8}$$

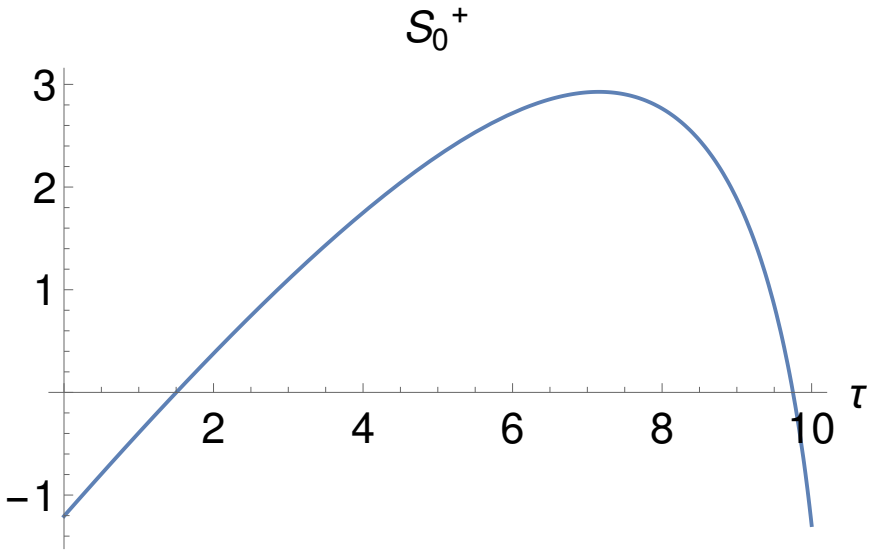

Figure 4.1: Graph of Stability Switch in Terms of Time Delay for Model 4.1. The Function Is $S_0(\tau)$ from Equation 4.9.

Then we can introduce the functions $I \to \mathbf{R}$,

$$S_n(\tau) = \tau - \tau_n(\tau), \quad n \in \mathbf{N}_0, \quad \tau \in I \tag{4.9}$$

Finally, we can use the following theorem by Beretta and Kuang (2002).

Theorem 4.3.1. *Assume that $\omega(\tau)$ is a positive real root of 4.2 defined for $\tau \in I$, $I \subseteq \mathbf{R}_{+0}$, and some $\tau^* \in I$,*

$$S_n(\tau^*) = 0 \tag{4.10}$$

for some $n \in N_0$. Then a pair of simple conjugate pure imaginary roots $\lambda_+(\tau^*) = i\omega(\tau^*)$,$\lambda_-(\tau^*) = -i\omega(\tau^*)$ of 4.2 exists at $\tau = \tau^*$ and crosses the imaginary axis from left to right if $\delta(\tau^*) > 0$ and crosses the imaginary axis from right to left if $\delta(\tau^*) < 0$, where

$$\delta_+(\tau^*) = sign\left\{\frac{dRe\lambda}{d\tau}\right\} = sign\left\{\frac{dS_n(\tau)}{d\tau}\right\} \tag{4.11}$$

We can illustrate Theorem 4.3 by plotting the functions of $S_n(\tau)$ in Figure (4.1) together with Figure (4.2). We can observe that for $\tau = 1$ we have a stable steady state.

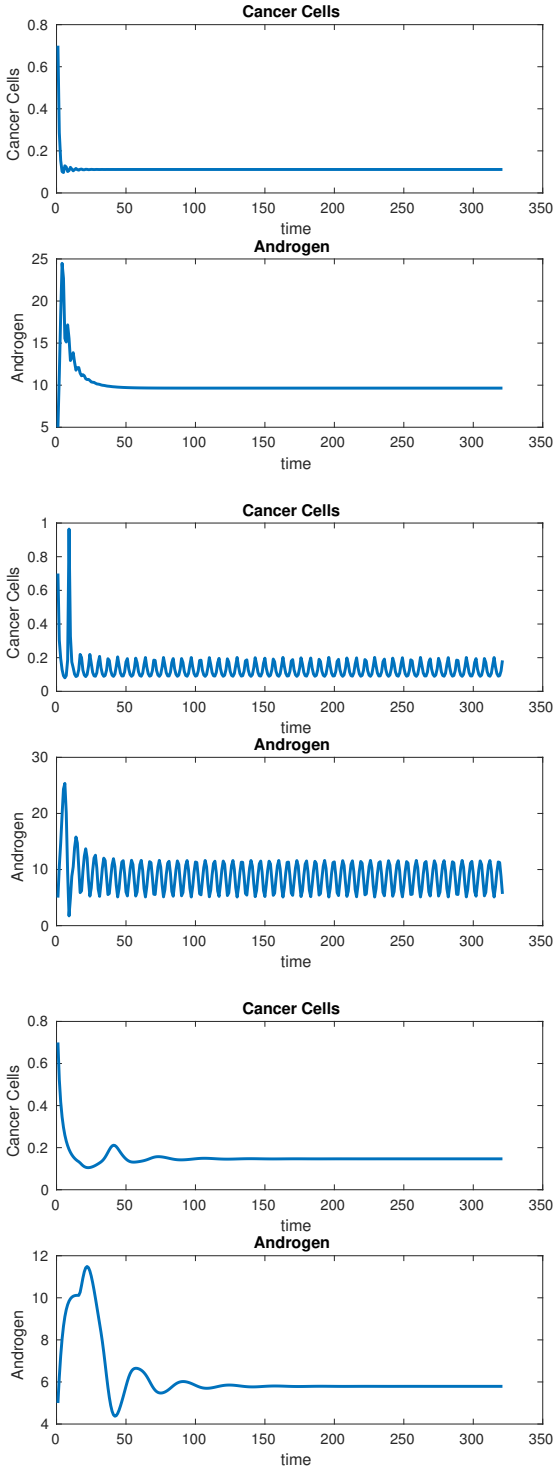

Figure 4.2: Simulation for System 4.1. Top: $\tau = 1$ with Local Stability, Middle: $\tau = 6$ with the Emergence of Periodic Solutions, Bottom: $\tau = 11$ with Stability Regained.

Table 4.1: Parameter Definitions, Units, and Ranges.

Parameters	Definition	Range	Units
μ	Max prolif. rate	.001-.09	day^{-1}
q	Min cell quota	.1 - .5	nM
b	Prostate baseline PSA	0.1-2.5	10^{-3} $\mu g/L/nM/day$
σ	Tumor PSA prod. rate	.001-.9	$\mu g/L/nM/mm^3/day$
ϵ	PSA clearance rate	.001-.01	day^{-1}
d	Maximum cell death rate	.0001-.09	day^{-1}
δ	Density death rate	.1-9 10^{-5}	$1/\text{day}/mm^3$
R	CDR half-satur. level	0-3	nM
γ_1	Testes androgen prod.	20	day^{-1}
γ_2	Secondary androgen prod.	0.001-.01	day^{-1}
Q_m	Maximum androgen	15-30	nM
ν	Death rate decay rate	.01	unitless
τ	Androgen absorption delay	.5 - 1	days

As τ increases, S_n crosses the horizontal axis with a positive slope and the real part of the eigenvalues crosses the imaginary axis from right to left and there is the emergence of periodic solutions. Similarly, S_n crosses the horizontal axis with a negative slope at $\tau = 9.5$ and the real part of the eigenvalues crosses the imaginary axis from right to left and there is the steady state becomes stable again. Therefore, we have fully characterized the stability behavior of our model for a given set of parameter values. Now, we move to the analysis of a model without the delay dependent parameter.

4.4 Mathematical Analysis: No Delay Dependent Parameter

For mathematical analysis we shall reduce our model to:

$$\begin{aligned} x'(t) &= \mu\left(1-\frac{q}{Q(t-\tau)}\right)x(t-\tau) - \frac{dR}{R+Q(t)}x(t) - \delta x^2(t) \\ Q'(t) &= \gamma(Q_m - Q(t)) - \mu\left(1-\frac{q}{Q(t-\tau)}\right)Q(t)\frac{x(t-\tau)}{x(t)} \end{aligned} \tag{4.12}$$

where the parameters are the same as model 4.1.

Since performing analysis with a time dependent delay is very challenging we aim to simplify the model and check whether it is sufficient to fit the data and also provide helpful insights. Now we proceed to show, positivity, boundedness, and stability analysis. The steady state for the system is $E^* = (x^*, Q^*)$, where $x^* = \frac{\mu}{\delta}(1-\frac{q}{Q^*})$, and $Q^* = \frac{\gamma Q_m + \mu q}{\gamma+\mu}$.

4.4.1 Existence, Uniqueness, Positivity, and Boundedness

Before we do our local stability analysis we need to show that solutions are positive and bounded. For the following we use the notation:

$$\begin{pmatrix} x' \\ Q' \end{pmatrix} = \begin{pmatrix} g_1\left(x(t), Q(t), x(t-\tau), Q(t-\tau)\right) \\ g_2\left(x(t), Q(t), x(t-\tau), Q(t-\tau)\right) \end{pmatrix}$$

With corresponding initial data $\phi_1(t)$, $\phi_2(t)$ for $x(t)$ and $Q(t)$.

Theorem 4.4.1. *The solutions of system (4.12) with initial conditions* $0 < \phi_1(t) < x_m$ *and* $q < \phi_2(t) < Q_m$*, where* $x_m = \frac{\mu}{\delta}(1-\frac{q}{Q_m})$ *then the solution stays in that region for all* $t > 0$*.*

Proof. Clearly, $x(t)$ and $Q(t)$ remain positive since

$$g_1(0, x(t-1), Q(t), Q(t-1)) \geq 0$$

and

$$g_2(x(t), x(t-1), 0, Q(t-1)) \geq 0.$$

Now, we show $Q(t)$ is bounded above by Q_m. Suppose $Q(t) = Q_m$ at $t = t_1$, then

$$Q'(t_1) = -\mu(1 - \frac{q}{Q(t_1 - \tau_1)})\frac{x(t_1 - \tau_2)}{x(t)} < 0$$

However, since $Q'(t_1) > 0$ this is a contradiction and $Q(t)$ cannot reach Q_m. Next, we show that $x(t)$ is bounded above. Suppose at $t = t_2$, $x(t_2) = x_m$ for the first time. Then $x(t)$ must be increasing. So,

$$\begin{aligned} x'(t_1) &= f_1\left(Q(t_1 - \tau)\right) x(t_1 - \tau) - \frac{dR}{R + Q(t)} x_m - \delta x_m^2 && (4.13) \\ &< \mu(1 - \frac{q}{Q_m})x_m - \frac{dR}{R + Q(t)} x_m - \delta x_m^2 < 0 && (4.14) \end{aligned}$$

This is a contradiction, since $x'(t_2) > 0$, and $x(t)$ cannot reach x_m. □

4.4.2 Local Stability Analysis

The characteristic equation of the system evaluated at the steady state (x^*, Q^*) is given by:

$$\lambda^2 + \lambda\left(c + de^{-\lambda\tau}\right) + a + be^{-\lambda\tau} \tag{4.15}$$

where,

$$\begin{aligned} a &= \frac{dR\left(-\mu qR + \gamma Q*^2 + Q^*R(\gamma + \mu)\right) + 2\delta x^*(Q^* + R)^2(Q^*(\gamma + \mu) - \mu q)}{Q^*(Q^* + R)^2} \\ b &= \frac{\mu\left(dR\left(qR + Q*^2\right) + (Q^* + R)^2(q(\gamma + \mu + 2\delta x^*) - Q^*(\gamma + \mu))\right)}{Q^*(Q^* + R)^2} \\ c &= \frac{dQ^*R + (Q^* + R)(Q^*(\gamma + \mu + 2\delta x^*) - \mu q)}{Q^*(Q^* + R)} \\ d &= \mu\left(\frac{2q}{Q^*} - 1\right) \end{aligned}$$

The characteristic equation (4.15) is an exponential polynomial with infinitely many solutions. Local stability occurs if all of the eigenvalues satisfy $\Re(\lambda) \leq 0$ for all λ (Kuang (1993)).

For $\omega > 0$, let $i\omega$ be a root of (4.15), then by separating real and imaginary part it follows that

$$\begin{cases} a\cos(\tau\omega) + b - \omega^2\cos(\tau\omega) & = -c\omega\sin(\tau\omega) \\ -a\sin(\tau\omega) - d\omega + \omega^2\sin(\tau\omega) & = c\omega\cos(\tau\omega) \end{cases} \tag{4.16}$$

which leads to

$$\omega^4 + \omega^2\left(c^2 - 2a - d^2\right) + a^2 - b^2 = 0 \tag{4.17}$$

It is easy to see that if the conditions

$$(C1) \quad c^2 - 2a - d^2 > 0$$

$$(C2) \qquad a^2 - b^2 > 0$$

hold, then (4.15) has no positive roots. Hence, all roots of (4.15) have negative real part. However, if condition

$$(\text{C3}) \qquad\qquad a^2 - b^2 < 0$$

holds, then (4.15) has at least one positive real root. Substituting ω_0 into 4.16 yields

$$\tau_j = -\frac{1}{\omega_j}\cos^{-1}\left(\frac{-a^2 + 2a\omega_j^2 - b^2 + c^2\omega_j^2 + d^2\omega_j^2 - \omega_j^4}{2\left(ab - b\omega_j^2 - cd\omega_j^2\right)}\right) + \frac{2k\pi}{\omega_j}$$

where $j = 1, 2, 3, 4$, $k = 0, 1, 2, \ldots$. Then $\pm i\omega_j$ is a pair of purely imaginary roots of 4.15. Let

$$\tau_j^0 = \min\{\tau_j\}$$

Then taking the derivative of the characteristic polynomial yields

$$\frac{d\lambda}{d\tau} = -\frac{e^{\tau\lambda(\tau)}\lambda(\tau)\left(a + c\lambda(\tau) + \lambda(\tau)^2\right)}{a\tau e^{\tau\lambda(\tau)} + c\tau e^{\tau\lambda(\tau)}\lambda(\tau) + ce^{\tau\lambda(\tau)} + d + \tau e^{\tau\lambda(\tau)}\lambda(\tau)^2 + 2e^{\tau\lambda(\tau)}\lambda(\tau)}$$

$$\begin{aligned}\left[\frac{d\lambda}{d\tau}\right]^{-1}_{\lambda=i\omega} &= \Re\left[\frac{e^{-i\tau\omega}\left(-ice^{i\tau\omega} - id + 2\omega e^{i\tau\omega}\right)}{\omega\left(-a - ic\omega + \omega^2\right)} + \frac{i\tau}{\omega}\right] \\ &= \Re\left[\frac{(\cos(\tau\omega) - i\sin(\tau\omega))((c + 2i\omega)\sin(\tau\omega) + (2\omega - ic)\cos(\tau\omega) - id)}{\omega\left(a^2 - 2a\omega^2 + c^2\omega^2 + \omega^4\right)}\right] \\ &= \frac{-2a + c^2 + d^2 + 2\omega^2}{a^2 - 2a\omega^2 + c^2\omega^2 + \omega^4}\end{aligned}$$

Thus, if condition (C1) holds, then $\Re(\lambda) > 0$. Based on the Hopf bifurcation theorem (Kuang (1993)), we have the following results.

Theorem 4.4.2. *For system (4.1-4.1), assume that (C1) and (C2) are satisfied, then the positive equilibrium E^* is asymptotically stable. If (C3) is satisfied, then when $\tau \in (0, \tau_j^0)$ the system is stable ,and undergoes a Hopf bifurcation at E^* when $\tau = \tau_j^0$.*

4.5 Stability of Hopf Bifrucation

In the previous section, we have obtained sufficient conditions to guarantee that system (1.2) undergoes the Hopf bifurcation at τ_j^0. In this section, we shall study the bifurcation properties. The method we used is based on the normal form method and the center manifold theory presented in Hassard *et al.* (1981).

Let $x_1(t) = x(t) - x^*$ and $x_2(t) = Q(t) - Q^*$. Then, we normalize the delay with the scaling $t \to \frac{t}{\tau}$. Then, the system can be rewritten as:

$$\begin{pmatrix} \dot{} \\ x_2 \\ x_2 \end{pmatrix} = (\tau_j^0 + k)K_1 \begin{pmatrix} x_1(t) \\ x_2(t) \end{pmatrix} + (\tau_j^0 + k)K_2 \begin{pmatrix} x_1(t-1) \\ x_2(t-1) \end{pmatrix} + (\tau_j^0 + k)\begin{pmatrix} f_1 \\ f_2 \end{pmatrix} \quad (4.18)$$

Where,

$$K_1 = \begin{pmatrix} -(D_1(Q^*) + 2\delta x^*) & -x^* D_1'(Q^*) \\ -\frac{Q^* F_1(Q^*)}{x^*} & -F_1(Q^*) \end{pmatrix}$$

$$K_2 = \begin{pmatrix} F_1(Q^*) & x^* F_1'(Q^*) \\ -Q^* F_1(Q^*) & -Q^* F_1'(Q^*) \end{pmatrix}$$

$$\begin{aligned} f_1 =& -(x^* + x_1(t)) D_1(Q^* + x_2(t)) - D_2(x^* + y) \\ & + (x^* + x_1(t-1)) F_1(Q^* + x_2(t-1)) + x_1(t) D_1(Q^*) - x_1(t-1) F_1(Q^*) \\ & + x^* x_2(t) D_1'(Q^*) + 2y\delta x^* - x^* x_2(t-1) F_1'(Q^*) \\ f_2 =& \gamma(Q_m - (Q^* + x_2(t))) - Q^* x^* F_1(Q^* + x_2(t-1)) \frac{1}{x^* + x_1(t-1)} \\ & - Q^* x_1(t) F_1(Q^* + x_2(t-1)) \frac{1}{x^* + x_1(t-1)} \\ & - x^* x_2(t) F_1(Q^* + x_2(t-1)) \frac{1}{x^* + x_1(t-1)} \\ & - x_1(t) x_2(t) F_1(Q^* + x_2(t-1)) \frac{1}{x^* + x_1(t-1)} + Q^* x_1(t) F_1(Q^*) \frac{1}{x^*} \\ & + x^* x_2(t) F_1(Q^*) \frac{1}{x^*} \\ & + Q^* x^* x_2(t-1) \frac{1}{x^*} F_1'(Q^*) + Q^* x^* x_1(t-1) F_1(Q^*) \frac{1}{x^*} \end{aligned}$$

Define the linear operator $L(\mu) : \mathbb{C} \to \mathbb{R}^2$ and the nonlinear operator $f(\cdot, \mu) : \mathbb{C} \to \mathbb{R}^2$ by:

$$L_\mu(\phi) = (\tau_j^0 + \mu) K_1 \begin{pmatrix} \phi_1(0) \\ \phi_2(0) \end{pmatrix} + (\tau_j^0 + \mu) K_2 \begin{pmatrix} \phi_1(-1) \\ \phi_2(-1) \end{pmatrix}$$

and

$$f(\phi, \mu) = (\tau_j^0 + \mu) \begin{pmatrix} f_1 \\ f_2 \end{pmatrix} \tag{4.19}$$

where $\phi = (x_1(t), x_2(t))^T \in \mathbb{C}$.

By the Riesz representation theorem, there exists a 2×2 matrix function $\eta(\theta, \mu)$, $-1 \leq \phi \leq 0$ whose elements are of bounded variation such that

$$L_\mu(\phi) = \int_{-1}^{0} d\eta(\theta, \mu)\phi(\theta) \qquad \text{for} \qquad \phi \in \mathbb{C}([-1, 0], \mathbb{R}^2) \tag{4.20}$$

In fact, we can choose

$$\eta(\theta, \mu) = (\tau_j^0 + \mu)K_1\delta(\theta) + (\tau_j^0 + \mu)K_2\delta(\theta + 1)$$

where δ is the Dirac delta function. For $\phi \in \mathbb{C}^1([-1, 0], \mathbb{R}^2)$, define

$$A(\mu)\phi = \begin{cases} \frac{d\phi(\theta)}{d\theta}, & \phi \in [-1, 0) \\ \int_{-1}^{0} d\eta(\mu, s)\phi(s), & \phi = 0 \end{cases}$$

and

$$R(\mu)\phi = \begin{cases} 0, & \phi \in [-1, 0) \\ f(\mu, \phi), & \phi = 0 \end{cases}.$$

Then, the system is equivalent to

$$u'(t) = A(\mu)u_t + R(\mu)u_t$$

,

where $u(t) = (x_1(t), x_2(t))^T$, $u_t = u(t + \theta)$, for $\phi \in [-1, 0]$.

For $\psi \in \mathbb{C}^1([0, 1], (\mathbb{R}^2)^*)$, define

$$A^*\psi = \begin{cases} \frac{d\psi(\theta)}{d\theta}, & s \in [-1, 0) \\ \int_{-1}^{0} d\eta(t, 0)\psi(-t), & s = 0 \end{cases}$$

and a bilinear inner product

$$\langle \psi(s), \phi(\theta) \rangle = \bar{\phi}(0)\theta(0) - \int_{-1}^{0} \int_{\xi=0}^{\theta} \bar{\psi}(\xi - \theta)d\eta(\theta)\phi(\xi)d\xi \tag{4.21}$$

where $\eta(\theta) = \eta(\theta, 0)$. In addition, by Theorem 4.4.2 we know that $\pm i\omega_0\tau_j^0$ are eigenvalues of $A(0)$. Thus, they are also eigenvalues of A^*. Let $q(\theta)$ be the eigenvector of $A(0)$ corresponding to $i\omega_0\tau_j^0$ and $q^*(s)$ be the eigenvector of A^* corresponding to $-i\omega_0\tau_j^0$.

Let $q(\theta) = (1, \nu_1)^T e^{i\omega_0\tau_j^0\theta}$ and $q^*(s) = D(1, \nu_1)e^{i\omega_0\tau_j^0 s}$. From the above discussion, it is easy to know that $A(0)q(0) = i\omega_0\tau_j^0 q(0)$ and $A^*(0)q^*(0) = -i\omega_0\tau_j^0 q^*0)$. That is

$$\tau_j^0 \begin{pmatrix} -(D_1(Q^*) + 2\delta x^*) & -x^* D_1'(Q^*) \\ -Q^* F_1(Q^*)\frac{1}{x^*} & F_2(Q^*) - F_1(Q^*) \end{pmatrix} q(0) +$$

$$\tau_j^0 \begin{pmatrix} F_1(Q^*) & x^* F_1'(Q^*) \\ -Q^* F_1(Q^*) & -Q^* F_1'(Q^*) \end{pmatrix} q(-1) = i\omega_0\tau_j^0 q(0)$$

and,

$$\tau_j^0 \begin{pmatrix} -(D_1(Q^*) + 2\delta x^*) & -Q^* F_1(Q^*)\frac{1}{x^*} \\ -x^* D_1'(Q^*) & F_2(Q^*) - F_1(Q^*) \end{pmatrix} q^*(0) +$$

$$\tau_j^0 \begin{pmatrix} F_1(Q^*) & -Q^* F_1(Q^*) \\ x^* F_1'(Q^*) & -Q^* F_1'(Q^*) \end{pmatrix} q^*(-1) = -i\omega_0\tau_j^0 q^*(0)$$

Thus, we can easily obtain:

$$q(\theta) = \left(1, \frac{Q^*}{x^*}\frac{F_1(Q^*)\left(e^{i\omega_0} - 1\right)}{F_1(Q^*) - Q^* F_1'(Q^*)e^{-i\omega_0} - i\omega_0}\right)^T e^{i\omega_0\tau_j^0\theta}$$

$$q^*(s) = D\left(1, \frac{x^*\left(F_1'(Q^*)e^{-i\omega_0} - D_1'(Q^*)\right)}{F_1(Q^*) + Q^* F_1'(Q^*)e^{-i\omega_0} + i\omega_0}\right)^T e^{i\omega_0\tau_j^0 s}$$

In order to assure $\langle \bar{q^*}(s), q(\theta)\rangle = 1$, we need to determine the value of D. From 4.21 we have

$$\begin{aligned}
\langle \bar{q^*}(s), q(\theta)\rangle &= \bar{q}^*(0)q(0) - \int_{-1}^{0}\int_{\xi=0}^{\theta} \bar{q}^*(\xi-\theta)d\eta(\theta)q(\xi)d\xi \\
&= \bar{q}^*(0)q(0) - \int_{-1}^{0}\int_{\xi=0}^{\theta} \bar{D}\,(1,\bar{\nu}_1^*)\, e^{-i\omega_0\tau_j(\xi-\theta)}d\eta(\theta)\,(1,\nu_1)^T\, e^{i\omega_0\tau_j\xi}d\xi \\
&= \bar{q}^*(0)q(0) - \bar{q}^*(0)\int_{-1}^{0} \theta e^{i\omega_0\tau_j\theta}d\eta(\theta)q(0) \\
&= \bar{q}^*(0)q(0) - \bar{q}^*(0)\begin{pmatrix} F_1(Q^*) & x^*F_1'(Q^*) \\ -Q^*F_1(Q^*) & -Q^*F_1'(Q^*)\end{pmatrix} e^{-i\omega_0\tau_j}q(0)
\end{aligned}$$

So we have,

$$D = \frac{1}{1+\nu_1\nu_1^* + \tau_j e^{-i\omega_0\tau_j}\left(F_1(Q^*) + \nu_1 x^* F_1'(Q^*) + \frac{\nu_1^* Q^* F_1(Q^*)}{x^*} - \nu_1\nu_1^* Q^* F_1(Q^*)\right)}$$

$$\bar{D} = \frac{1}{1+\nu_1\bar{\nu}_1^* + \tau_j e^{-i\omega_0\tau_j}\left(F_1(Q^*) + \nu_1 x^* F_1'(Q^*) + \frac{\bar{\nu_1^*} Q^* F_1(Q^*)}{x^*} - \nu_1\bar{\nu}_1^* Q^* F_1(Q^*)\right)}$$

Lemma 4.5.1. The system (6) is equivalent to

$$\dot{x}(t) = A(\mu)x_t + R(\mu)x_t, \tag{4.22}$$

where $A(\mu)$ is linear. Besides, there exists an inner product $< \cdot, \cdot >$ and eigenvectors $q(\theta)$ and $q^*(\theta)$ respectively of $A(0)$ and A^* such that $< q^*(s), q(\theta) >= 1$, where A^* is the associate operator of A.

Using the same notations as in 4.22, we first compute the coordinates to describe the center manifold C_0 at $\mu = 0$. Let x_t be the solution of Equation 4.18 when $\mu = 0$. Define

$$
\begin{aligned}
x_2(t) &= \langle q^*, x_t \rangle \\
W(t,\theta) &= x_t(\theta) - 2\Re(x_2(t)q(\theta)) \\
&= x_t(\theta) - (x_2(t)q(\theta) + \bar{z}(t)\bar{q}(\theta))
\end{aligned} \tag{4.23}
$$

On the center manifold C_0 we have

$$
W(t,\theta) = W(z,\bar{z},\theta) \tag{4.24}
$$

where,

$$
W(z,\bar{z},\theta) = W_{20}(\theta)\frac{z^2}{2} + W_{11}(\theta)z\bar{z} + W_{02}\frac{\bar{z}^2}{2} + W_{30}(\theta)\frac{z^3}{6} + \dots \tag{4.25}
$$

z and $\bar{z}$ are local coordinates for the center manifold C_0 in the direction of q^* and $\bar{q}^*$. Note that W is real if x_t is real. We only consider real solutions. For solution $x_t \in C_0$ of 4.18, since $\mu = 0$, we have

$$
\begin{aligned}
\dot{z}(t) &= i\omega_0\tau_j^0 z + \bar{q}^*(0)f(0, W(z,\bar{z},0) + 2R_e(x_2(t)q(t))) = i\omega_0\tau_j^0 z + \bar{q}^*(0)f_0(z,\bar{z}) \\
&= i\omega_0\tau_j^0 z + g(z,\bar{z})
\end{aligned}
$$

where,

$$
g(z,\bar{z}) = g_{20}(\theta)\frac{z^2}{2} + g_{11}(\theta)z\bar{z} + g_{02}(\theta)\frac{\bar{z}^2}{2} + g_{21}(\theta)\frac{z^2\bar{z}}{2} \tag{4.26}
$$

Now, we obtain the coefficients in g. Notice that we have that $x_t(\theta) = (x_{1t}(\theta), x_{2t}(\theta))$ and $q(\theta) = (1,\nu_1)^T e^{i\omega_0\tau_j^0\theta}$. So, from (4.23 and 4.25), it follows that

$$x_t(\theta) = W(t,\theta) + 2R_e(x_2(t)q(\theta)) \tag{4.27}$$

$$= W_{20}(\theta)\frac{z^2}{2} + W_{11}(\theta)z\bar{z} + W_{02}\frac{\bar{z}^2}{2} + (1,\nu_1)^T e^{i\omega_0\tau_j^0\theta}z(t) + (1,\bar{\nu}_1)^T e^{-i\omega_0\tau_j^0\theta}\bar{z}(t) + \dots \tag{4.28}$$

and then we have

$$x_{1t}(0) = z + \bar{z} + W_{20}^{(1)}(0)\frac{z^2}{2} + W_{11}^{(1)}(0)z\bar{z} + W_{02}^{(1)}(0)\frac{\bar{z}^2}{2} + \dots$$

$$x_{2t}(0) = \nu_1 z + \bar{\nu_1}\bar{z} + W_{20}^{(2)}(0)\frac{z^2}{2} + W_{11}^{(2)}(0)z\bar{z} + W_{02}^{(2)}(0)\frac{\bar{z}^2}{2} + \dots$$

$$x_{1t}(-1) = ze^{-i\omega_0\tau_j^0\theta} + \bar{z}e^{i\omega_0\tau_j^0\theta} + W_{20}^{(1)}(-1)\frac{z^2}{2} + W_{11}^{(1)}(-1)z\bar{z} + W_{02}^{(1)}(-1)\frac{\bar{z}^2}{2} + \dots$$

$$x_{2t}(-1) = \nu_1 ze^{-i\omega_0\tau_j^0\theta} + \bar{\nu_1}\bar{z}e^{i\omega_0\tau_j^0\theta} + W_{20}^{(2)}(-1)\frac{z^2}{2} + W_{11}^{(2)}(-1)z\bar{z} + W_{02}^{(2)}(-1)\frac{\bar{z}^2}{2} + \dots$$

It follows together with 4.19 that

$$
\begin{aligned}
g_{20} &= -\nu_1 D_1'\left(Q^*\right) - \frac{1}{2}\nu_1^2 x^* D_1''\left(Q^*\right) + \nu_1 F_1'\left(Q^*\right) e^{-2i\omega_0 {\tau_j}^0} + \frac{1}{2}\nu_1^2 x^* F_1''\left(Q^*\right) e^{-2i\omega_0 {\tau_j}^0} \\
&- \delta - \frac{\overline{\nu_1}^* \nu_1 e^{-2i\omega_0 {\tau_j}^0}\left(2F_1\left(Q^*\right) e^{i\omega_0 {\tau_j}^0} + 2\nu_1 x^* F_1'\left(Q^*\right) e^{i\omega_0 {\tau_j}^0}\right)}{2x^*} \\
&- \frac{\overline{\nu_1}^* \nu_1 e^{-2i\omega_0 {\tau_j}^0}\left(Q^*\left(\nu_1 x^* F_1''\left(Q^*\right) + 2F_1'\left(Q^*\right)\right)\right) + 2i\omega_0}{2x^*} \\
g_{02} &= -\overline{\nu_1} D_1'\left(Q^*\right) - \frac{1}{2}\overline{\nu_1}^2 x^* D_1''\left(Q^*\right) + \overline{\nu_1} F_1'\left(Q^*\right) e^{2i\omega_0 {\tau_j}^0} + \frac{1}{2}\overline{\nu_1}^2 x^* F_1''\left(Q^*\right) e^{2i\omega_0 {\tau_j}^0} \\
&- \delta - \frac{\overline{\nu_1}^* \overline{\nu_1} e^{i\omega_0 {\tau_j}^0}\left(Q^* e^{i\omega_0 {\tau_j}^0}\left(\overline{\nu_1} x^* F_1''\left(Q^*\right) + 2F_1'\left(Q^*\right)\right) + 2\overline{\nu_1} x^* F_1'\left(Q^*\right) + 2F_1\left(Q^*\right)\right)}{2x^*} \\
&+ \frac{2i\omega_0}{2x^*} \\
g_{11} &= -\overline{\nu_1} D_1'\left(Q^*\right) - \nu_1 \overline{\nu_1} x^* D_1''\left(Q^*\right) + \overline{\nu_1} F_1'\left(Q^*\right) + \nu_1 \overline{\nu_1} x^* F_1''\left(Q^*\right) - \nu_1 D_1'\left(Q^*\right) \\
&+ \nu_1 F_1'\left(Q^*\right) - 2\delta + \overline{\nu_1}^*(-\nu_1 \overline{\nu_1} F_1'\left(Q^*\right) e^{-i\omega_0 {\tau_j}^0} - \nu_1 \overline{\nu_1} F_1'\left(Q^*\right) e^{i\omega_0 {\tau_j}^0} \\
&- \frac{\overline{\nu_1} F_1\left(Q^*\right) e^{-i\omega_0 {\tau_j}^0}}{x^*} - \nu_1 \overline{\nu_1} Q^* F_1''\left(Q^*\right) \\
&- \frac{\overline{\nu_1} Q^* F_1'\left(Q^*\right)}{x^*} - \frac{\nu_1 F_1\left(Q^*\right) e^{i\omega_0 {\tau_j}^0}}{x^*} - \frac{\nu_1 Q^* F_1'\left(Q^*\right)}{x^*})
\end{aligned}
$$

$$
\begin{aligned}
g_{21} = & -\frac{1}{2}D_1''\left(Q^*\right)\nu_1^2+\frac{1}{2}e^{-i\omega_0{\tau_j}^0}F_1''\left(Q^*\right)\nu_1^2-\frac{1}{2}e^{-2i\omega_0{\tau_j}^0}\overline{\nu_1}\overline{\nu_1{}^*}F_1''\left(Q^*\right)\nu_1^2 \\
& -\overline{\nu_1}\overline{\nu_1{}^*}F_1''\left(Q^*\right)\nu_1^2-\frac{e^{-i\omega_0{\tau_j}^0}\overline{\nu_1{}^*}\alpha_2F_1'\left(Q^*\right)\nu_1^2}{x^*}-\frac{e^{-2i\omega_0{\tau_j}^0}\overline{\nu_1{}^*}\alpha_2Q^*F_1''\left(Q^*\right)\nu_1^2}{2x^*} \\
& -e^{-i\omega_0{\tau_j}^0}\alpha_5\nu_1-e^{-i\omega_0{\tau_j}^0}\overline{\nu_1{}^*}\alpha_6\nu_1 \\
& +\frac{e^{-i\omega_0{\tau_j}^0}\overline{\nu_1{}^*}\alpha_1F_1\left(Q^*\right)\nu_1}{\left(x^*\right)^2}+\frac{e^{i\omega_0{\tau_j}^0}\overline{\nu_1}\overline{\nu_1{}^*}F_1'\left(Q^*\right)\nu_1}{x^*}+\frac{e^{-2i\omega_0{\tau_j}^0}\overline{\nu_1}\overline{\nu_1{}^*}\alpha_2F_1'\left(Q^*\right)\nu_1}{x^*} \\
& +\frac{e^{-2i\omega_0{\tau_j}^0}\overline{\nu_1{}^*}\alpha_1Q^*F_1'\left(Q^*\right)\nu_1}{\left(x^*\right)^2}+\frac{e^{-i\omega_0{\tau_j}^0}\overline{\nu_1}\overline{\nu_1{}^*}\alpha_2Q^*F_1''\left(Q^*\right)\nu_1}{x^*}-\frac{\overline{\nu_1}\overline{\nu_1{}^*}F_1'\left(Q^*\right)\nu_1}{x^*} \\
& +\frac{e^{-i\omega_0{\tau_j}^0}\overline{\nu_1{}^*}\alpha_2\alpha_3F_1\left(Q^*\right)}{2x^*}+\frac{\overline{\nu_1{}^*}\alpha_4Q^*F_1\left(Q^*\right)}{2\left(x^*\right)^2}-2\delta{W_{11}}^{(1)}(0)+\frac{i\overline{\nu_1{}^*}\omega_0{W_{11}}^{(1)}(0)}{x^*} \\
& -\delta{W_{20}}^{(1)}(0)-{W_{11}}^{(2)}(0)D_1'\left(Q^*\right)-\frac{1}{2}\overline{\nu_1}{W_{20}}^{(1)}(0)D_1'\left(Q^*\right) \\
& -\frac{1}{2}{W_{20}}^{(2)}(0)D_1'\left(Q^*\right)+e^{-i\omega_0{\tau_j}^0}{W_{11}}^{(2)}(-1)F_1'\left(Q^*\right) \\
& +\frac{e^{-i\omega_0{\tau_j}^0}\overline{\nu_1{}^*}\alpha_2Q^*{W_{11}}^{(2)}(-1)F_1'\left(Q^*\right)}{x^*}+\frac{1}{2}e^{i\omega_0{\tau_j}^0}\overline{\nu_1}{W_{20}}^{(1)}(-1)F_1'\left(Q^*\right) \\
& +\frac{1}{2}e^{i\omega_0{\tau_j}^0}{W_{20}}^{(2)}(-1)F_1'\left(Q^*\right) \\
& -\frac{1}{2}\overline{\nu_1}\overline{\nu_1{}^*}{W_{20}}^{(2)}(-1)F_1'\left(Q^*\right)-\frac{1}{2}e^{i\omega_0{\tau_j}^0}\overline{\nu_1}\overline{\nu_1{}^*}{W_{20}}^{(2)}(0)F_1'\left(Q^*\right) \\
& -\frac{1}{2}\overline{\nu_1}x^*{W_{20}}^{(2)}(0)D_1''\left(Q^*\right) \\
& -\frac{1}{2}e^{i\omega_0{\tau_j}^0}\overline{\nu_1}\overline{\nu_1{}^*}Q^*{W_{20}}^{(2)}(-1)F_1''\left(Q^*\right)+\frac{1}{2}e^{i\omega_0{\tau_j}^0}\overline{\nu_1}x^*{W_{20}}^{(2)}(-1)F_1''\left(Q^*\right) \\
& -\frac{\overline{\nu_1{}^*}\alpha_2Q^*{W_{20}}^{(2)}(-1)F_1'\left(Q^*\right)}{2x^*}+\frac{i\overline{\nu_1{}^*}\omega_0}{\left(x^*\right)^2}-\frac{e^{-i\omega_0{\tau_j}^0}\overline{\nu_1}\overline{\nu_1{}^*}\alpha_7F_1\left(Q^*\right)}{2\left(x^*\right)^2} \\
& -\frac{\overline{\nu_1}\overline{\nu_1{}^*}\alpha_7Q^*F_1'\left(Q^*\right)}{2\left(x^*\right)^2}-\frac{\overline{\nu_1{}^*}3Q^*F_1\left(Q^*\right)}{\left(x^*\right)^3}
\end{aligned}
$$

Where,

$$\alpha_1 = x^* {W_{11}}^{(1)}(-1)\left(-e^{i\omega_0 {\tau_j}^0}\right) + e^{2i\omega_0\ {\tau_j}^0} + 1$$

$$\alpha_2 = e^{i\omega_0 {\tau_j}^0} - 1$$

$$\alpha_3 = 2{W_{11}}^{(2)}(0) - {W_{20}}^{(2)}(0)e^{i\omega_0 {\tau_j}^0}$$

$$\alpha_4 = {W_{20}}^{(1)}(0)e^{i\omega_0 {\tau_j}^0} + 2{W_{11}}^{(1)}(-1) - 2{W_{11}}^{(1)}(0) + {W_{20}}^{(1)}(-1) - 2{W_{20}}^{(1)}(0)$$

$$\alpha_5 = \overline{\nu_1} D_1''(Q^*)\, e^{i\omega_0 {\tau_j}^0} - \overline{\nu_1} F_1''(Q^*) + {W_{11}}^{(1)}(0) D_1'(Q^*)\, e^{i\omega_0 {\tau_j}^0} - {W_{11}}^{(1)}(-1) F_1'(Q^*)$$
$$+ x^* {W_{11}}^{(2)}(0) D_1''(Q^*)\, e^{i\omega_0 {\tau_j}^0} - x^* {W_{11}}^{(2)}(-1) F_1''(Q^*)$$

$$\alpha_6 = F_1'(Q^*)\left({W_{11}}^{(2)}(-1)e^{i\omega_0 {\tau_j}^0} + {W_{11}}^{(2)}(0)\right) + Q^* {W_{11}}^{(2)}(-1) F_1''(Q^*)$$

$$\alpha_7 = x^*\left({W_{20}}^{(1)}(-1) - {W_{20}}^{(1)}(0)\right) e^{i\omega_0 {\tau_j}^0} - 2$$

Since W_{11} and W_{20} are in g_{21} we need to solve for them.

$$\begin{aligned}
\dot{W} &= \dot{x}_t - \dot{z}q - \dot{\bar{z}}\bar{q} \\
&= \begin{cases} AW - 2Re\{\bar{q}^*(0) f_0 q(\theta)\}, & \theta \in [-1, 0) \\ AW - 2Re\{\bar{q}^*(0) f_0 q(\theta)\} + f_0, & \theta = 0 \end{cases} \\
&= AW + H(z, \bar{z}, \theta)
\end{aligned}$$

where,

$$H(z, \bar{z}, \theta) = H_{20}(\theta)\frac{z^2}{2} + H_{11}(\theta) z\bar{z} + H_{02}(\theta)\frac{\bar{z}^2}{2} + \ldots \tag{4.29}$$

Substituting the corresponding series into (14) and comparing the coefficients, we obtain

$$(A - 2i\omega_0\tau_j^0)W_{20}(\theta) = -H_{20}(\theta)$$
$$AW_{11}(\theta) = -H_{11}(\theta)$$

From (a) and (b) we know that for $\theta \in [-1, 0)$.

$$H(z, \bar{z}, \theta) = -\bar{q}^*(0)f_0q(\theta) - q^*(0)\bar{f}_0\bar{q}(\theta) - \bar{g}(z, \bar{z})\bar{q}(\theta) \tag{4.30}$$

Comparing the coefficient with (15) we get:

$$-g_{20}q(\theta) - \bar{g}_{02}\bar{q}(\theta) = H_{20}(\theta)$$
$$-g_{11}q(\theta) - \bar{g}_{11}\bar{q}(\theta) = H_{11}(\theta)$$

From (16) and (18) and the definition of A, it follows that

$$\dot{W}(\theta) = 2i\omega_0\tau_j^0W_{20} + g_{20}q(\theta) + \bar{g}_{02}\bar{q}(\theta) \tag{4.31}$$

Notice that $q(\theta) = (1, \nu_1)^T e^{i\omega_0\tau_j^0\theta}$. Hence,

$$W_{20}(\theta) = \frac{ig_{20}}{\omega_0\tau_j^0}q(0)e^{i\omega_0\tau_j^0\theta} + \frac{i\bar{g}_{02}}{3\omega_0\tau_j^0}\bar{q}(0)e^{-i\omega_0\tau_j^0\theta} + E_1e^{2i\omega_0\tau_j^0\theta} \tag{4.32}$$

where $E_1 = (E_1^{(1)}, E_1^{(2)}) \in \mathbb{R}^2$ is a constant vector. Similarly, from (16) and (19), we obtain

$$W_{11}(\theta) = -\frac{g_{11}}{\omega\tau_j^0}q(0)e^{i\omega_0\tau_j^0\theta} + \frac{i\bar{g}_{11}}{\omega_0\tau_j^0}\bar{q}(0)e^{-i\omega_0\tau_j^0\theta} + E_2 \tag{4.33}$$

where $E_2 = (E_1^{(1)}, E_1^{(2)}) \in \mathbb{R}^2$ is also a constant vector. In what follows, we will seek appropriate E_1 and E_2. From the definition of A and (16), we obtain

$$\int_{-1}^{0} d\eta(\theta)W_{20}(\theta) = 2i\omega_0\tau_jW_{20}(0) - H_{20}(0)$$
$$\int_{-1}^{0} d\eta(\theta)W_{11}(\theta) = -H_{11}(\theta)$$

where $\eta(\theta) = \eta(0, \theta)$. By (14), we have

$$H_{20}(0) = -g_{20}q(0) - \bar{g}_{02}\bar{q}(0) + 2\tau_j^0 \begin{pmatrix} A_1 \\ A_2 \end{pmatrix}$$

where

$$\begin{aligned} A1 = & -\nu_1 D_1'(Q^*) - \frac{1}{2}\nu_1^2 x^* D_1''(Q^*) + \nu_1 F_1'(Q^*) e^{-2i\omega_0 {\tau_j}^0} \\ & + \frac{1}{2}\nu_1^2 x^* F_1''(Q^*) e^{-2i\omega_0 {\tau_j}^0} - \delta \\ A2 = & -\frac{\nu_1 e^{-2i\omega_0 {\tau_j}^0} \left(2F_1(Q^*) e^{i\omega_0 {\tau_j}^0} + 2\nu_1 x^* F_1'(Q^*) e^{i\omega_0 {\tau_j}^0}\right)}{2x^*} \\ & - \frac{\nu_1 e^{-2i\omega_0 {\tau_j}^0} \left(Q^* \left(\nu_1 x^* F_1''(Q^*) + 2F_1'(Q^*)\right)\right) + 2i\omega_0}{2x^*} \end{aligned}$$

$$H_{11}(0) = -g_{11}q(0) - \bar{g}_{11}\bar{q}(0) + 2\tau_j^0 \begin{pmatrix} B_1 \\ B_2 \end{pmatrix}$$

where

$$\begin{aligned} B_1 = & -\overline{\nu_1} D_1'(Q^*) - \nu_1 \overline{\nu_1} x^* D_1''(Q^*) + \overline{\nu_1} F_1'(Q^*) \\ & + \nu_1 \overline{\nu_1} x^* F_1''(Q^*) - \nu_1 D_1'(Q^*) + \nu_1 F_1'(Q^*) - 2\delta \\ B_2 = & \left(-\nu_1 \overline{\nu_1} F_1'(Q^*) e^{-i\omega_0 {\tau_j}^0} - \nu_1 \overline{\nu_1} F_1'(Q^*) e^{i\omega_0 {\tau_j}^0}\right. \\ & \left. - \frac{\overline{\nu_1} F_1(Q^*) e^{-i\omega_0 {\tau_j}^0}}{x^*} - \nu_1 \overline{\nu_1} Q^* F_1''(Q^*)\right. \end{aligned}$$

Substituting (21) and (25) into 23 and noticing that

$$\begin{aligned} \left(i\omega_0 \tau_j^0 I - \int_{-1}^{0} e^{i\omega_0 \tau_j^0 \theta} d\eta(\theta)\right) q(0) = 0 \\ \left(-i\omega_0 \tau_j^0 I - \int_{-1}^{0} e^{-i\omega_0 \tau_j^0 \theta} d\eta(\theta)\right) \bar{q}(0) = 0 \end{aligned}$$

we obtain

$$\left(2i\omega_0\tau_j I - \int_{-1}^{0} e^{2i\omega_0\tau_j^0\theta} d\eta(\theta)\right) E_1 = 2\tau_j^0 \begin{pmatrix} A_1 \\ A_2 \end{pmatrix}$$

This leads to

$$\begin{pmatrix} 2i\omega_0 + D_1(Q^*) + 2\delta x^* - F_1(Q^*)e^{-2i\omega_0\tau_j} & x^* D_1^{'} \\ \frac{Q^*}{x^*} F_1(Q^*)(1 + e^{-2i\omega_0\tau_j}) & F_1(Q^*)(1 + Q^* e^{-2i\omega_0\tau_j}) + 2i\omega_0 \end{pmatrix} E_1$$
$$= 2 \begin{pmatrix} A_1 \\ A_2 \end{pmatrix}$$

Solving this system for E_1 we get

$$E_1 =$$
$$2 \begin{pmatrix} 2i\omega_0 + D_1(Q^*) + 2\delta x^* - F_1(Q^*)e^{-2i\omega_0\tau_j} & x^* D_1^{'} - x^* F_1^{'}(Q^*)e^{-2i\omega_0\tau_j} \\ \frac{Q^*}{x^*} F_1(Q^*)(1 + x^* e^{-2i\omega_0\tau_j}) & F_1(Q^*)(1 + Q^* e^{-2i\omega_0\tau_j}) + 2i\omega_0 \end{pmatrix}^{-1} \times$$
$$\begin{pmatrix} A_1 \\ A_2 \end{pmatrix}$$

Then, we can obtain,

$$\begin{pmatrix} -D_1(Q^*) - 2\delta x^* + F_1(Q^*) & -x^* D_1^{'} + x^* F_1^{'}(Q^*) \\ -\frac{Q^*}{x^*} F_1(Q^*) - Q^* F_1(Q^*) & -F_1(Q^*)(1 + Q^*) \end{pmatrix} E_2 = \begin{pmatrix} B_1 \\ B_2 \end{pmatrix}$$

Which leads to

$$E_2 =$$
$$\begin{pmatrix} -D_1(Q^*) - 2\delta x^* + F_1(Q^*) & -x^* D_1^{'} + x^* F_1^{'}(Q^*) \\ -\frac{Q^*}{x^*} F_1(Q^*) - Q^* F_1(Q^*) & -F_1(Q^*)(1+Q^*) \end{pmatrix}^{-1} \begin{pmatrix} B_1 \\ B_2 \end{pmatrix}$$

Thus, we can determine W_{20} and W_{11} from (21) and (22). Furthermore, $g_{21}z$ in (13) can be expressed by the parameters and delay. Thus, we can compute the following values:

$$C_1(0) = \frac{i}{2\omega\tau_j^0}\left(g_{20}g_{11}|g_{11}|^2 - \frac{||g_{02}|^2}{3}\right) + \frac{g_{21}}{2} \tag{4.34}$$

$$\nu_2 = -\frac{Re\{C_1(0)\}}{Re\{\lambda'(\tau_j^0)\}} \tag{4.35}$$

$$\beta_2 = 2Re\{C_1(0)\} \tag{4.36}$$

$$P_2 = -\frac{I_m\{C_1(0) + \nu_2 I_m\{\lambda'(\tau_j^0)\}}{\omega_0\tau_j^0} \tag{4.37}$$

which determine the qualities of bifurcating periodic solutions in the center manifold at the critical value τ_j^0,

Theorem 4.5.1. *In equations (27-30) the sign of ν_2 determines the direction of the Hopf bifurcation. Thus, if $\nu_2 > 0$, then the Hopf bifurcation is supercritical and the bifurcating periodic solution exists for $\tau > \tau^0$. If $\nu_2 < 0$, then the Hopf bifurcation is subcritical and the bifurcating periodic solution exists for $\tau < \tau^0$. β_2 determines the stability of the bifurcating periodic solution: The bifurcating periodic solutions are stable if $\beta_2 < 0$ and unstable if $\beta_2 > 0$. P_2 determines the period of the bifurcating periodic solutions: the period increases if $P_2 > 0$ and decreases if $P_2 < 0$.*

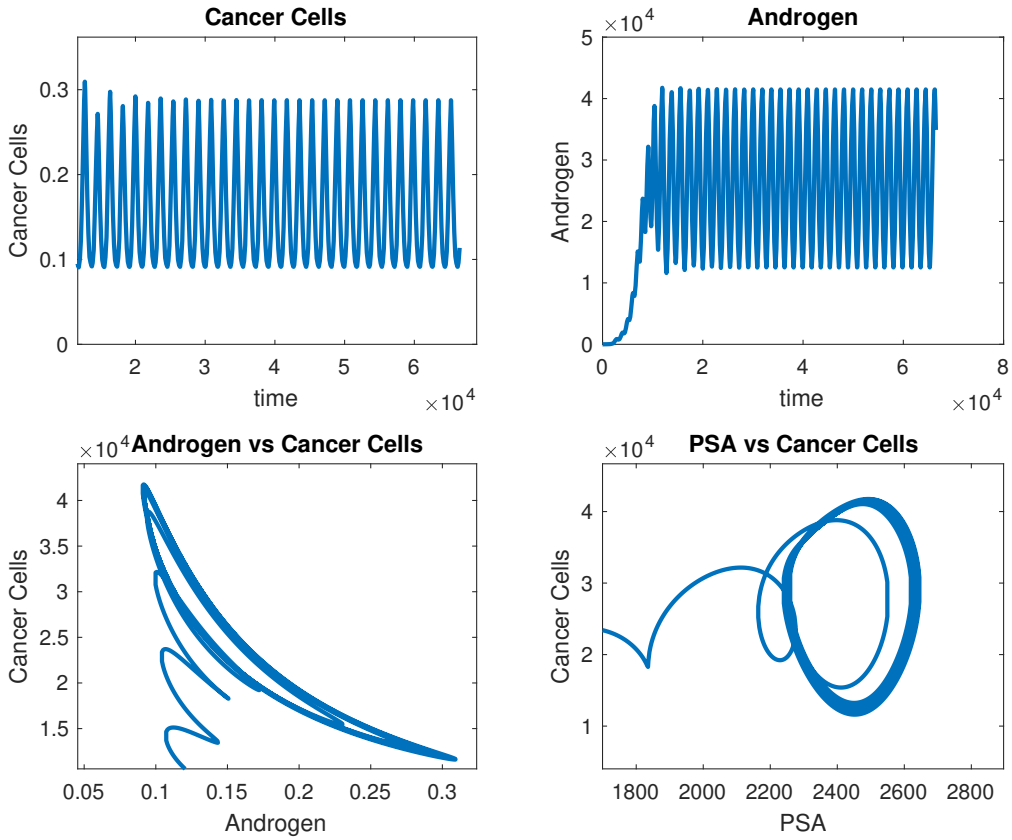

Figure 4.3: Simulation of System 4.12 with $\tau > \tau_j^0$. We Have Emergence of Oscillating Solutions.

4.6 Parameter Estimation

Now we compare models (4.1) and (4.12) ability to estimate clinical data. Figure 4.4 shows a sample data fitting for both models for a single patient. Table 4.2 shows the statistics of the mean square error of PSA and androgen for both models. We can notice that model (4.1) performs consistently better but not at a very significant level. However, Figure 4.5 shows that model (4.12) has an identifiability problem of the time delay. For model (4.1), when all other parameters are fixed, there is a single τ that best fits the data. For model (4.12), under the same conditions, we have multiple values that yield the same MSE. Having multiple time delays that yield the same

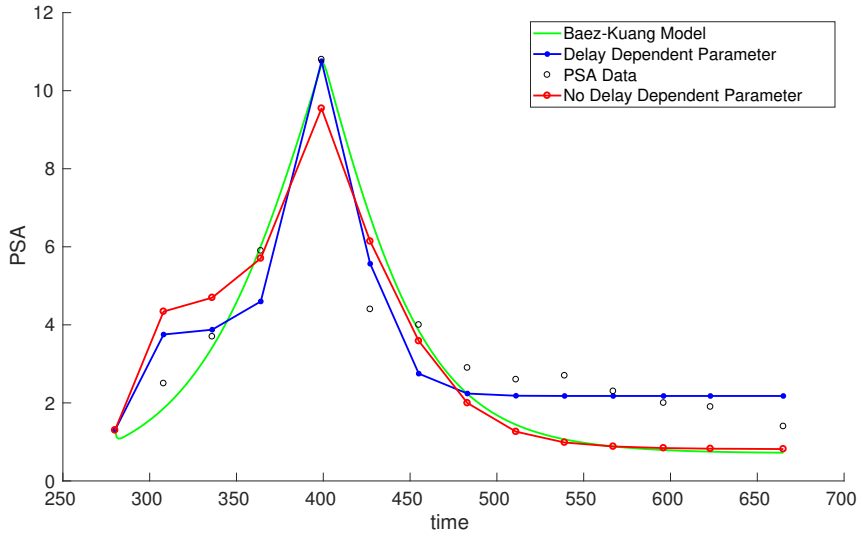

Figure 4.4: Simulation of Data Fitting of PSA for a Single Patient for Baez-Kuang Model (2.2-2.5), Model with Delay Dependent Parameter (4.1), and Model with No Delay Dependent Parameter (4.12). They Can Fit PSA Close to the Same Accuracy but the Model with Delay Dependent Parameter Has Some Improvement Towards the Last Data Points.

Table 4.2: Comparison of MSE for Androgen and PSA for the First 1.5 Cycles.

	PSA			**Androgen**		
	Min	**Mean**	**Max**	**Min**	**Mean**	**Max**
Model 4.1	0.2001	5.6087	22.1370	0.7744	14.0644	45.3743
Model 4.12	0.461	10.3993	30.45	0.7744	15.071	47.3895
Model 2.2-2.5	0.973	8.676	71.847	5.0351	100.10	710.26

MSE means that we cannot draw insights from the delay parameter and defeats the purpose of incorporating the time delay in the first place.

4.7 Conclusion

This work remarked the importance of biological realism. The inclusion of delay dependent parameters shows more complicated and interesting dynamics. In addition,

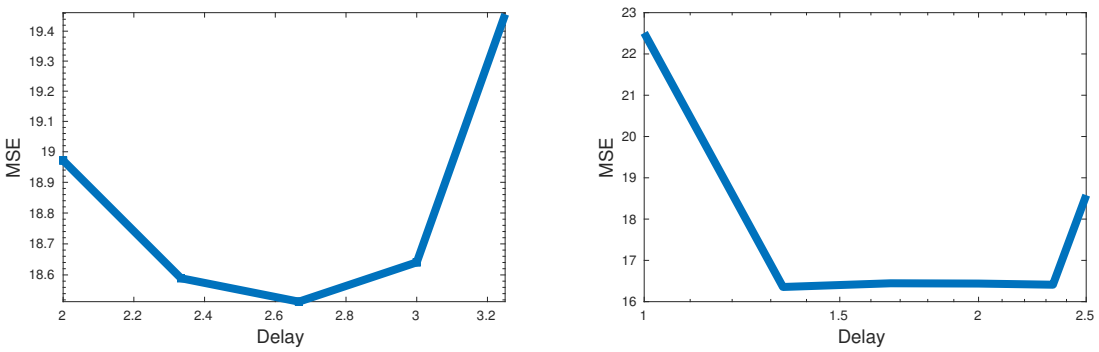

Figure 4.5: Time Delay τ as a Function of MSE. Left:Model 4.1 . Right: Model 4.12. Model 4.1 Has a Unique Minimum and Model 4.1 Does Not.

the biological accuracy of the delay dependent parameter model in turn produced more reliable parameter estimations by allowing better identification of the time delay. By better estimation parameters we were able to have better overall parameter estimations that yielded a Mean Square Error that is superior to the non-delay versions of this model. That is, with a single extra parameter, τ, we are able to improve our data fitting results when we incorporate the delay dependent parameter compared to the Baez-Kuang model 2.2-2.5. Therefore, with this new supporting evidence from clinical data fittings our goal is to extend this work and use an Ensemble Kalman filter to make predictions about resistance using these models.

Chapter 5

DISCUSSION & FUTURE WORK

The main goal of this research is to produce a model that is simple enough to be used by physicians as a treatment tool and has enough biological mechanisms to capture the individual characteristics of each patient in order to provide personalized accurate forecasts of PSA dynamics. In chapter 2, we proposed two novel mathematical models to understand the dynamics of prostate cancer androgen resistance. We provided evidence for the potential that these novel models could provide in assisting physicians predict androgen resistance. Furthermore, these models present a framework where mathematical analysis is more tractable and predictions of resistance could be more reliable as simpler models have less unknown parameters and uncertainty. In chapter 3, we took the models proposed in chapter 2 and tested whether they were reliable in making predictions. First, we did a systematic testing of models in literature and we demonstrated that among the most cited models in literature only the Baez-Kuang model is identifiable. Then we applied the ensemble Kalman filter to estimate the most likely state of the system as well as the most likely parameter that produce those states. In chapter 4, we extended the work of chapter 2 and presented another extension to model prostate cancer dynamics. We included a time delay to model the time it takes for prostate cells to use testosterone for growth. We took two approaches for including the time delay. First, we apply the delay directly without adjusting for the difference in growth at $t-\tau$ with model (4.12). Then we include a delay dependent parameter in model (4.1) to take into account the death at time $t-\tau$. Model (4.1) yielded more interesting dynamics as well as making the time delay identifiable as shown in Figure 4.5.

A model that is able to capture the possible pathways resistance should be ideal if we want to model androgen resistance development in patients. However, in order to make data driven conclusions we must work at the level of detail at which there is data available. We discovered in Chapter 3 that when we model separate population types such as in model 3.16-3.19 we can't identify the populations uniquely. The unidentifiable problem might yield incorrect conclusions about the prognosis of a patient. Therefore, since data is only available for PSA and testosterone serum levels we can only model the proportion of the total population that is becoming resistant over time. That is, we cannot distinguish from sensitive cells having mutations such as in the first four pathways to resistance presented in Chapter 1 or the lurker pathway in which originally present resistant cells take over the tumor as androgen resistance selects for those cells. If data becomes available at a finer scale any future work on this area should include the mechanisms of the different pathways and consider modeling the individual populations.

This work has encompassed a diversity of approaches to modeling androgen resistance in prostate cancer. Even though this work has been extensive there are logical continuation of this work as well as approaches that we did not consider. The first natural extension of Chapter 3 is to make predictions on resistance using an the ensemble Kalman filter via the method proposed in Chapter 2. After the natural continuation a different approach would be to use Machine Learning classification algorithms to make predictions on resistance and presented as a classification problem. However, there is extensive literature that points to this type of algorithms been not as effective when data is as limited as the one we have in this dissertation.

Audoly, S., G. Bellu, L. D'Angiò, M. P. Saccomani and C. Cobelli, "Global identifiability of nonlinear models of biological systems", (2001).

Baek, S. J., B. R. Hunt, E. Kalnay, E. Oott and I. Szunyogh, "Local ensemble Kalman filtering in the presence of model bias", Tellus, Series A: Dynamic Meteorology and Oceanography **58**, 3, 293–306 (2006).

Baez, J. and Y. Kuang, "Mathematical Models of Androgen Resistance in Prostate Cancer Patients under Intermittent Androgen Suppression Therapy", Applied Sciences **6**, 11, 352 (2016).

Banks, H. T., S. Dediu and S. L. Ernstberger, "Sensitivity functions and their uses in inverse problems", Journal of Inverse and Ill-Posed Problems **15**, 7, 683–708 (2007).

Bard, R. L., J. J. Fütterer and D. Sperling, *Image guided prostate cancer treatments* (Springer Science & Business Media, 2013).

Beretta, E. and Y. Kuang, "Modeling and analysis of a marine bacteriophage infection with latency period", Nonlinear Analysis: Real World Applications **2**, 1, 35–74 (2001).

Beretta, E. and Y. Kuang, "Geometric stability switch criteria in delay differential systems with delay dependent parameters", SIAM Journal on Mathematical Analysis **33**, 5, 1144–1165 (2002).

Berges, R. R., J. Vukanovic, J. I. Epstein, M. CarMichel, L. Cisek, D. E. Johnson, R. W. Veltri, P. C. Walsh and J. T. Isaacs, "Implication of cell kinetic changes during the progression of human prostatic cancer", Clinical cancer research **1**, 473–480 (1995).

Bruchovsky, N., L. Klotz, J. Crook, S. Malone, C. Ludgate, W. J. Morris, M. E. Gleave and S. L. Goldenberg, "Final results of the Canadian prospective Phase II trial of intermittent androgen suppression for men in biochemical recurrence after radiotherapy for locally advanced prostate cancer: Clinical parameters", Cancer **107**, 2, 389–395 (2006a).

Bruchovsky, N., L. Klotz, J. Crook, S. Malone, C. Ludgate *et al.*, "Final results of the canadian prospective phase ii trial of intermittent androgen suppression for men in biochemical recurrence after radiotherapy for locally advanced prostate cancer", Cancer **107**, 2, 389–395 (2006b).

Bruchovsky, N., L. Klotz, J. Crook, N. Phillips, J. Abersbach and S. Goldenberg, "Quality of life, morbidity, and mortality results of a prospective phase ii study of intermittent androgen suppression for men with evidence of prostate-specific antigen relapse after radiation therapy for locally advanced prostate cancer", Clinical genitourinary cancer **6**, 1, 46–52 (2008).

Bryce, A. H. and E. S. Antonarakis, "Androgen receptor splice variant 7 in castration-resistant prostate cancer: Clinical considerations", International Journal of Urology **23**, 8, 646–653 (2016).

Carrassi, A. and S. Vannitsem, "State and parameter estimation with the extended Kalman filter: An alternative formulation of the model error dynamics", Quarterly Journal of the Royal Meteorological Society **137**, 655, 435–451 (2011).

Crook, J. M., C. J. O'Callaghan, G. Duncan, D. P. Dearnaley, C. S. Higano, E. M. Horwitz, E. Frymire, S. Malone, J. Chin, A. Nabid, P. Warde, T. Corbett, S. Angyalfi, S. L. Goldenberg, M. K. Gospodarowicz, F. Saad, J. P. Logue, E. Hall, P. F. Schellhammer, K. Ding and L. Klotz, "Intermittent Androgen Suppression for Rising PSA Level after Radiotherapy", New England Journal of Medicine **367**, 10, 895–903 (2012).

Deaths, P. C., "Cancer Statistics , 2011 The Impact of Eliminating Socioeconomic and Racial Disparities on Premature Cancer Deaths", (2011).

Denmeade, S. R. and J. T. Isaacs, "A history of prostate cancer treatment", Nature Reviews Cancer **2**, 5, 389–396 (2002).

Droop, M., "Some thoughts on nutrient limitation in algae1", Journal of Phycology **9**, 3, 264–272 (1973).

Eisenberg, M. C. and M. A.L. Hayashi, "Determining identifiable parameter combinations using subset profiling", Mathematical Biosciences **256**, 116–126 (2014).

Eisenberg, M. C., S. L. Robertson and J. H. Tien, "Identifiability and estimation of multiple transmission pathways in cholera and waterborne disease", Journal of Theoretical Biology **324**, 84–102 (2013).

Everett, R. A., A. M. Packer and Y. Kuang, "Can Mathematical Models Predict the Outcomes of Prostate Cancer Patients Undergoing Intermittent Androgen Deprivation Therapy?", Biophysical Reviews and Letters **09**, 02, 173–191 (2014).

Feldman, B. and D. Feldman, "The development of androgen-independent prostate cancer", Nature Reviews Cancer **1**, 1, 34–45 (2001).

Folkman, J., "New perspectives in clinical oncology from angiogenesis research", European Journal of Cancer **32**, 14, 2534–2539 (1996).

Gleave, M., "Prime time for intermittent androgen suppression", European urology **66**, 2, 240–2 (2014).

Gonnet, P., S. Dimopoulos, L. Widmer and J. Stelling, "A specialized ODE integrator for the efficient computation of parameter sensitivities.", BMC systems biology **6**, 46 (2012).

Gottesman, M. M., "Mechanisms of cancer drug resistance", Annual review of medicine **53**, 1, 615–627 (2002).

Guo, Q., Z. Lu, Y. Hirata and K. Aihara, "Parameter estimation and optimal scheduling algorithm for a mathematical model of intermittent androgen suppression therapy for prostate cancer", Chaos **23**, 4, 43125 (2013).

Hassard, B. D., N. D. Kazarinoff and Y.-H. Wan, *Theory and applications of Hopf bifurcation*, vol. 41 (CUP Archive, 1981).

Heinlein, C. and C. Chang, "Androgen receptor in prostate cancer", Endocrine reviews **25**, 2, 276–308 (2004).

Hirata, Y., K. Akakura, C. S. Higano, N. Bruchovsky and K. Aihara, "Quantitative mathematical modeling of PSA dynamics of prostate cancer patients treated with intermittent androgen suppression", Journal of Molecular Cell Biology **4**, 3, 127–132 (2012a).

Hirata, Y., S. Azuma and K. Aihara, "Model predictive control for optimally scheduling intermittent androgen suppression of prostate cancer", Methods **67**, 3, 278–281 (2014a).

Hirata, Y., S.-i. Azuma and K. Aihara, "Model predictive control for optimally scheduling intermittent androgen suppression of prostate cancer", Methods **67**, 3, 278–281 (2014b).

Hirata, Y., N. Bruchovsky and K. Aihara, "Development of a mathematical model that predicts the outcome of hormone therapy for prostate cancer", Journal of Theoretical Biology **264**, 2, 517–527 (2010).

Hirata, Y., G. Tanaka, N. Bruchovsky and K. Aihara, "Mathematically modelling and controlling prostate cancer under intermittent hormone therapy", Asian Journal of Andrology **14**, 2, 270–277 (2012b).

Holohan, C., S. Van Schaeybroeck, D. B. Longley and P. G. Johnston, "Cancer drug resistance: an evolving paradigm", Nature reviews. Cancer **13**, 10, 714 (2013).

Hunt, B. R., E. J. Kostelich and I. Szunyogh, "Efficient data assimilation for spatiotemporal chaos: A local ensemble transform Kalman filter", Physica D: Nonlinear Phenomena **230**, 1-2, 112–126 (2007).

Hussain, M., C. Tangen, D. Berry, C. Higano, E. Crawford *et al.*, "Intermittent versus continuous androgen deprivation in prostate cancer", New England Journal of Medicine **368**, 14, 1314–1325 (2013).

Ideta, A., G. Tanaka, T. Takeuchi and K. Aihara, "A mathematical model of intermittent androgen suppression for prostate cancer", Journal of nonlinear science **18**, 6, 593–614 (2008).

Jackson, T., "A mathematical model of prostate tumor growth and androgen-independent relapse", Discrete and Continuous Dynamical Systems - Series B **4**, 1, 187–201 (2003).

Jackson, T., "A mathematical investigation of the multiple pathways to recurrent prostate cancer: Comparison with experimental data", Neoplasia **6**, 697–704 (2004a).

Jackson, T., "A mathematical model of prostate tumor growth and androgen-independent relapse", Discrete and Continuous Dynamical Systems - B **4**, 1, 187–202 (2004b).

Jacquez, J. A. and P. Greif, "Numerical parameter identifiability and estimability: Integrating identifiability, estimability, and optimal sampling design", Mathematical Biosciences **77**, 1-2, 201–227 (1985).

Jain, H., S. Clinton, A. Bhinder and A. Friedman, "Mathematical modeling of prostate cancer progression in response to androgen ablation therapy", Proceedings of the National Academy of Sciences **108**, 49, 19701–19706 (2011).

Jain, H. and A. Friedman, "Modeling prostate cancer response to continuous versus intermittent androgen ablation therapy", Discrete and Continuous Dynamical Systems - B **18**, 4, 945–967 (2013a).

Jain, H. and A. Friedman, "A partial differential equation model of metastasized prostatic cancer", Mathematical Biosciences and Engineering **10**, 3, 591–608 (2013b).

Jazwinski, A. H., *Stochastic processes and filtering theory* (Courier Corporation, 2007).

Karantanos, T., C. P. Evans, B. Tombal, T. C. Thompson, R. Montironi and W. B. Isaacs, "Understanding the mechanisms of androgen deprivation resistance in prostate cancer at the molecular level", European urology **67**, 3, 470–9 (2015).

Khayat, D. and G. Hortobagyi, *Progress in Anti-Cancer Chemotherapy*, no. v. 4 in Progress in Anti-Cancer Chemotherapy (Springer Paris, 2013).

Klotz, L. and P. Toren, "Androgen deprivation therapy in advanced prostate cancer: is intermittent therapy the new standard of care?", Current Oncology **19**, Suppl 3, S13 (2012).

Kuang, Y., *Delay differential equations: with applications in population dynamics*, vol. 191 (Academic Press, 1993).

Kuang, Y., J. Nagy and S. Eikenberry, *Introduction to Mathematical Oncology* (CRC Press, 2016).

Lahoz, W., B. Khattatov and R. Ménard, "Data assimilation: Making sense of observations", Data Assimilation: Making Sense of Observations pp. 1–718 (2010).

Miao, H., X. Xia, A. S. Perelson and H. Wu, "On Identifiability of Nonlinear ODE Models and Applications in Viral Dynamics", SIAM Review **53**, 1, 3–39 (2011).

Moradkhani, H., S. Sorooshian, H. V. Gupta and P. R. Houser, "Dual state-parameter estimation of hydrological models using ensemble Kalman filter", Advances in Water Resources **28**, 2, 135–147 (2005).

Morken, J., A. Packer, R. Everett, J. Nagy and Y. Kuang, "Mechanisms of resistance to intermittent androgen deprivation in patients with prostate cancer identified by a novel computational method", Cancer Research **74**, 14, 3673–3683 (2014).

Nishiyama, T., "Serum testosterone levels after medical or surgical androgen deprivation: a comprehensive review of the literature.", Urologic oncology **32**, 1, 38.e17–28 (2013).

Portz, T., Y. Kuang and J. D. Nagy, "A clinical data validated mathematical model of prostate cancer growth under intermittent androgen suppression therapy", AIP Advances **2**, 1, 0–14 (2012).

Quaiser, T. and M. Monnigmann, "Systematic identifiability testing for unambiguous mechanistic modeling - application to JAK-STAT, MAP kinase, and NF-κB signaling pathway models", BMC Systems Biology **3**, 50 (2009).

Raue, A., J. Karlsson, M. P. Saccomani, M. Jirstrand and J. Timmer, "Comparison of approaches for parameter identifiability analysis of biological systems", Bioinformatics **30**, 10, 1440–1448 (2014).

Raue, A., C. Kreutz, T. Maiwald, J. Bachmann, M. Schilling, U. Klingmüller and J. Timmer, "Structural and practical identifiability analysis of partially observed dynamical models by exploiting the profile likelihood", Bioinformatics **25**, 15, 1923–1929 (2009).

Rodriguez-Fernandez, M., J. a. Egea and J. R. Banga, "Novel metaheuristic for parameter estimation in nonlinear dynamic biological systems.", BMC bioinformatics **7**, 483 (2006).

Roy, A. and B. Chatterjee, "Androgen action.", Critical reviews in eukaryotic gene expression **5**, 2, 157–176 (1995).

Saccomani, M. P. and L. D'Angiò, "Examples of testing global identifiability with the DAISY software", IFAC Proceedings Volumes (IFAC-PapersOnline) **15**, PART 1, 48–53 (2009).

Shafi, A., A. Yen and N. Weigel, "Androgen receptors in hormone-dependent and castration-resistant prostate cancer", Pharmacology & Therapeutics **140**, 3, 223–238 (2013).

Suzuki, Y., D. Sakai, T. Nomura, Y. Hirata and K. Aihara, "A new protocol for intermittent androgen suppression therapy of prostate cancer with unstable saddle-point dynamics", Journal of Theoretical Biology **350**, 1–16 (2014).

Swanson, K., L. True, D. Lin, K. Buhler, R. Vessella and J. Murray, "A quantitative model for the dynamics of serum prostate-specific antigen as a marker for cancerous growth: an explanation for a medical anomaly", The American journal of pathology **158**, 2195–2199 (2001).

Tao, Y., Q. Guo and K. Aihara, "A partial differential equation model and its reduction to an ordinary differential equation model for prostate tumor growth under intermittent hormone therapy", Journal of Mathematical Biology pp. 1–22 (2013).

Tilley, W. D., G. Buchanan, T. E. Hickey and J. M. Bentel, "Mutations in the androgen receptor gene are associated with progression of human prostate cancer to androgen independence.", Clinical Cancer Research **2**, 2, 277–285 (1996).

Tsao, C.-K., A. Small, M. Galsky and W. Oh, "Overcoming castration resistance in prostate cancer", Current opinion in urology **22**, 3, 167–74 (2012).

Vollmer, R., "Tumor length in prostate cancer", Am J Clin Pathol pp. 77–82 (2008).

Wu, H., H. Zhu, H. Miao and A. S. Perelson, "Parameter identifiability and estimation of HIV/AIDS dynamic models", Bulletin of Mathematical Biology **70**, 3, 785–799 (2008).

Yang, X. and T. Delsole, "Using the ensemble Kalman filter to estimate multiplicative model parameters", Tellus, Series A: Dynamic Meteorology and Oceanography **61**, 5, 601–609 (2009).

Yue, H., M. Brown, J. Knowles, H. Wang, D. S. Broomhead, D. B. Kell, S. Broomhead and D. B. Kell, "Insights into the behaviour of systems biology models from dynamic sensitivity and identifiability analysis: a case study of an NF-kappaB signalling pathway.", Molecular bioSystems **2**, 12, 640–649 (2006).

APPENDIX A

CODE FOR CHAPTER 2

```
function fitting_all
%{
This files takes the patients numbers from variable LIST and performs parameter
estimation using fmincon. Parameters are stored for each patient in p#.mat, and for
every patient in par_all.mat.

Parameter estimation can be done for one_pop,two_pop,portz,and hirata models.

Created by Javier Baez Sep 2016
%}

for yy = 4
% model = 'one_pop';                              % Choose which model to run fittings
n = 3;                                            % number of periods to fit

if yy == 1
model = 'one_pop';
elseif yy == 2
model = 'two_pop';
elseif yy == 3
model = 'portz';
elseif yy == 4
model = 'hirata';
end

switch model                                     % Number of parameters
case 'one_pop'
nParams = 12;
case 'two_pop'
nParams = 20;
case 'hirata'
nParams = 10;
case 'portz'
nParams = 21;
otherwise
warning('Unexpected model, choose a different one')
return;
end
%%%%%%%%% Initialization of arrays and variables %%%%%%%%%%%%%
LIST = [1,2,6,7,12,14:17,19,24:25,28:32,36:37,39:42,...
44,51:52,54,55,58,60:64,66,71,75,...
77:79,83:88,91,93:97,99:102,104:109]; % patient numbers
totalPatients = length(LIST);     % total number of patients
patients = cell(1,62);      % creates a cell array to hold patient data
counter = 1;     % counter for patients and change array
ind = cell(1,totalPatients);   % initializes the index for the S structure
change = ones(1,n+1);         % vector stores times when treatment changed
par_store = zeros(nParams,totalPatients);  % used to store parameter values for each fit
options = optimset('Algorithm','interior-point','TolX',1e-13...
,'TolFun',1e-13,'TolCon',1e-13,'MaxIter',1000);    % Optimizer Options
```

```
%%%%%%%% Creates Structure to store all patient data %%%%%%%%%%%
for ii = LIST;
patient = strcat('patient',num2str(ii));   % Patient with corresp number
file = strcat('Data/',patient,'.txt');     % Complete name of file
    patient#.txt
var = load(file);                          % holds variable just loaded
patients(counter) = {var};                 % stores patient data into
    cell patients
x = strcat('a',num2str(counter));          % Creates index for
    structure S
ind{counter} = x;                          % puts all indexed in ind
    cell array
counter = counter+ 1;                      % increases counter
end
S = cell2struct(patients,ind,2);              % cell to structure
%%%%%%%%%% Runs the fitting for the selected patients %%%%%%%%
for i =1:totalPatients
try                                % In case of error for loop will move
    to next iteration
name = ['p',num2str(LIST(i))];     % where parameters will be saved
index = char(ind(i));              % Index to calll specific patients
patient = S.(index);               % calls specific patient from list S
t = patient(:,2);                  % time vector in days
psa = patient(:,3);                % psa vector of values
androgen= patient(:,4);            % androgen vector of value
treatment = patient(:,6);          % treatment vector of values
%%%%%%%%%%%%%%%% Finds periods of on and off treatment %%%%%%%%%
jj = 1;
change(1) = 1;                            % Treatment starts at t = 0
for a = 1:length(treatment)
if treatment(a) ~= mod(jj,2) % When treatment change occurs
jj = jj + 1;
change(jj) = a;            % Stores time in change vector
end
end
change(jj+1) = length(treatment);      % Last day of treatment
%%%%%%%%%%%%%%%%%%%%%% Bounds For Parameters %%%%%%%%%%%
switch model
case 'one_pop'
a = max(androgen(change(2):change(4)));
% um              % q             % R                % d            % dd
            % gamma1
LB(1) = 0.01;  LB(2) = 0;     LB(3) =0;         LB(4) = 0;     LB(5) =
    0.000001; LB(6) = 18;
UB(1) = .1;     UB(2) = .5;    UB(3) = 1;        UB(4) = .01;  UB(5) =
    .00009;   UB(6) = 21;
% gamma2         % Qmax         % b              % sigma        % epsilon
          % u
LB(7) = 0;       LB(8) = a-4;  LB(9) = 0;       LB(10) = 0;    LB(11) =
    .01;      LB(12) = 0;
UB(7) = .001;    UB(8) = a;     UB(9) = 0.0025; UB(10) = 1;    UB(11) = 1;
          UB(12) = 0;
x0 = [androgen(1);100;psa(1);.09]; %collects init cond in a column
    vector
case 'two_pop'
a = max(androgen);
b = min(androgen(change(1):change(4)));
```

```
% um              % q1              % q2              % c1
LB(1) = 0.01;     LB(2) = b+.1;     LB(3) = 0;        LB(4) = 0.00001;
UB(1) = 0.1;      UB(2) = b+.5;     UB(3) = b +.1;    UB(4) = .0001;
%  c2             %  K1             % K2              % b
LB(5) = 0.00001; LB(6) = 0;         LB(7) = 0;        LB(8) = 0;
UB(5) = 0.0001;  UB(6) = 1;         UB(7) = 1;        UB(8) = 0.0025;
%  sigma1         % epsilon         % d1              % d2
LB(9) = 0;        LB(10) = 0.01;    LB(11) = 0.002;   LB(12) = 0;
UB(9) = 1;        UB(10) = 1;       UB(11) = .09;     UB(12) = .001;
%  R1             %  R2              % gamma1         %  gamma2
LB(13) = 0;       LB(14) = 0;        LB(15) = 20;     LB(16) = 0;
UB(13) = 3;       UB(14) = 3;        UB(15) = 20;     UB(16) = .001;
% dd1                % dd2                % Qm              % parameter u
LB(17) = 0.000001;  LB(18) = 0.000001;    LB(19) = a - 4;  LB(20) = 0;
UB(17) = .00009;    UB(18) = .00009;      UB(19) = a;      UB(20) = 0;
x0 = [androgen(1);99;1;psa(1)]; %collects init cond in a column vector
case 'hirata'
% Taken from Everett et. al.
% w11o          % w21          % w22o          % w31          % w32
    w33o
LB(1) = -.15;  LB(2) = .0006; LB(3) = -.015; LB(4) = .0003; LB(5) = 0;
    LB(6) = 0.002;
UB(1) = -.015; UB(2) = .002;  UB(3) = .0009; UB(4) = .001;  UB(5) = 0;
    UB(6) = 0.003;
% w11f           % w12f          % w22f             % w33f
LB(7) = .001;   LB(8) = .049;  LB(9) = 0.002;    LB(10) = -.13;
UB(7) = .003;   UB(8) = .18;   UB(9) = 0.008;    UB(10) = -0.0044;
x0 = [psa(1)*.95;psa(1)*.05;0]; %collects init cond in a column vector
case 'portz'
% um            % qx          % qy          % dx           % dy
        % c1
LB(1) = 0.01; LB(2) = .175;  LB(3) = .1;   LB(4) = 0.15; LB(5) = 0.215;
      LB(6) = .01;
UB(1) = .1;  UB(2) = .29;  UB(3) = .21;   UB(4) = .4;   UB(5) = .4;
    UB(6) = .015;
% Kxyn          % c2           % Kyxn           % n          % qm
        % vm
LB(7) = .05;   LB(8) = .01;  LB(9) = 1.2;    LB(10) = 1;  LB(11) = 2;
    LB(12) = .075;
UB(7) = .08;   UB(8) = .015;  UB(9) = 1.7;    UB(10) = 1;  UB(11) = 5;
     UB(12) = .275;
% vh          % b            % sigmax       % sigmay          %  rhoxm
           % rhoym
LB(13) =  2;   LB(14) = 0.02; LB(15) = 0 ;  LB(16) = 0;    LB(17) = .3;
        LB(18) = 1;
UB(13) = 4;   UB(14) = 0.09;  UB(15) = .4;   UB(16) = .4;    UB(17) =
    1.3;     UB(18) = 1.3;
% m           % sigma0        % delta
LB(19) = 1;   LB(20) = 0;     LB(21) = 0.008;
UB(19) = 1;   UB(20) = .04;   UB(21) = 0.08;
x0 = [99;1;.5;.5;psa(1)];
end
%%%%%%%%%%%%%%%%%%%%%% Optimization Step
    %%%%%%%%%%%%%%%%%%%%%%%%%%%%%%%%%%
IC = UB; % initial parameter values
[params,~] =
    fmincon(@(params)objective(params,psa,androgen,t,change,x0,n,model)...
```

```
,IC,[],[],[],[],LB,UB,[],options); % Finds optimized parameters
%%%%%%%%%%%%%%%%%%%%%%%%%%%%%%%%%%%%%%%%%%%%%%%%%%%%%
par_store(:,i) = params; % stores parameters in a matrix to be used later for predictions and errors
cd(strcat('parameters_',model))
save(name,'params')      % saves parameters for individual patients in file p(patient#).mat
cd ..
catch ME
disp(ME)         % If an error occurs it will be displayed
end

end

%%
save(strcat('par_all_',model,'.mat'),'par_store') % saves the matrix of all patients parameter values
end
end

%%%%%%%%%%%%%%%% Minimizes the Error %%%%%%%%%%%%%%%%%%%%%%%%%%%%%%%%%%%%%%%%
function [err]= objective(params,psadata,and_data,tdata,change,x0,n,model)
%{
This function serves as the objective function that fmincon uses to find
optimal parameter values.
params  =  vector of parameters to fit
psadata =  psa data
change  =  vecotor that with the time steps at which treatmet is switched
tdata   =  time data
n       =  the number of periods of treatment to fit
%}
psadata = psadata(change(1):change(n+1));
and_data = and_data(change(1):change(n+1));
[Y1run] = run_model(params,tdata,change,x0,n,model,and_data);

switch model
case 'one_pop'
PSA = Y1run(:,3);
AND = Y1run(:,1);
errp = sum((PSA-psadata).^2/length(PSA));
erra = sum((AND-and_data).^2/length(AND));
err = errp + erra;
fprintf('PSA Error = %.4f \t Androgen Error = %.4f \n',errp, erra);

case 'two_pop'
PSA = Y1run(:,4);
AND = Y1run(:,1);
errp = sum((PSA-psadata).^2/length(PSA));
erra = sum((AND-and_data).^2/length(AND));
err = errp + erra;
fprintf('PSA Error = %.4f \t Androgen Error = %.4f \n',errp, erra);

case 'portz'
PSA = Y1run(:,5);
```

```
err = sum((PSA-psadata).^2/length(PSA));
fprintf('PSA Error = %.4f \n',err);

case 'hirata'
PSA = Y1run(:,1) + Y1run(:,2) + Y1run(:,3);
err = sum((PSA-psadata).^2/length(PSA));
fprintf('PSA Error = %.4f \n',err);

end
end
%%%%%%%%%%%%%%%% Runs the Model and Generates synthetic data %%%%%%%%%%%%
function [y] = run_model(params,tdata,change,x0,n,model,androgen)
y = [];                                     % Initial vector for solution
tint = tdata(change(n+1));                  % Time interval to run solution
for k = 1:n                                 % K number of cycles of treatment
u = 1 - mod(k,2);
switch model
case 'one_pop'
if tint(end) >= tdata(change(k))
[~,Yrun]=ode15s(@(t,x) one_pop(t,x,[params(1:end-1),u]) ,...
tdata(change(k):change(k+1)),x0);
x0 = [Yrun(end,1);Yrun(end,2);Yrun(end,3);Yrun(end,4)];
if k < n
y = [y; Yrun(1:end-1,:)]; %#ok<AGROW>
elseif k == n
y = [y; Yrun(1:end,:)];   %#ok<AGROW>
end
end
case 'two_pop'
if tint(end) >= tdata(change(k))
[~,Yrun]=ode15s(@(t,x) two_pop(t,x,[params(1:end-1),u]) ,...
tdata(change(k):change(k+1)),x0);
x0 = [Yrun(end,1);Yrun(end,2);Yrun(end,3);Yrun(end,4)];
if k < n
y = [y; Yrun(1:end-1,:)]; %#ok<AGROW>
elseif k == n
y = [y; Yrun(1:end,:)];   %#ok<AGROW>
end
end
case 'portz'
if tint(end) >= tdata(change(k))
%                   options = odeset('AbsTol',1e-14,'RelTol',1e-14);
[~,Yrun]=ode23tb(@(t,x)
    portz(t,x,params,androgen,change(k):change(k+1)) ,...
tdata(change(k):change(k+1)),x0);
x0 = [Yrun(end,1);Yrun(end,2);Yrun(end,3);Yrun(end,4);Yrun(end,5)];
if k < n
y = [y; Yrun(1:end-1,:)]; %#ok<AGROW>
elseif k == n
y = [y; Yrun(1:end,:)];   %#ok<AGROW>
end
end
case 'hirata'
```

```
if tint(end) >= tdata(change(k))
[~,Yrun]=ode15s(@(t,x) hirata(t,x,params,u) ,...
tdata(change(k):change(k+1)),x0);
x0 = [Yrun(end,1);Yrun(end,2);Yrun(end,3)];
if k < n
y = [y; Yrun(1:end-1,:)]; %#ok<AGROW>
elseif k == n
y = [y; Yrun(1:end,:)];    %#ok<AGROW>
end
end
end
end
end
% model ODE functions
function dxdt = one_pop(~,x,p)
% collect parameter values to pass to ODE function
mu = p(1);        q = p(2);       R = p(3);   d = p(4); dd = p(5);
gamma1 = p(6);    gamma2 = p(7); Qm = p(8); b = p(9); sigma = p(10);
epsilon = p(11); u = p(12);
%separates solutions
Q = x(1); X = x(2); P = x(3);V = x(4);
%%%%%%%%%%%%%%%%%%% ODE system %%%%%%%%%%%%%%%%%%%%%%%%%%%%%%%%%%%%%%%%%%%%%%%%
dX = mu*(1-q/Q)*X - V*R*X/(Q+R)- abs(dd)*X^2;
dA = (gamma1*u +gamma2)*(Qm -Q)- mu*(Q-q);
dP = abs(b)*Q + abs(sigma)*X*Q - abs(epsilon)*P;
dV = -d*V;
%%%%%%%%%%%%%%%%%%%%%%%%%%%%%%%%%%%%%%%%%%%%%%%%%%%%%%%%%%%%%%%%%%%%%%%%%%%%%%
dxdt = [dA; dX; dP; dV]; %Puts the ode in a column vector
end

function dxdt = two_pop(~,x,p)
% collect parameter values to pass to ODE function
um = p(1);          q1= p(2);          q2= p(3);       c1= p(4);          c2=
    p(5);  K1= p(6);
K2= p(7);          b= p(8);          sigma1= p(9);   epsilon= p(10);    d1=
    p(11);  d2= p(12);
R1= p(13);          R2= p(14);         gamma1= p(15); gamma2= p(16);     dd1
    = abs(p(17));
dd2 = abs(p(18)); Qm = abs(p(19)); u= p(20);
%separates solutions
Q = x(1); X = x(2); Y = x(3); P = x(4);
%%%%%%%%%%%%%%%%%%%  Parameters for ODE System
    %%%%%%%%%%%%%%%%%%%%%%%%%%%%
if q1>Q
ux = 0;
else
ux = abs(um)*(1 - abs(q1)/Q);
end
if q2 > Q
uy = 0;
else
uy = abs(um)*(1 - abs(q2)/Q);
end
Dx = abs(d1)*R1/(Q+R1);      Dy = abs(d2)*R2/(Q+R2);
mxy = abs(c1)*K1/(Q + K1); myx = abs(c2)*Q/(Q + K2);
%%%%%%%%%%%%%%%%%%% ODE system %%%%%%%%%%%%%%%%%%%%%%%%%%%%%%%%%%%%%%%%%%%%%%%%
dX = (ux - Dx  - abs(dd1)*X -  mxy)*X + myx*Y;
```

```
dY = (uy - Dy  - abs(dd2)*Y - myx)*Y + mxy*X;
dA = (abs(gamma1)*u +abs(gamma2))*(Qm -Q) - (ux*Q*X + uy*Q*Y)/(X+Y);
dP = b*Q + sigma1*(Y*Q + X*Q) - epsilon*P;
%%%%%%%%%%%%%%%%%%%%%%%%%%%%%%%%%%%%%%%%%%%%%%%%%%%%%%%%%%%%%%%%%%%%%%%%%%%%
dxdt = [dA; dX; dY;dP]; %Puts the ode in a column vector
end

function dxdt = hirata(~,x,p,treat)
% collect parameter values to pass to ODE function
w110 = p(1);    w11f = p(7);
w21  = p(2);    w12f = p(8);
w220 = p(3);    w22f = p(9);
w31 = p(4);     w33f = p(10);
w32 = p(5);
w33 = p(6);
%separates solutions
X1 = x(1); X2 = x(2); X3 = x(3);
%%%%%%%%%%%%%%%%%%%% ODE system %%%%%%%%%%%%%%%%%%%%%%%%%%%%%%%%%%%%%%%%%%%%
if treat == 0
%%%%%%%%%%%%%%%%%%%% On Treatment %%%%%%%%%%%%%%%%%%%%%%%%%%%%%%%%%%%%%%%%%%
dX1 = w110*X1;
dX2 = w21*X1 + w220*X2;
dX3 = w31*X1 + w32*X2 + w33*X3;
%%%%%%%%%%%%%%%%%%%% Of Treatment %%%%%%%%%%%%%%%%%%%%%%%%%%%%%%%%%%%%%%%%%%
elseif treat == 1
dX1 = w11f*X1;
dX2 = w12f*X1 + w22f*X2;
dX3 = w33f*X3;
end
dxdt = [dX1; dX2; dX3]; %Puts the ode in a column vector
end

function dxdt = portz(t,x,p,androgen,trange)
% Parameter Values
um = p(1);      qx = p(2);      qy = p(3);      dx = p(4);      dy = p(5);
        c1 = p(6);
Kxyn = p(7);    c2 = p(8);     Kyxn = p(9);     n = p(10);      qm =
    p(11);     vm = p(12);
vh = p(13);     b = p(14);     sigmax = p(15);  sigmay = p(16);rhoxm =
    p(17); rhoym = p(18);
m = p(19);    sigma0 = p(20); delta  = p(21);
%separates solutions
X = x(1); Y = x(2); Qx = x(3); Qy = x(4); P = x(5);
% Androgen function constructed from data
A = androgen(trange(end)) +
    (androgen(trange(1))-androgen(trange(end)))*exp(-(t-trange(1)));
% Combines parameters to form expressions used in model
Qxn = Qx^n; Qyn = Qy^n;
Qxm = Qx^m; Qym = Qx^m;
ux = um*(1 - qx/Qx);
uy = um*(1 - qy/Qy);
mxy = c1*Kxyn/(Qxn + Kxyn);
myx = c2*Qyn/(Qyn + Kyxn);
vx = ((qm - Qx)/(qm - qx))*vm*(A/(A + vh));
vy = ((qm - Qy)/(qm - qy))*vm*(A/(A + vh));
% Portz et. al. Model
dX = (ux - dx - mxy)*X + myx*Y;
```

```
348 dY = (uy - dy - myx)*Y + mxy*X;
349 dQx = vx - ux*Qx - b*Qx;
350 dQy = vy - uy*Qy - b*Qy;
351 dP = sigmax*X*Qxm/(Qxm + rhoxm) + sigmay*Y*Qym/(Qym + rhoym) +
        sigma0*(X + Y) - delta*P;
352 %Puts the ode in a column vector
353 dxdt = [dX; dY; dQx; dQy; dP];
354 end
```

APPENDIX B

LOCAL IDENTIFIABILITY USING THE FISHER INFORMATION MATRIX

Lets expand equation 3.2 about an initial estimate of parameters $\mathbf{p_0}$ via Taylor series:

$$\mathbf{y}(t_i) = \mathbf{H}(\mathbf{x}(t_i), \mathbf{p_0}) + \sum_{j=1}^{n} \frac{\partial H_i^0}{\partial p_j} \Delta p_j + \epsilon_i$$

Here, $\frac{\partial H_i^0}{\partial p_j}$ is the derivative evaluated at $\mathbf{p_0}$. The error of high order terms is contained in ϵ_i. Then, the sum of squared deviations is given by:

$$A = \sum_{i=1}^{n} [y_i - H_i^0 - \sum_{j=1}^{q} \frac{\partial H_i^0}{\partial p_j} \Delta p_j]^2,$$

A is simply the square of the sum of the higher order terms in the Taylor expansion. The number n is the number of observations. That is A is zero at $\mathbf{p} = \mathbf{p_0}$. Taking the derivative with respect to Δp_k of A and setting equal to zero gives the normal equations for estimates $\hat{\Delta p_k}$.

$$\sum_{j=1}^{q} \sum_{i=1}^{n} \frac{\partial H_i^0}{\partial p_j} \frac{\partial H_i^0}{\partial p_k} \hat{\Delta p_j} = \sum_{i=1}^{n} (y_i - H_i^0) \frac{\partial H_i^0}{\partial p_k}, k = 1, \ldots, p$$

Let $z_i = y_i - H_i^0$, so $z = (z_1, \ldots, z_n)^T$, $\hat{\Delta p} = (\hat{\Delta p_1}, \ldots, \hat{\Delta p_q})^T$. Define the matrix S by

$$S = \begin{pmatrix} s_{11}(t_i) & \ldots & s_{1,n}(t_i) \\ \vdots & \ddots & \vdots \\ s_{m,1}(t_i) & \ldots & s_{m,n}(t_i) \end{pmatrix}$$

where,

$$s_{ij}(t_k) = \frac{\partial H_i(t, \mathbf{p})}{\partial p_j}. \tag{B.1}$$

The sum of squares and normal equations are then given by

$$A = (z - S\Delta\theta)^T (z - S\Delta\theta) \tag{B.2}$$

$$S^T S \hat{\Delta\theta} = S^T z \tag{B.3}$$

The rank of $S^T S$ determines model identifiability. If one of the parameters does not appear in the observations. For example p_j. Then, $\frac{\partial H_i^0}{\partial p_i} = 0$ for $i = 1, \ldots, n$. In consequence, column j of S is null, so row j and column j of $S^T S$ are null and $|S^T S| = 0$. It happens that $|S^T S| \neq 0$ is a sufficient not necessary condition for local model identifiability (Jacquez and Greif (1985)). If a system has $|S^T S| \neq 0$ then as a consequence all of its parameters are observable. Then, we shall look at the correlations between the parameters.

APPENDIX C

GLOBAL IDENTIFIABILITY USING TRANSFER FUNCTIONS

Since Hirata's Model is linear we can use the transfer function method for parameter identifiability (Jacquez and Greif (1985)). Let us express Hirata's model as

$$\begin{aligned} \dot{\mathbf{x}} &= \mathbf{A}\mathbf{x} && \text{(C.1)} \\ \mathbf{x}(0) &= [x_{01}, x_{02}, x_{03}]^T && \text{(C.2)} \\ y(t) &= x_1(t) + x_2(t) + x_3(t) && \text{(C.3)} \end{aligned}$$

where $\mathbf{x}$ is a 3 dimensional vector with components x_1, x_2, and x_3. $\mathbf{A}$ is a 3x3 matrix and the output is denoted by $y(t)$. We study Hirata's off-treatment phase given by eq 3.9. We can solve for $\mathbf{x}(t)$ analytically, and apply the Laplace transformation to obtain:

$$\begin{aligned} \phi(s) = & \quad L\{y\}(s) \\ = & \quad \frac{x_{01}}{s - w_{11}^0} + \frac{x_{02}}{s - w_{22}^0} + \frac{x_{02} w_{12}^0}{(s - w_{11}^0)(w_{11}^0 - w_{22}^0)} \\ & - \frac{x_{02} w_{12}^0}{(s - w_{22}^0)(w_{11}^0 - w_{22}^0)} + \frac{x_{03}}{s - w_{33}^0} \\ = & \quad \frac{a_1 s^2 - a_2 s + a_3}{s^3 - a_4 s^2 + a_5 s - a_6} \end{aligned}$$

where,

$$\begin{aligned} a_1 &= x_{01} + x_{02} + x_{03} \\ a_2 &= -(x_{02} + x_{03}) w_{11}^0 + x_{02} w_{12}^0 \\ &\quad -(x_{01} + x_{02} - x_{03}) w_{22}^0 - (x_{01} + x_{02}) w_{33}^0 \\ a_3 &= w_{33}^0 (x_{02} w_{11}^0 - x_{02} w_{12}^0 + x_{01} w_{22}^0) \\ a_4 &= (w_{11}^0 + w_{22}^0 + w_{33}^0) \\ a_5 &= (w_{11}^0 w_{22}^0 + w_{22}^0 w_{33}^0 + w_{11}^0 w_{33}^0) \\ a_6 &= w_{11}^0 w_{22}^0 w_{33}^0 \end{aligned}$$

and $\phi(s)$ is the transfer function and $L\{y\}(s)$ is the Laplace transform of $y(t)$. Then the model parameters are structurally identifiable, if the transfer function $\phi(s)$, can be expressed uniquely in terms of its parameters $\mathbf{p}$. Lets assume that x_{01}, x_{02}, and x_{03} are known - we want to test the best case scenario. This is possible if we assume all cancer cells are x_1 type cells in the beginning. Then, equations $a1 - a5$ reduce to:

$$\begin{aligned} b_1 &= -w_{11}^0 + w_{12}^0 - w_{22}^0 - w_{33}^0 \\ b_2 &= w_{33}^0 (w_{11}^0 - w_{12}^0 + w_{22}^0) \\ b_3 &= (w_{11}^0 + w_{22}^0 + w_{33}^0) \\ b_4 &= (w_{11}^0 w_{22}^0 + w_{22}^0 w_{33}^0 + w_{11}^0 w_{33}^0) \\ b_5 &= w_{11}^0 w_{22}^0 w_{33}^0 \end{aligned}$$

Now, we can test global identifiability by introducing new parameters $\hat{w}_{00}^0, \hat{w}_{11}^0, \hat{w}_{22}^0$, and $\hat{w}_{01}^0$. Then we set $(b_1 - b_5)$ equal to the same equation but with the new parameters

and testing if we can uniquely identify the parameters. The result of this procedure yields:

$$\{w_{11}^0 = \hat{w_{11}^0}, w_{11}^0 = \hat{w_{22}^0}, w_{33}^0 = \hat{w_{33}^0}, w_{12}^0 = \hat{w_{12}^0}\}$$

and

$$\{w_{11}^0 = \hat{w_{22}^0}, w_{11}^0 = \hat{w_{00}^0}, w_{33}^0 = \hat{w_{33}^0}, w_{12}^0 = \hat{w_{12}^0}\}$$

as the solutions. Thus, w_{11}^0 and w_{22}^0 are indistinguishable from each other and not identifiable. Since all parameters appear in the system of equations they are all *observable parameters*. This same process can be applied to solve the transfer function for the on-treatment phase of Hirata's Model eq 3.8. For the on-treatment phase, all parameters are observable but none of the parameters are identifiable.

APPENDIX D

CODE FOR CHAPTER 3

```
LIST = [1,2,6,7,12,14:17,19,24:25,28:32,36:37,39:42,...
44,51:52,54,55,58,60:64,66,71,75,...
77:79,83:88,91,93:97,99:102,104:109]; % patient numbers
total = length(LIST);      % total number of patients

errors = [];
pat_count = [];
max_p = 30;
pcount = 1;
for  x = LIST
try
change = [];
load(strcat('parameters/p',num2str(x),'.mat'),'params')
% Complete name of file patient#.txt
file = strcat('Data/',strcat('patient',num2str(x)),'.txt');
patient = load(file);

tdata = patient(:,2);psa = patient(:,3);androgen= patient(:,4);
treatment = patient(:,6);
n = 4;
jj = 1;
change(1) = 1;
for a = 1:length(treatment)
if treatment(a) == mod(jj,2)
a = a+1;
else
jj = jj + 1 ;
change(jj) = a;
end
end
change(jj+1) = length(treatment);

par_noise= 0;k = 100; kk= 12;

par_range = 1:15;
par1 = params;

% noise = 0;
cancer(1) = 20;
x0 = [androgen(1),cancer(1),psa(1),.09];

par_names = {'mu','q','R','k','dd','gamma1','gamma2',...
'Amax','sigma0','sigma1','epsilon','all'};

IC = zeros(k,4);
pn = 1:11;

if kk == 12
params = params + params*par_noise;
else
par_range(4+kk) = [];
pn(kk) =[];
params(kk) = params(kk) + params(kk)*par_noise ;
end

par = params(pn);
```

```
58
59 len_t = length(tdata);
60 len_p = length(par);
61 len_pn = length(pn);
62
63 par_ensemble = zeros(k,len_pn);
64 maxp = ones(len_t,len_p);
65 minp = ones(len_t,len_p);
66 meanp = ones(len_t,len_p);
67 deviation = ones(len_t,len_p);
68 %------------------------------ Loading Data ---------
69 s = x0;                % True initial conditions
70 for i = 1:length(s)
71 a = s(i)*.90; b = s(i)*1.8;
72 % Initial Conds for Enssemble
73 IC(:,i) = (b-a).*rand(1,k) + a;
74 end
75 for i = 1:length(pn)
76 a1 = par(i)*.8;  b1 = par(i)*1.9;
77 par_ensemble(:,i) = (b1-a1).*rand(1,k) + a1;
78
79 deviation(:,i) = std(par_ensemble(:,i));
80 maxp(:,i)      = max(par_ensemble(:,i));
81 minp(:,i)      = min(par_ensemble(:,i));
82 meanp(:,i)     = mean(par_ensemble(:,i));
83 end
84 %---------------- Variables for LETKF ------------
85 R = .6;           % Uncertainty of PSA (2.94% - 4.21%)
86 CAST = zeros(length(par_range),k);   % Forcast matrix - filled using ii
87 I = eye(k);                          % Identity matrix for calculations
88 p = .12;              % error parameter of model (1 to 4);
89 Wa = zeros(k,k);                     % Big W (a = hat)
90 total_t = change(n);                 % Total time for Kalman filter
91 % Stores states solutions from Kalman filter
92 sol1 = psa(1)*ones(1,total_t);
93 sol2 = androgen(1)*ones(1,total_t);
94 sol3 = cancer(1)*ones(1,total_t);
95
96 for jj = 1:1:total_t % setting the ode function to move one time step
97
98 time = [tdata(jj) tdata(jj+1)];    % Time between Measurement
99
100 for ii = 1:1:k % Running the ode45 on the ensembles
101
102 if jj == 1 % Start with IC to initiate the Kalman Filter
103 y0 = [IC(ii,1);IC(ii,2);IC(ii,3);IC(ii,4)];
104 params(pn) = par_ensemble(ii,:);
105 else
106 y0 = [Xa(1,ii);Xa(2,ii);Xa(3,ii);Xa(4,ii)];
107 params(pn) = Xa(5:end,ii);
108 end
109
110 % Runs the model and stores output
111 [t, y] = run_dynd_full(params,tdata,change,time,y0);
112
113 % Collect last y value to preform the Kalman Filter
114 CAST(:,ii) = [y(end,1:4), params(pn)]; % CAST stands for FORECAST;
```

```
end
%-------------------- Plotting Commands ----------------------------------
sol1(jj) = (y(1,3));
sol2(jj) = (y(1,1));
sol3(jj) = (y(1,2));
sol4(jj) = (y(1,4));

X_bar = mean(CAST,2); % X_bar := x-bar(b); the '2' across ;

% Xb := the difference matrix X-double-bar(b)
for i = 1:length(par_range)
if i == 1
Xb = CAST(1,:)- X_bar(1);
else
Xb = [Xb ; CAST(i,:)- X_bar(i)];
end
end

% H := Predicted levels from each ensemble. 0 for augmented states
H = [CAST(1,:)', CAST(3,:)',zeros(100,11)];

y_bar = mean(H); % y_bar := average of predicted PSA
Yb(:,1) = H(:,1) - y_bar(1);  % Yb := Difference between Predicted and
    mean
Yb(:,2) = H(:,2) - y_bar(2);  % Yb := Difference between Predicted and
    mean
Yb(:,3:13) = zeros(100,11);

C = Yb.*(1/R); % Step 4 cook book; R is the uncertainty in PSA -
    defined on top
Pa = ((k-1)*I./p + C*Yb'); %p-twidle
[V, D] = eig(Pa);
lambda = max(0, diag(D));
Z = zeros(k);

for j = 1:k
if lambda(j)>0
Z(:,j) = V(:,j)/lambda(j);
end
end

Pa = Z*V';

for j = 1:k
if lambda(j)>0
Z(:,j) = V(:,j)/sqrt(lambda(j));
end
end

Wa = sqrt(k-1)*(Z*V');

% Put the observed PSA in here
wa = Pa*C*([androgen(jj);psa(jj);zeros(11,1)]-[y_bar(1);...
y_bar(2);zeros(11,1)]);

for gg = 1:1:k
Wa(:,gg) = Wa(:,gg) + wa; % Add wa to each column of Wa
```

```
end

% Finally, we can create the forecast for X1, and PSA
Xa = (Xb*Wa);
for ll = 1:1:k
Xa(:,ll) = Xa(:,ll) + X_bar;
end

Xa(1:end,:) = abs(Xa(1:end,:));

for i = 1:length(par)
maxp(jj+1,i)= max(Xa(4+i,:));
minp(jj+1,i)= min(Xa(4+i,:));
meanp(jj+1,i)= mean(Xa(4+i,:));
deviation(jj+1,i)= std(Xa(4+i,:));
end

disp(jj)
end

catch ME
disp('Something Wrong')
errors = [errors pcount];
end

params1 = [meanp(change(4),:),0];

params = par1;
PSAall4 = [];
last = 6;
lengthPred4 = tdata(change(4):change(6));
for in = 1:100%:length(Xa(1,:))
params2 = [Xa(5:end,in)',0];


x04 = [sol2(end), sol3(end),sol1(end),sol4(end)];
[T4run2,Y4run2]=ode23tb(@(t,x)
    base_dyn_d_full(t,x,[params2(1:end-1),1]),...
tdata(change(4)):tdata(change(5)),x04);
x05 = [Y4run2(end,1);Y4run2(end,2);Y4run2(end,3);Y4run2(end,4)];
[T5run2,Y5run2]=ode23tb(@(t,x)
    base_dyn_d_full(t,x,[params2(1:end-1),0]),...
tdata(change(5)):tdata(change(6)),x05);
Y4 = [Y4run2(:,3);Y5run2(:,3)];
PSAall4 = [PSAall4,Y4'];
plot([T4run2;T5run2],[Y4run2(:,3);Y5run2(:,3)])
hold on
% check if outlier and remove it from the list

end
plot(tdata(change(4):change(6)),psa(change(4):change(6)),'o')
for i = 2:length(PSAall4)
  min_p(i) = min(PSAall4(:,i));
  max_p(i) = max(PSAall4(:,i));
end
end
```

APPENDIX E

CODE FOR CHAPTER 4

```
function [perrors, aerrors] = run_model_delaydependence_mse
x = [1 6 14 15 17 19 24 25 28 29 30 32 36 37 39 44 51 ...
52 54 55 58 60 62 63 64 66 75 77 79 83 87 88 91 ...
93 100 101 102 105]; % list of patients
perrors = [];
aerrors = [];
for ii = x
%%%%%%%%%%%%%%%%% Initialization of arrays and variables %%%%%
nParams = 13;
options = optimset('Algorithm','interior-point','TolX',1e-13,...
'TolFun',1e-13,'TolCon',1e-13,'MaxIter',100);                    %
    Optimizer Options
change = [];                                          % Initialize change
    Vector
load(strcat('par_delay_dependence',num2str(ii),'.mat'),'params')
% Complete name of file patient#.txt
file = strcat('Data/',strcat('patient',num2str(ii)),'.txt');
patient = load(file);
tdata = patient(:,2);psa = patient(:,3);androgen=
    patient(:,4);treatment = patient(:,6);
%%%%%%%%%% Finds periods of on and off treatment %%%%%%%%
jj = 1;
change(1) = 1;                              % Treatment starts at t = 0
for a = 1:length(treatment)
if treatment(a) ~= mod(jj,2) % When treatment change occurs
jj = jj + 1;
change(jj) = a;            % Stores time in change vector
end
end
change(jj+1) = length(treatment);      % Last day of treatment

% noise = 0;

a = max(androgen(change(2):change(4)));
% um              % q             % R               % d             % dd
            % gamma1
LB(1) = 0.0001;  LB(2) = 0;     LB(3) = 0;      LB(4) = .001;     LB(5) =
    0.000001; LB(6) = 18;
UB(1) = .009;     UB(2) = .5;    UB(3) = 1;      UB(4) = .1;    UB(5) =
    .00009;    UB(6) = 21;
% gamma2          % Qmax          % b               % sigma          %
    epsilon          % u
LB(7) = 0;       LB(8) = 5;  LB(9) = 0.01;     LB(10) = 0;     LB(11) =
    .01;      LB(12) = 0;
UB(7) = 4;    UB(8) = 9;     UB(9) = 0.5;       UB(10) = 1;     UB(11) =
    1.5;      UB(12) = 0;

% x0
LB(13) = .1;
UB(13) = 20;

%for i = .5:1:12
lag =2;
global l;
l = lag;
IC = UB/2; % initial parameter values

```

```
Y= run_one_pop(params,tdata,change,n,lag,androgen,psa);

perrors = [perrors,immse(Y(3,:)',psa(change(2):change(n+1)))];
aerrors = [aerrors,immse(Y(1,:)',androgen(change(2):change(n+1)))];
end

function [y] = run_one_pop(params,tdata,change,last,lag,androgen,psa)
y = [];
opts = ddeset('Jumps',lag,'RelTol',1e-5,'AbsTol',1e-5);
for k = 2:last
params(12) = 1 - mod(k,2);
if k == 2
HQ = @(t) interp1(tdata,androgen,t);
HP = @(t) interp1(tdata,psa,t);
x0 = params(13);
else
HQ = @(t) interp1(tdata(change(k-1):change(k)),S(1,:),t);
HP = @(t) interp1(tdata(change(k-1):change(k)),S(3,:),t);
x0 = S(2,end);
end
sol=dde23(@ddex1de,lag,...
ddex1hist(tdata(change(k-1):change(k)),HQ,HP,x0),...
tdata(change(k):change(k+1)),opts,params(1:end));
[S,~] = deval(sol,tdata(change(k):change(k+1)));
if k < last
y = [y, S(1:3,1:end-1)];
elseif k == last
y = [y, S(1:3,1:end)];
end
end
end

function s = ddex1hist(t,HQ,HP,x0)
% Constant history function for DDEX1.
H1 = HQ(t);
H2 = HP(t);
H1= H1(end,1);
H2 = H2(end,1);
s = [H1;x0;H2];
end
%
    ------------------------------------------------------------------------
function dydt = ddex1de(~,x,Z,p)
mu          = p(1);
q           = p(2);
R           = p(3);
d           = p(4);
del         = p(5);
gamma1      = p(6);
gamma2      = p(7);
Qm          = p(8);
b           = p(9);
sigma       = p(10);
epsilon     = p(11);
c           = p(12);

Ql= Z(1,1);
```

```
105 Xl = Z(2,1);
106
107 %separates solutions
108 Q = x(1); X = x(2); P = x(3);
109 %%%%%%%%%%%%%%%%%%%% ODE system %%%%%%%%%%%%%%%%%%%%%%%%%%%%%%%%%%%%%%%%%%%%
110 dQ = (gamma1*c +gamma2)*(Qm -Q)- mu*(1-q/Ql)*Q*(Xl/X)*exp(-l*d);
111 dX = mu*(1-q/Ql)*Xl*exp(-l*d) - d*R*X/(Q+R)- abs(del)*X^2;
112 dP = abs(b)*Q + abs(sigma)*X*Q - abs(epsilon)*P;
113 %%%%%%%%%%%%%%%%%%%%%%%%%%%%%%%%%%%%%%%%%%%%%%%%%%%%%%%%%%%%%%%%%%%%%%%%%%%%
114 dydt = [dQ; dX; dP]; %Puts the ode in a column vector
115 end
116 end
```